Analysis of Hybrid CSMA/CA-TDMA Channel Access Schemes with Application to Wireless Sensor Networks

by

Bharat Shrestha

A Thesis submitted to the Faculty of Graduate Studies of
The University of Manitoba
in Partial Fulfilment of the Requirements for the degree of

Doctor of Philosophy

Department of Electrical and Computer Engineering
University of Manitoba
Winnipeg

Supervisor: Prof. E. Hossain

ABSTRACT

A wireless sensor network consists of a number of sensor devices and coordinator(s) or sink(s). A coordinator collects the sensed data from the sensor devices for further processing. In such networks, sensor devices are generally powered by batteries. Since wireless transmission of packets consumes significant amount of energy, it is important for a network to adopt a medium access control (MAC) technology which is energy efficient and satisfies the communication performance requirements. Carrier sense multiple access with collision avoidance (CSMA/CA), which is a popular access technique because of its simplicity, flexibility and robustness, suffers poor throughput and energy inefficiency performance in wireless sensor networks. On the other hand, time division multiple access (TDMA) is a collision free and delay bounded access technique but suffers from the scalability problem. For this reason, this thesis focuses on design and analysis of hybrid channel access schemes which combine the strengths of both the CSMA/CA and TDMA schemes.

In a hybrid CSMA/CA-TDMA scheme, the use of the CSMA/CA period and the TDMA period can be optimized to enhance the communication performance in the network. If such a hybrid channel access scheme is not designed properly, high congestion during the CSMA/CA period and wastage of bandwidth during the TDMA period result in poor communication performance in terms of throughput and energy efficiency. To address this issue, distributed and centralized channel access schemes are proposed to regulate the activities (such as transmitting, receiving, idling and going into low power mode) of the sensor devices. This regulation during the CSMA/CA period and allocation of TDMA slots reduce traffic congestion and thus improve the network performance. In this thesis work, time slot allocation methods in hybrid CSMA/CA-TDMA schemes are also proposed and analyzed to improve the network performance. Finally, such hybrid CSMA/CA-TDMA schemes are used in a cellular layout model for the multihop wireless sensor network to mitigate the hidden terminal collision problem.

Acknowledgment

First and foremost, I would like to thank my advisor Professor Ekram Hossain for his constant support, guidelines, comments and direction to this work. His comments were always motivational to me.

I would like to express my sincere thanks to Dr. Sergio Camorlinga for his support and helpful comments. It has been a great experience for me to work with him at TRLabs Winnipeg. I am very thankful towards TRLabs Winnipeg for providing research facilities and financial support. Also, it was an honor for me to receive grants from NSERC to support this work financially. I am grateful to InfoMagnetics Technologies Corporation Winnipeg for the sponsorship of the project at TRLabs Winnipeg.

I am also thankful to Dr. Kaewon Choi for his suggestions, insightful comments and guidance. I would like to thank Dr. Dusit Niyato for his support and suggestions. I would like to thank my friends Dr. Phond Phunchongharn, Dr. Khajonpong Akkarajitsakul and Dr. Surachai Chieochan for their support and suggestions to make my study at the University of Manitoba beautiful. I would also like to thank all my friends at the University of Manitoba for their moral support.

I am also grateful to our Nepali friends and Nepali community for making my stay in Winnipeg enjoyable. Finally, I am happy to dedicate this work to my parents, my wife and family members because their support and encouragement brought me to this point.

To My Family

Table of Contents

List of Tables

List of Figures

Chapter 1

Introduction

1.1 Wireless Sensor Networks

A wireless sensor network is composed of a number of sensor devices and sink(s) or coordinator(s). A sensor device is a battery-powered device which has the capability of transmitting and receiving signal wirelessly. The sensor devices transmit the sensed data towards the sink or coordinator. The sink or coordinator sends the collected data to the control unit for further processing (as shown in Figure 1.1). Wireless sensor networks have been widely used in a broad range of applications including field surveillance, industrial control system, and monitoring applications in health-care systems [1, 2]. Because the sensor devices generally have low processing power, limited battery power, small memory size and suffer from collisions and interference in wireless transmissions, optimizing the operation of a wireless sensor network is challenging.

Since wireless sensor devices are powered by battery, energy consumption is a major issue to be addressed while designing the communication protocols between the sensor devices and the sink or coordinator. Sensor devices consume a significant amount of energy while transmitting and receiving data [3]. Sensor devices do not transmit with high power to achieve longer life time of the battery. Therefore, short-range communication protocols are suitable for wireless sensor networks. This thesis focuses on designing such communication protocols. In this context, collision mitigation, sleep and wakeup scheduling and improving successful data transmission rate without degrading latency are the major issues which need to be addressed. In particular, an efficient medium access control (MAC) protocol which is responsible for handling the access to the shared wireless medium has to be designed for the

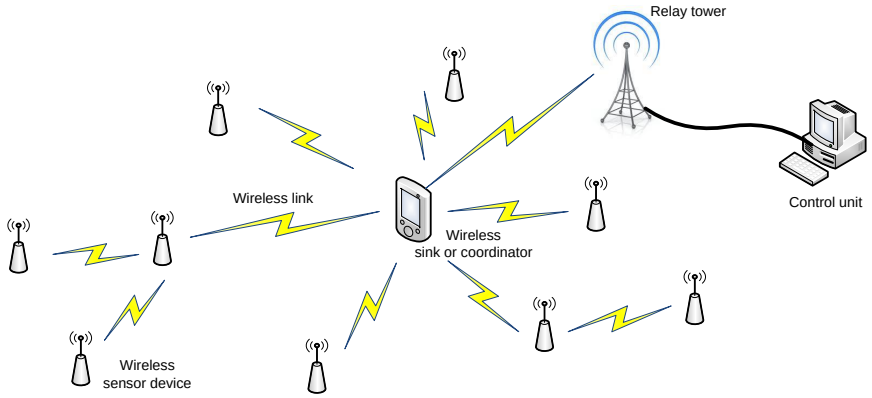

Figure 1.1. *A wireless sensor network.*

wireless sensor network. Note that self organization, routing, and security are examples of some other issues which are also important in the design of wireless sensor networks [1].

The design of a MAC protocol depends on the requirement of the wireless sensor network. For example, in a wireless sensor network where the sensor devices have low volume of data traffic to transmit and require mobility, contention-based MAC protocols are desirable. In a contention-based MAC protocol, the devices compete to access the shared transmission medium. If two or more devices compete at the same time, the data transmission is unsuccessful. The contention-based MAC protocols are simple and flexible in terms of synchronization requirement and robust to the change in network structure. In a small wireless sensor network where the sensor devices have a requirement of high rate of data transmission at low or no mobility, contention-free MAC protocols are desirable. In a contention-free MAC protocol, the devices are scheduled to access the medium one at a time so that the transmission is guaranteed to be successful. In addition, the design of the MAC protocol requires to balance the tradeoff between rate of successful data transmission, energy consumption, and latency because one can be maximized at the expense of the other [1]. A hybrid MAC protocol, which combines the contention-based and contention-free MAC protocols, can be designed to support a broad range of requirements of the wireless sensor networks. The research work presented in this thesis deals with the design of such hybrid MAC protocols. Note that such a MAC protocol can incorporate both active

period and inactive periods in the superframe structure allowing the devices to go into the sleep mode during inactive period. For designing the hybrid MAC protocol, in this work, only the active period of the superframe is considered. Application of the protocol for a special type of sensor network, namely, the body area sensor network is also demonstrated.

1.2 Wireless Body Area Sensor Networks

Wireless body area sensor network (WiBASE-Net) [4] is an emerging technology that can be used in medical, entertainment, and fitness applications. In a WiBASE-Net, several wearable or implanted sensor devices, for instance electrocardiogram (ECG) sensor, blood pressure sensor, temperature sensor, respiratory sensor, pulse oximeter, and accelerometer, are deployed throughout the body. A body controller unit (BCU) collects data from the Body Sensor Units (BSUs) or sensor devices deployed in the body of a patient. With necessary processing, the BCU is also responsible for transmitting medical data to the health professionals at medical control center in a required format via external network or the Internet as shown in Figure 1.2. The Institute of Electrical and Electronics Engineers (IEEE) 802.15.1 [5]-based and the IEEE 802.15.4 [6]-based technologies are suitable communication protocols for WiBASE-Nets [7]. For health monitoring and other pervasive health care applications, WiBASE-Net technologies provide flexible networking solutions by replacing bulky wired systems. For example, health professionals can monitor patients remotely sitting in front of their personal computer or mobile device whereas patients can move with unobtrusive sensor devices.

WiBASE-Net technology will be a basic element of next generation wireless medical services. Examples of some potential applications of body area sensor network are clinical intensive care, general clinical patient care (e.g., respiratory, wearable heart rate monitoring), home care, mobile care, supervised rehabilitation (e.g., muscle tension sensing and stimulation, fall detection), personal health support, and medical process evaluation applications. In addition, a WiBASE-Net is useful for non-medical services such as in entertainment albeit with different requirements. WiBASE-Net is targeted to meet the requirements of low power consumption to be safe for human

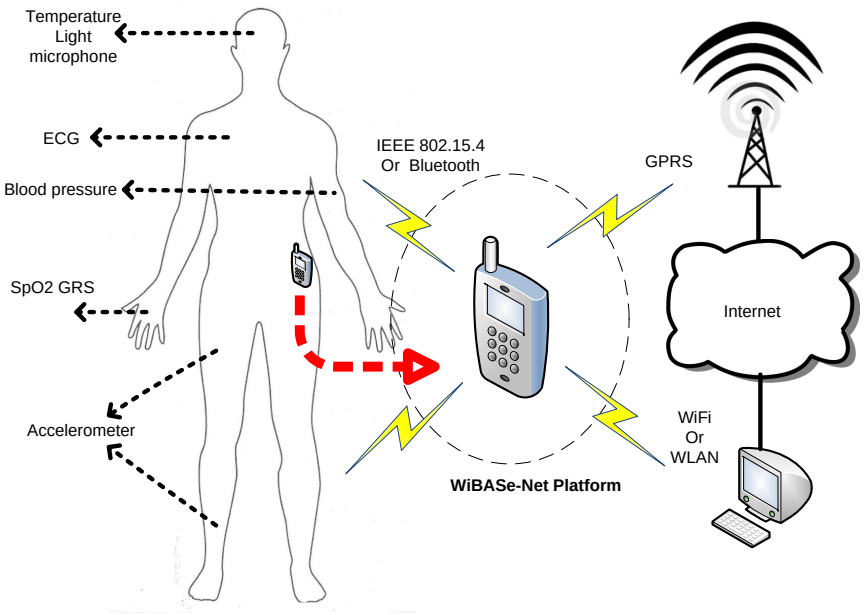

Figure 1.2. *A wireless body area sensor network.*

tissue, short range communications (within human body) causing no interference to other networks, reliable data transmissions, security and low latency. Some of the basic features of a WiBASE-Net are as follows:

- Operating on, inside, or in the vicinity of the body
- Limited range (e.g., 0.01 to 2 meters)
- Channel model includes human body effects (absorption, health effects)
- Low power consumption (e.g., 0.1 to 1 mW) for each sensor device
- Scalable data rate (e.g., 0.01 to 100 kbps)
- Different classes of QoS for high reliability, asymmetric traffic, and power constrained
- Optimized low complexity MAC and networking layers.

The issue of communications between the BCU and the BSUs is important in designing such a WiBASE-Net. Such communications have to maximize the utilization of the network bandwidth (e.g., support as many BSUs as possible), satisfy the latency requirements for data transmission from BSUs to the BCU, and also need to be energy-efficient. In this research, we deal with the problem of optimizing the

communication performance in a hybrid carrier sense multiple access with collision avoidance-time division multiple access (CSMA/CA-TDMA) medium access-based WiBASE-Net. In particular, we exploit the guaranteed time slots (GTS) in the superframe of the hybrid CSMA/CA-TDMA scheme for efficient data transmissions from the sensor devices to the controller unit.

1.3 Medium Access Control (MAC) Protocols

The MAC protocol in a wireless sensor network defines a set of rules which regulate the activities of sensor devices in the network. The activities of a sensor device refer to transmitting data packet, receiving data packet, idling or sleeping. If a MAC protocol is not designed properly, it results in the wastage of energy in wireless sensor devices because of collisions, overhearing, idling, over emitting and on-off transitions [8]. Also, fairness among the sensor devices could not be achieved. In addition to wastage of energy and unfairness, improper design of the MAC protocol results in degradation of the performance of the devices in terms of throughput and delay. The problem of designing MAC protocols for wireless sensor networks has been extensively studied in the literature [2, 1, 3, 8, 9]. The design of MAC protocols should consider the specific requirements of the wireless sensor network. In general, the MAC protocols can be classified into contention-based and contention-free MAC protocols.

In a contention-based MAC protocol, a common wireless medium or channel is shared by the sensor devices. The performance of a device depends on the medium or channel access probabilities of the all sensor devices in the network. For example, in ALOHA [1], a sensor device transmits whenever it has data packet(s). It waits for an acknowledgment from the destination device. If the acknowledgment is not received, it retransmits the data packet after a backoff interval the duration of which is determined by using a backoff algorithm. Note that two or more devices could transmit data packets simultaneously resulting in collisions. The number collisions could be reduced if devices listen before transmitting as in the carrier sense multiple access (CSMA) protocol. In the CSMA protocol, each device first senses the medium to see if any other device is transmitting. If the medium is free (or idle), then the device starts transmitting a data packet. If the medium is busy, the device

backs off. With such modification, the sensor devices achieve a better communication performance than ALOHA.

Over the time, many variations of the ALOHA and CSMA protocols such as slotted ALOHA, p-persistent CSMA, and CSMA with collision avoidance (CSMA/CA) have been developed. In CSMA/CA, some improvements over CSMA have been made to resolve the collisions. The devices take random backoff before starting the carrier sensing. To cope with switching, propagation and processing time, the devices require the medium to be idle for at least a period called inter frame space (IFS) before packet transmission begins. The devices take random backoff from a contention window if the medium is found busy. Also, handshake signaling, which is optional, has been introduced to resolve the collisions. The CAMA/CA-based MAC protocol is gaining its popularity as a simple, flexible and robust random access MAC protocol albeit collision is unavoidable. Some examples of contention-based MAC protocols are SMAC and WISE MAC [1]. These are not as popular as CSMA/CA because SMAC requires synchronization between the devices whereas the WISE MAC requires a device to transmit long preamble before the packet is transmitted.

In a contention-free MAC protocol, time is divided into frames and frames are further divided into time slots. A specific time slot(s) during a frame is assigned to a device for packet transmission. The time slot is allocated to the device and no other devices contend to transmit during this time slot. This protocol eliminates the collision problem inherent in the CSMA-based protocols. The contention-free MAC protocols can be broadly classified into static time division multiple access (TDMA) and dynamic TDMA MAC protocols. In the static TDMA MAC protocols, the devices are assigned static time slots for packet transmission for the entire duration of communication. Many TDMA slot allocation algorithms have been developed to allocate conflict-free slots to the devices [10]. One problem with such protocols is the under-utilization of the TDMA slots because of variable traffic load at the devices. Also, the TDMA slot allocation algorithm has to be re-run in case some devices change their positions. In the dynamic TDMA MAC protocols, the TDMA slots are allocated to the needy devices by a coordinator following a defined procedure. For example, in the IEEE 802.15.4 MAC protocol (i.e., in ZigBee networks) [6], a coordinator allocates time slots in a first-come first-served fashion to the device who requests for the time

slot. A polling-based MAC protocol can also be considered in this category. For example, in the IEEE 802.15.1 MAC (i.e., in Bluetooth networks) [5], a coordinator polls a device to transmit packet in the next immediate time slot.

The contention-based and contention free MAC protocols can be combined together to form a hybrid MAC protocol. ZMAC [10] is an example of hybrid MAC protocol. In the ZMAC protocol, the devices are allocated static TDMA slots. The slot owner has the highest priority to access the TDMA slot. The larger the size of the backoff window, the lower is the priority. If the slot owner has no packet to transmit, then rest compete using CSMA/CA to access the slot. At low traffic, the ZMAC protocol behaves as the CSMA/CA protocol whereas at high traffic it behaves as a TDMA protocol. The problem with ZMAC is the requirement of static TDMA slot allocation. The examples of hybrid MAC protocols which adopt the dynamic TDMA MAC include the IEEE 802.15.4 MAC [6] and the IEEE 802.15.3c MAC [11] where the TDMA slots are allocated to the devices upon requests. This thesis particularly focuses on such hybrid MAC protocols incorporating CSMA/CA and dynamic TDMA.

1.3.1 Carrier Sense Multiple Access with Collision Avoidance (CSMA/CA)

CSMA/CA is a popular access technique for packet transmissions in wireless sensor networks because of its simplicity, flexibility, and robustness. It does not need synchronization and does not depend on the topology of the network. CSMA/CA has been adopted in its various form by many IEEE standards for wireless communication technology such as the IEEE 802.15.4 [6], IEEE 802.15.3c [11], and IEEE 802.11 [12] standards. Figure 1.3 shows the basic operation of CSMA/CA. To cope with the propagation delay and processing time, there should be a gap between transmissions of any two packet frames. This gap is called inter frame space (IFS). Before carrier sensing, a device takes a random backoff. The size of backoff is selected randomly from a window called contention window ($cw \in [cw_{min}, cw_{max}]$). Randomness in the backoff reduces collisions but is unable to eliminate it completely. There is still chance that two or more devices start sensing the medium simultaneously and collision occurs. If collision occurs (i.e., the sender does not receive the acknowledgment packet

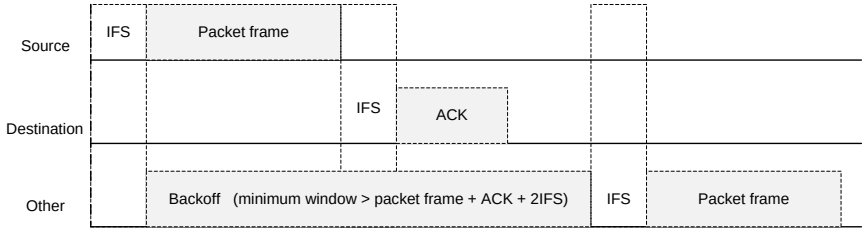

Figure 1.3. *Packet transmission using CSMA/CA.*

from the receiver), the devices repeat the backoff process to retransmit the packet.

In CSMA/CA, *hidden terminal collision* is also a problem. As shown in Figure 1.4, device A and device C are hidden terminals because they are out of range of each other. Device A and device C are unable to hear each other, and therefore, sense the medium to be free. When both start transmission, device B suffers collision. In CSMA/CA, handshake signaling called request-to-send/clear-to-send (RTS/CTS) can be used to resolve the hidden terminal problem. As shown in right side of the Figure 1.4, device A first sends the RTS message to device B. Device B broadcasts the CTS message. Upon receipt of the CTS message, device C freezes its transmission preventing the collision at device B. However, there is possibility of collisions between RTS messages. As shown in Figure 1.5, simultaneous transmission between device A to device B and device D to device C is possible. The RTS/CTS handshaking prevents device D from transmission which results in the *exposed terminal problem*. Moreover, since the RTS/CTS handshaking involves signaling exchanges, it is not favorable for the power-limited sensor devices. Therefore, collisions are almost unavoidable in CSMA/CA networks.

There are two types of CSMA/CA techniques, namely, the un-slotted CSMA/CA and the slotted CSMA/CA. In un-slotted CSMA/CA, time synchronization is not important for the devices (e.g., in the IEEE 802.15.4 MAC protocol in the non-beacon enabled mode). In slotted CSMA/CA, the devices are required to be synchronized with the coordinator. The TDMA slot is further divided into multiple unit backoff period (UBP). The devices start each activity (backoff, carrier sensing, transmitting or receiving) at the boundary of the UBP. The IEEE 802.15.4 MAC protocol adopts slotted CSMA/CA in the beacon enabled mode.

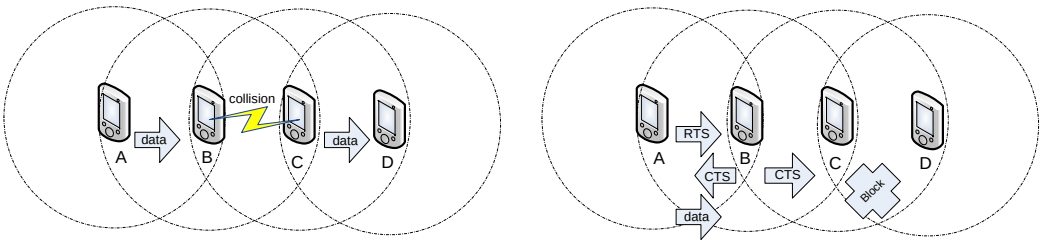

Figure 1.4. *Hidden terminal collision problem and the RTS/CTS-based solution.*

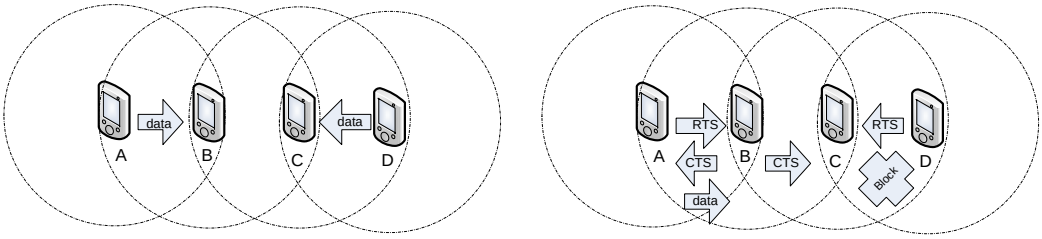

Figure 1.5. *Simultaneous transmission and the exposed terminal problem resulting from RTS/CTS.*

1.3.2 Time Division Multiple Access (TDMA)

The superframe structure of a TDMA MAC protocol is shown in Figure 1.6. Time is divided into superframes and a superframe is divided into equal time slots. The length of a superframe depends on the maximum number of slots M. In TDMA MAC protocol, a TDMA slot allocation algorithm is used to allocate slots to the devices in the network. Each device transmits packet in the assigned TDMA slot(s). The allocation of slots can be done in a centralized way or in a distributed way. In a distributed TDMA slot allocation method, devices exchange information with each other to obtain the conflict-free TDMA slots. In a centralized method, a coordinator allocates slots to the devices associated with it. A central controller can exist to allocate slots to the multiple coordinators. In multihop networks, the challenge is to minimize the maximum number of slots, because the longer the superframe length, the larger is the delay. To resolve the problem due to a longer superframe length, a dynamic TDMA slot allocation algorithms can be applied. This MAC protocol is inherently collision-free and hence energy efficient. Synchronization might not be a serious issue in a TDMA MAC protocol because of the recent advancement in

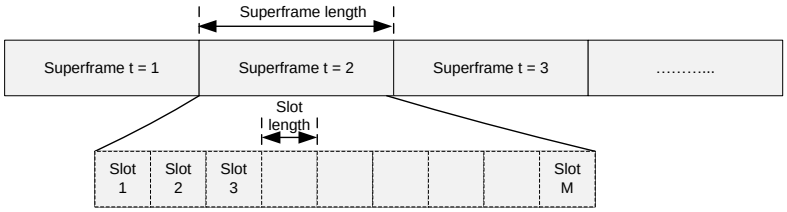

Figure 1.6. *TDMA superframe structure.*

microprocessing technology but scalability is a problem. The TDMA MAC protocol is unable to handle the new devices who want to join the network.

1.3.3 Hybrid CSMA/CA-TDMA

A superframe structure of a hybrid CSMA/CA-TDMA MAC protocol which adopts the dynamic TDMA is shown in Figure 1.7. The coordinator is responsible for controlling the sensor devices which sends information about time synchronization and reservation of TDMA slots through the beacon frame at the start of the superframe. Since the superframe is divided into CSMA/CA period and TDMA period, a limited number of slots are available for the devices. The coordinator allocates the TDMA slots to the devices based on their requirements following a defined procedure. Also, the coordinator can allocate the slots to the devices based on their requests. The devices which do not have time critical data can use only CSMA/CA period to transmit their data packets. Because of collisions, their data packets might be delayed to reach the destination. However, data packets are guaranteed to reach the destination within a bounded delay when TDMA slots are used; therefore, a TDMA slot is also called the guaranteed time slot (GTS). In the superframe of a hybrid CMSMA/CA-TDMA MAC, the minimum length of CSMA/CA period is maintained all the time so that the devices are able to send their request packets either for obtaining the TDMA slot(s) or for joining the network. The IEEE 802.15.4 MAC protocol is an example of such a hybrid MAC protocol. In such a hybrid MAC protocol, maintaining the optimal CSMA/CA and TDMA period for the optimal network performance is a challenging problem.

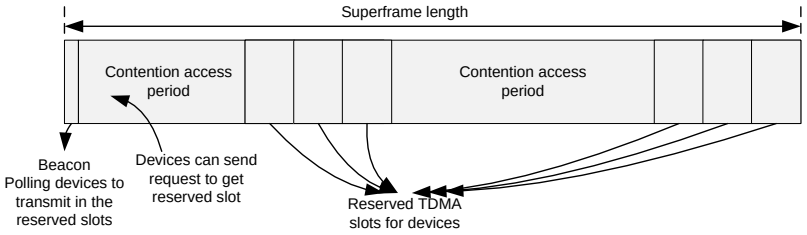

Figure 1.7. *Superframe structure for hybrid CSMA/CA-TDMA scheme.*

1.4 Wireless Communications Standards

There have been a huge number of MAC protocols developed for wireless sensor networks. A few of them have been standardized to be implemented universally. The IEEE 802.11 and IEEE 802.15 task groups are working on the short range, very low power and highly reliable wireless communication protocols. Such standard protocols applicable to wireless sensor networks are as follows:

- ZigBee using IEEE 802.15.4 [13]
- WiFi using IEEE 802.11 [14]
- Bluetooth using IEEE 802.15.1 [15].

1.4.1 ZigBee Using IEEE 802.15.4

ZigBee [13] is a wireless networking protocol designed for automation and control networks which require low data rate, low power consumption and low cost. It sits on the IEEE 802.15.4 MAC [6] and PHY layers and supports user defined network, transport and application layers. The IEEE 802.15.4 MAC uses un-slotted CSMA/CA channel access mechanism when beacon is not enabled and uses slotted CSMA/CA mechanism otherwise. ZigBee operates on the unlicensed industrial, scientific and medical (ISM) band in the 2.4 GHz (also in the 915 MHz Americas and in the 868 MHz band in Europe). The data rate is 250 kbps at 2.4GHz, 40 kbps at 915 MHz and 20 kbps at 868 MHz. The expected transmission range is 10 to 75 meters. The radio uses Direct Sequence Spread Spectrum signaling with OQPSK modulation scheme at 2.4 GHz band and BPSK in other bands. There are 16 channels in the 2.4 GHz to 2.4835 GHz band. In the network layer, it uses Ad Hoc On Demand Distance Vector

(AODV) routing protocol. ZigBee uses a simple master slave configuration in star network and can support 254 nodes in the network. ZigBee's application domains are health care applications, mobile phone applications, building automations, etc. ZigBee is a registered trademark of ZigBee alliance which is an association of over 285 companies working together to enable reliable, cost-effective, low-power, wirelessly networked, monitoring and control products based on an open global standard.

1.4.2 WiFi Using IEEE 802.11

Wireless fidelity (WiFi) [14] runs on the MAC and physical layer of IEEE 802.11 standard [12]. The IEEE 802.11 MAC was designed for wireless local area networks with data rate of 1Mbps to 2 Mbps to handle mobile and portable devices. However, various amendments have been done to the IEEE 802.11 to achieve high data rate up to 1.3Gbps with the help of various modulation schemes, coding schemes, spectrum use and antenna systems. The IEEE 802.11 MAC protocol also operates in 2.4 GHz and 5 GHz band. The IEEE 802.11 MAC supports two types of access methods: point coordination function (PCF) and distributed coordination function (DCF). In PCF, a point coordinator (PC) controls the access of channel as in contention-free MAC protocol. The PC polls the devices to transmit packet in a specified time slots based on their requirement.

In DCF, a variation of the CSMA/CA is used as the channel access method. In DCF, to reduce the number of collisions, the concept of network allocation vector (NAV) is introduced as a method for virtual carrier sensing. When a device detects any packet transmission in the channel, it defers its transmission activity until the NAV expires. The duration of NAV is set according to the time taken to complete the transmission of the data packet successfully. Another notable difference of DCF with CSMA/CA is that, while in backoff, a node freezes the backoff counter if channel is sensed busy. It resumes the backoff counter after the channel is sensed to be free. Because of high power consumption and its physical layer design for high speed data transfer applications, WiFi is not suitable for wireless sensor networks.

1.4.3 Bluetooth Using IEEE 802.15.1

Bluetooth [15] is a communication protocol based on the IEEE 802.15.1 standard [5] and it is intended for handling voice, images and file transfer applications in wireless ad hoc networks. Similar to ZigBee, Bluetooth operates in the 2.4 GHz band. It has a data rate of 1 Mbps which is higher than that of ZigBee, and with Bluetooth version 2, it can support a data rate up to 3 Mbps. It uses 79 Radio Frequency (RF) channels with 1 MHz carrier spacing. For standard and basic rate transmission, it uses the Gaussian Frequency Shift Keying (GFSK) modulation scheme with bandwidth bit product BT = 0.5. The transmit power is in the range of 1 to 100 mW with corresponding transmission range from 1m to 100m. The radio technology uses Frequency Hopping Spread Spectrum (FHSS) coding and has 1600 hopping/s over 79 channels with 625 μs default time slot. It uses Time Division Duplexing (TDD) for data receive and transmit separation. Bluetooth enabled devices form a piconet of maximum 8 devices in a master-slave fashion but can support many parked and standby devices. In each piconet, the master assigns hop sequences to the slaves and the slaves have to synchronize with that hopping sequence. There can be more than one piconet. A device can be master in one piconet and slave in another piconet. Multiple piconets form a scatternet. Because of its energy consumption in transition from parked or standby to active and in frequency hopping, this protocol is not suitable for wireless sensor networks.

1.5 Overview of IEEE 802.15.4 Medium Access Control Protocol

In this section, we present the details of the IEEE 802.15.4 MAC protocol which is a standard hybrid CSMA/CA-TDMA MAC protocol. The IEEE 802.15.4 (ZigBee) and IEEE 802.15.1 (Bluetooth) are widely accepted MAC protocols for low-power and short-range communications. Particularly, in a wireless sensor network, the IEEE 802.15.4 MAC offers some advantages over the IEEE 802.15.1 MAC which are as follows:

- Low duty cycle feature for low power consumption

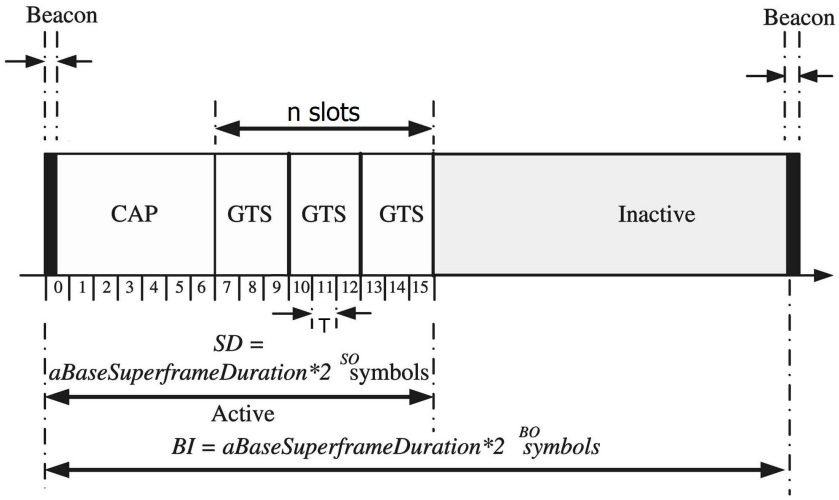

Figure 1.8. *Superframe structure in the IEEE 802.15.4 standard (source [71]).*

- Low device connection time
- Hybrid transmission scheme (contention-based and contention-free)
- Radio controller can handle 256 devices while a Bluetooth controller can handle at most 7 active devices at the same time.

The IEEE 802.15.4 standard [6] specifies a MAC protocol for low data rate short-range wireless networks such as medical wireless sensor networks. It supports two operating modes: beacon-enabled and non-beacon-enabled modes. In the non-beacon-enabled mode, the un-slotted CSMA/CA protocol is used. In the beacon-enabled mode, the network coordinator transmits beacon to synchronize and provide necessary information to the devices.

In the IEEE 802.15.4 MAC, time is divided into superframes (Figure 1.8). The active period consists of two parts: contention-access period (CAP) and contention-free period (CFP). During CAP, the wireless devices use a slotted CSMA/CA protocol. The slotted CSMA/CA mechanism is shown in Figure 1.9. It starts clear channel assessment (CCA) right after the backoff counter reaches to zero. If it finds the channel to be clear, then it performs a second CCA before transmitting a packet. If it finds the channel to be busy, then it increases the backoff window exponent (BE) by one, but not exceeding macMaxBE, and repeats the random backoff. During CFP, trans-

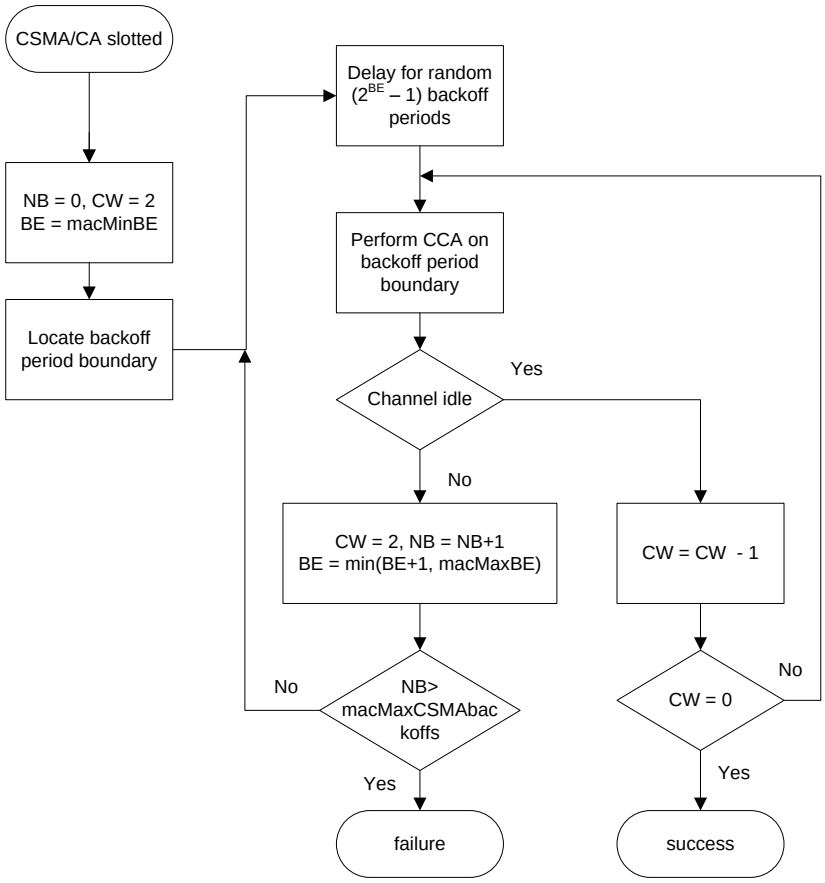

Figure 1.9. *Flowchart for the slotted CSMA/CA protocol in the IEEE 802.15.4 MAC.*

missions are performed without using CSMA and GTS is allocated for either uplink or downlink transmission. The coordinator can allocate a maximum of seven GTSs to a device. The coordinator maintains beacon interval, slot length, active period (SD), and inactive period in the beacon order (BO) and super frame order (SO) as shown in Figure 1.8.

Whenever a device requires a certain guaranteed bandwidth for transmission, the device sends a GTS request using CSMA/CA during CAP. Upon receiving the request, the coordinator first checks the availability of GTS slots in which the length of CAP must not be shorter than aMinCAPLength. The coordinator informs the device about the allocation of slot in the GTS descriptor in the next beacon frame (Figure 1.8). The GTS deallocation can be performed by the coordinator or by the device itself. For

device initiated deallocation, it sends a GTS request with characteristic type subfield set to zero using CSMA/CA during CAP. Similarly, if the coordinator does not receive data from the device in the GTS for at least $2f$ super frames, the coordinator will deallocate the GTS with starting slot subfield set to zero in the GTS descriptor field of the beacon frame for that device, where $f = 2^{8-\mathrm{BO}}$ for $0 \leq \mathrm{BO} \leq 8$, and $f = 1$ for $9 \leq \mathrm{BO} \leq 14$.

1.6 Design Issues for Hybrid CSMA/CA-TDMA Scheme

The hybrid CSMA/CA-TDMA scheme offers several advantages to the wireless sensor networks such as scalability and collision free transmissions. New devices which want to associate to the network seek random access scheme during CSMA/CA period. Also, the devices seek random access during CSMA/CA period to send request for the TDMA slot or release the TDMA slot so that other needy devices can use it. The problem of CSMA/CA access scheme is that there is no guarantee to deliver the packet to destination in pre-defined time since there is always possibility of collision in transmissions using CSMA/CA. The devices which have time critical data seek collision free transmission through reserved TDMA slots. For this reason, such hybrid channel access scheme is explored in this research work. However, to take the full advantage of the hybrid channel access scheme, some issues listed below have to be taken into account while designing such channel access schemes.

1.6.1 Sizes of CSMA/CA and TDMA Periods

A superframe is divided into K equal slots. The superframe consists of TDMA period of M slots and CSMA/CA period of $K - M$ slots. Note that, increasing the TDMA period (M) decreases the CSMA/CA period which in turn increases congestion during the CSMA/CA period. The congestion refers to the state of a network where a number of devices are trying to get access to the channel and probability that packet transmission is successful is low. The congestion during the CSMA/CA period leads to increased collisions, higher number of retransmissions of packets, and wastage of

energy. Therefore, determining the optimal size of the CSMA/CA and TDMA periods to satisfy the network requirements and determining the activities (i.e., transmit, receive, backoff or sleep) of the devices are challenging for such hybrid channel access schemes.

1.6.2 Allocation of TDMA Slots

The transmission scheduling of the devices to meet their requirements is an important problem. For example, if the network size N is such that $N \gg M$, careful design of a TDMA slot allocation algorithm (i.e., allocating M slots to N devices) to meet the requirements such as maximizing the channel utilization is required. Such scheduling algorithms should work for minimum exchanges of messages.

1.6.3 Support for Multihop Networks

In a hybrid CSMA/CA-TDMA scheme, the devices are required to synchronize their clock with each other. For this reason, devices require to associate with a master or a coordinator in the network. In a multihop wireless sensor network, the hybrid channel access scheme should support the multiple coordinators as relays or gateways. In such case, management of multiple beacon frames and collision free transmissions is also a challenging problem.

The thesis addresses the above problems and proposes novel solutions which consider propagation in the wireless channel, traffic heterogeneity in the sensor nodes as well as energy efficiency of wireless transmission. The contributions of the thesis are summarized in the next section.

1.7 Contributions of the Thesis

The research work presented in this thesis deals with the communication problem between the sensor devices and the coordinator in a wireless sensor network. In particular, we are interested in designing an efficient channel access mechanism between the sensor devices and a coordinator to enhance the performance in terms of throughput and energy efficiency. As a channel access mechanism between sensor

devices and a coordinator, we consider hybrid channel access scheme which combines carrier sense multiple access with collision avoidance (CSMA/CA) and time-division multiple access (TDMA). Time is divided into contention access period (CAP) where sensor devices use CSMA/CA and contention free period (CFP) where sensor devices use TDMA. The CFP consists of a number of TDMA slots. Examples of such hybrid MAC protocols are the IEEE 802.15.4 MAC [6] and the IEEE 802.15.3c MAC [11]. The benefit of hybrid channel access scheme is that it has the power of collision free transmissions derived from TDMA and robustness and scalability derived from CSMA/CA. However, the contention access period and the contention-free period need to be used appropriately to meet the data communication requirement in a wireless sensor network. In this thesis, hybrid CSMA/CA-TDMA schemes are analyzed and enhanced for improved packet level performance (e.g., packet delivery ratio, energy consumption) of sensor devices in wireless sensor networks. The following sections summarize the contributions of the thesis.

1.7.1 Balanced Use of Contention Access Period and Contention-Free Period

In order for the sensor devices to use the contention free period (CFP), they need to get the information of transmission scheduling from the associated coordinator. We do not consider static allocation of TDMA slots to sensor devices as it leads to waste of bandwidth when sensor devices do not have data to transmit. In the case of distributed transmission scheduling during CFP, each sensor device sends a request to obtain the TDMA slots during CFP and the coordinator allocates the slot(s), if available, to the sensor device. In the case of centralized transmission scheduling during CFP, the coordinator collects the information such as traffic loads from all the sensor devices. After processing the information, the coordinator allocates slots to the sensor devices to meet the communication requirements of the network.

In **Chapter 2** of this thesis, we propose Markov decision process (MDP)-based distributed and centralized models to balance the use of both contention access and contention free periods in order to reduce transmission energy consumption. The proposed schemes consider the buffer status as an indication of congestion provided that the offered traffic does not exceed the channel capacity. The MDP develops a

policy which maps the buffer state to an action. Based on the policy, each device determines the best action from a set of actions (*go to low power mode, transmit packet during CAP, transmit packet during CFP and transmit packet during both CAP and CFP*). These channel access methods can save a considerable amount of energy when the network is congested. The network congestion can be the result of collisions, and/or high shadowing path-loss and/or increased number of collisions due to hidden nodes. The collision or path-loss enforces the devices to retransmit packets or go to further backoff stages which increase packet service time and thus result in delay and network congestion. In the centralized model, a coordinator requires knowledge of all devices to develop transmission strategy in distributed model, each device develops its transmission strategy based on the local information. We extend the schemes to consider the hidden node collision problem encountered due to the signal attenuation caused by channel fading. The simulation results show that the MDP-based distributed channel access scheme outperforms the legacy slotted CSMA/CA scheme. This scheme also works efficiently in a network consisting of heterogeneous nodes. The centralized model outperforms the distributed model and stands as a benchmark for the performance evaluation.

1.7.2 Analytical Modeling of the IEEE 802.15.4-Based Hybrid CSMA/CA-TDMA Scheme

In wireless sensor networks such as wireless body-area sensor networks, sensor devices have different bandwidth requirements and thus create heterogeneous traffics. For such networks, hybrid CSMA/CA-TDMA protocol such as the IEEE 802.15.4 MAC can be used in the beacon-enabled mode which supports guaranteed time slot (GTS) allocation for time-critical data transmissions. In **Chapter 3**, we develop a general discrete-time Markov chain model for the IEEE 802.15.4-based networks taking into account the slotted CSMA/CA and GTS transmission together in the heterogeneous traffic scenario and under non-saturated condition. For this purpose, the standard GTS allocation scheme of the IEEE 802.15.4 MAC is modified. For each non-identical device, the Markov model is solved and the average service time and the service utilization factor are analyzed in the non-saturated mode. Such a model for heterogeneous devices under non-saturated mode incorporating both contention

access period and contention-free period is novel in the literature. The analysis is validated by simulations using Network Simulator (NS) version 2.33. Also, the model is enhanced with a wireless propagation model and the performance of the MAC is evaluated in a wheelchair body-area sensor network scenario.

1.7.3 Improving Performance of the IEEE 802.15.4-Based Hybrid CSMA/CA-TDMA Scheme

In the IEEE 802.15.4 MAC-based hybrid CSMA/CA-TDMA scheme, a limited number of guaranteed time slots (i.e., TDMA slots) are available for time-critical or delay-sensitive data transmission. The semi-static slot allocation in the IEEE 802.15.4 standard results in wastage of bandwidth. In **Chapter 4**, we propose a GTS allocation scheme to improve reliability and bandwidth utilization in the IEEE 802.15.4-based wireless body area sensor networks (WiBASe-Nets). A knapsack problem is formulated to obtain optimal GTS allocation such that a minimum bandwidth requirement is satisfied for the sensor devices. This model is applicable to the network consisting of heterogeneous traffics. Simulation results show that the proposed scheme can achieve better GTS utilization and higher packet delivery ratio than the standard IEEE 802.15.4 scheme does.

1.7.4 Improving Performance of the Sensor Devices Under Uncertainty in the Queue Length in the Hybrid CSMA/CA-TDMA Scheme

In **Chapter 5**, we propose a dynamic queue-length-based time slot allocation scheme to improve channel utilization considering the uncertainty in queue length information. Due to the lack of a dedicated control channel from a device to the coordinator, the queue length in a device can be reported to the coordinator only in an intermittent manner. Arrival of traffic might follow a certain distribution. Therefore, queue length information received by the coordinator might not be the latest one at the time of slot allocation to the devices. To overcome this difficulty, the proposed scheme calculates the probability mass function (*pmf*) of the queue length and allocates slots during the TDMA period based on this *pmf*. The simulation results show that the proposed slot

allocation scheme outperforms the time slot allocation scheme which does not take into account the distribution of the queue length.

1.7.5 Mitigating the Hidden Node Collision Using the Hybrid CSMA/CA-TDMA Scheme

The hybrid CSMA/CA-TDMA channel access scheme can also be used to mitigate the hidden node collision problem in multihop wireless sensor networks. The RTS/CTS (Request to Send/Clear to Send)-based handshaking mechanism is not effective to solve this problem in multihop networks. Also, such a handshaking mechanism is not used in the IEEE 802.15.4-based networks in order to reduce energy consumption. Spatial scheduling of nodes is a classical approach to solve the hidden node problem. In **Chapter 6**, we apply this scheduling concept and present a network planning model to mitigate this problem without any control overhead by structuring a wireless wireless network in a cellular layout. The devices which are in the same cell are allocated the same time slot. These devices use the CSMA/CA protocol to transmit packet during the allocated slot. For this network model, we derive the required distance between a sender and a receiver so that the minimum required signal-to-interference ratio (SIR) at the receiver can be guaranteed in the worst-case scenario. We also present an analysis to estimate network size for given traffic under distance-dependent signal attenuation.

Chapter 2

Distributed and Centralized Channel Access Schemes

2.1 Introduction

Hybrid carrier-sense multiple access with collision avoidance (CSMA/CA) and time-division multiple access (TDMA) protocols such as the IEEE 802.15.4 standard-based medium access control (MAC) protocol [6] are useful in realizing low-power and low-rate wireless networks. TDMA is a collision-free channel access mechanism whereas CSMA/CA is a contention-based MAC protocol. TDMA is desirable to reduce collisions and to conserve power for channel access. However, CSMA/CA could be used by the wireless nodes to send the channel access request. In a hybrid CSMA/CA-TDMA-based wireless network with beacon-enabled mode (e.g., IEEE 802.15.4 network), wireless nodes synchronize their superframes with the coordinator by the help of a beacon frame.

The CSMA/CA operation requires a node to perform carrier sensing to make sure that the channel is free for transmission. The node competes with other nodes during contention access period (CAP) to get access to the channel and transmit packets to the coordinator using the CSMA/CA mechanism. On the other hand, a node can transmit packets in a collision-free manner using TDMA slots during contention-free period (CFP) without using any carrier-sensing mechanism. Whenever a node requires a certain guaranteed bandwidth for transmission, the node sends a reservation request for TDMA slot by using CSMA/CA during CAP. Upon receiving the request, the coordinator first checks the availability of the TDMA slots and it informs the node of the allocation of the TDMA slot. When a TDMA slot is allocated, the node

can turn off its receiver circuitry during CAP and go to low power mode to save its limited battery power. Transmission using TDMA slot also reduces congestion during CAP. Although reservation-based TDMA provides collision-free transmission, a node has to transmit the reservation request successfully during CAP. Some disadvantages of using only TDMA slot-based transmissions are: i) due to the fixed frame length, the packet transmission delay increases with increasing frame length (i.e., beacon interval), ii) the channel is under-utilized when traffic demand is low, and iii) when traffic demand is high, there is only fixed amount of allocated bandwidth (or limited number of TDMA slots).

Transmissions using CSMA/CA during CAP can avoid some of the above mentioned problems of the TDMA slot-based transmissions; however, only with CAP, packet transmission requirements (e.g., throughput, energy efficiency) may not be satisfied, especially when the network is congested. For transmissions during CAP, since the nodes compete with each other to get access to the channel, the network gets congested as the network size grows. Congestion drives the network into saturation worsening the performance in terms of latency and energy-consumption. In such a scenario, the nodes may have to take multiple backoffs before attempting their transmissions. Congestion may occur during CAP even when the total packet arrival rate into the network does not exceed the flow capacity of the contention period. Hidden node collision, which is a common problem in CSMA/CA-based wireless networks, also affects packet transmissions during CAP. An increased number of collisions results in an increase in the number of retransmissions and hence leads to reduced packet service rate. In a similar manner, signal attenuation due to channel fading as well as interference may lead to increased congestion in the network. The channel access scheme in the network should therefore be able to adapt to the network dynamics and perform efficiently in congestion scenarios. In particular, dynamic switching between the transmission modes using CAP and CFP would be desirable to achieve a superior channel access performance [16].

In this chapter, we model and analyze distributed and centralized channel access schemes that use both contention and contention-free accesses to cope with the above mentioned problems. For both of these schemes, to determine the strategy for data transmissions during a superframe, we formulate Markov Decision Process

(MDP) [17] models to decide whether to *transmit using contention period*, or *transmit using contention free period*, or *both*, or *not to transmit at all*. This work provides a method of changing the legacy CSMA/CA scheme to a hybrid CSMA/CA-TDMA scheme and improving the channel access performance of the nodes while preserving the scalability property of CSMA/CA. The novelty of the proposed channel access schemes is that they incorporate the notion of optimality in channel access considering the properties of both CSMA/CA and TDMA. The main contributions of this chapter can be summarized as follows:

- For low-power hybrid CSMA/CA-TDMA MAC protocol, we develop an MDP-based Distributed Channel Access (MDCA) scheme, which considers both the throughput and the energy consumption of the wireless nodes. In this scheme, a node is unaware of the traffic loads of the other nodes in the network and the coordinator does not require any information from the nodes. This scheme provides an improved TDMA slot utilization over the scheme proposed by Shrestha et al. [18].
- We develop an MDP-based Centralized Channel Access (MCCA) scheme, which improves the energy consumption rate compared to the existing hybrid CSMA/CA-TDMA schemes. However, it requires the traffic information of all the nodes available at the central controller and more computational efforts. This scheme stands as the benchmark for a hybrid CSMA/CA-TDMA scheme.
- We extend the models to consider the effect of channel fading.
- We provide a comprehensive performance evaluation of the proposed channel access schemes and comparison with the traditional channel access schemes.

We discuss the related work in Section 2.2. In Section 2.3, we describe the system model and assumptions and also introduce the proposed MDP-based MAC schemes. In Section 2.4, we formulate the MDP problem for the distributed channel access scheme. In Section 2.5, we present the MDP-based centralized channel access scheme. We analyze the effect of hidden node collision in Section 2.6. In Section 2.7, we present the performance evaluation results for the proposed channel access schemes. Section 2.8 summarizes the chapter. Table 2.1 lists the major notations used in this chapter.

2.2 Related Work

One of the pioneering works that deals with switching between contention access and contention free (i.e., TDMA) access was presented by Liu and Wu [16]. The model, which is designed for optical networks, switches contention access to contention free access when collision rate is high. Another related work can be found in [19] where each node in the network randomly selects a favored slot from the next window of slots. Some other work on hybrid MAC include those in [20], [21] and [10]. In the work by Cheng and Wu [20], the access point polls a node and the polled node transmits without contention while the rest of the nodes start the contention process. This method is not energy-efficient since the nodes have to overhear every packet. The model presented by Liu et al. [21] offers contention access, scheduled time-division multiple access (TDMA), and polling-based TDMA. Based on channel status and traffic request, the coordinator maintains the size of contention period and slot allocations. Rhee et al. [10] proposed the concept of hybrid CSMA/CA and TDMA schemes in static TDMA-based wireless networks. The nodes in the network are allocated conflict-free TDMA slots. If the slot owner has no packet to transmit, then non-slot owners compete to get access to the slot using CSMA/CA. Wang et al. [22] presented an improvement on the local framing scheduling model of [10]. Rana et al. [23] considered bandwidth-aware TDMA slot allocation. Because of their static nature, these models have scalability problem. The performance of the hybrid MAC protocol in the IEEE 802.15.4 standard [6] has been analyzed in the literature [24], [25]. Shrestha et al. [24] presented a general discrete-time Markov chain model taking into account the CSMA/CA and GTS-based transmissions together in a heterogeneous traffic scenario and non-saturated condition. Sheu et al. [25] used GTS to cope with the hidden node collision problem in the IEEE 802.15.4-based personal-area networks. Zhang et al. [26] analyzed the performance of contention/reservation interleaved hybrid MAC using soft reservation where owner can release the unused reserved time.

Some work in the literature dealt with sleeping mechanisms in the IEEE 802.15.4 MAC [27], [28], [29]. Jurdak et al. [27] implemented the IEEE 802.15.4-based RFID nodes considering only the non-beacon enabled mode. To save energy, such a node stays in sleep mode until it has data to transmit or the RFID tag is triggered to

receive data. Khanafe et al. [28], to save energy, proposed a strategy to force the nodes to go to sleep mode after each successful transmission. This strategy also helps reduce collision during CAP. Xiao et al. [29] presented a Markov-based model taking into account the sleep mechanism of the IEEE 802.15.4. All of these work focused only on contention-based channel access.

The use of contention access and TDMA access can be also optimized to enhance the performance (in terms of throughput and/or delay and/or energy) of the network. Shrestha et al. [30] presented a knapsack model taking into account the bandwidth demand from nodes to allocate the guaranteed time slots to improve the throughput performance in the IEEE 802.15.4 networks. Shrestha et al. [18] presented a Markov decision process model to make the best use of CSMA/CA and guaranteed time slots to enhance the throughput and energy performance of the IEEE 802.15.4 networks. However, the problem of under-utilization of TDMA slots degrades the network performance.

Some work (e.g., [31], [32]) considered the queue length-based TDMA slot allocation scheme to enhance the throughput and energy performance of hybrid random access and TDMA-based networks. In the model presented by Gilani et al. [31], the coordinator allocates slots to the nodes according to their queue lengths to improve the throughput and energy efficiency performance in the IEEE 802.15.4 networks. Similarly, in the model presented by Zhuo et al. [32], the coordinator takes the queue lengths of nodes as the indicator of traffic. The allocation of slots in these work is similar to that of longest queue first (LQF) scheduling method which is considered to be throughput maximal [33].

In the literature, MDP-based models have been used for optimizing channel access in a wireless network [34], [35], [36], and [37]. Seyedi and Sikdar [34] developed an MDP model for wireless body-area sensor networks to balance the tradeoff between energy consumption and packet error rate. Liu and Elhanany [35] presented a reinforcement learning-based solution for the MDP model to maximize the throughput and energy-efficiency in a wireless sensor network. Angen and Fine [36] considered the slotted ALOHA random access protocol and proposed an MDP model to take the optimal action. Based on the state (i.e., idle or backlogged), users choose their optimal transmit power and retransmission probability at the beginning of each time

slot. The model was also extended for the general case where users do not have the information about the backlogged users. Phan et al. [37] developed an MDP model for the transmission strategy of users in the IEEE 802.11 MAC-based wireless sensor networks. Using MDP, the users decide whether to transmit or defer transmission depending on the state (i.e., channel state, idle or active state of node) to minimize energy-consumption and frame error rate. Mastronarde and Schaar [38] presented a post-decision state to cope with unknown traffic and channel condition in the network.

To the best of our knowledge, the problem efficient channel access in a hybrid CSMA/CA-TDMA framework considering energy consumption, packet delivery ratio, the hidden node collision problem as well as traffic heterogeneity has not been addressed in the literature. The MDP-based transmission strategies presented in this work consider the above aspects and handle congestion in the network in a way to improve the channel access performance in terms of packet delivery ratio and energy consumption.

2.3 System Model, Assumptions, and the Hybrid CSMA/CA-TDMA Schemes

2.3.1 Network Model

We consider a star network topology with N nodes and a network coordinator. A node is indexed by n $(= 1, \cdots, N)$. Each node is within the carrier-sensing range of the other nodes when statistical variation in the channel propagation condition is not considered. Time is divided into superframes each of which has a contention period of T_{sf} unit backoff period (UBP) plus a beacon frame of length T_{beacon} UBP. The contention period (i.e., the superframe duration excluding beacon frame) is divided into K slots and the length of each slot is T_{slot} UBP (i.e., $T_{sf} = KT_{slot}$) as shown in Figure 2.1. A node can transmit η packets during a TDMA slot. The superframe structure, which is similar to the standard IEEE 802.15.4 superframe structure, is shown in Figure 2.1. The coordinator uses T_{beacon} UBP of the superframe to broadcast the beacon frame. Let M be the number of slots during CFP. The length of the CAP available for the nodes is $T_{cap} = T_{sf} - MT_{slot}$ UBP and the length of CFP

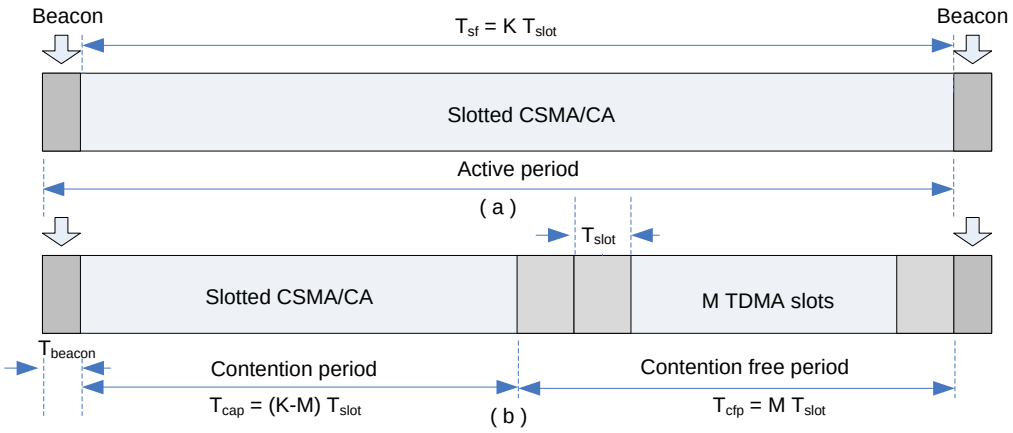

Figure 2.1. *Superframe structure: (a) with CFP length = 0, (b) with CFP length = M slots.*

is $T_{cfp} = MT_{slot}$ UBP. A node uses the slotted CSMA/CA protocol to access the medium during the CAP, while a node can only transmit on an assigned TDMA slot during the CFP. We refer to [6] for the detailed operation of the slotted CSMA/CA. Note that when $M = 0$, nodes use only CSMA/CA for data transmissions. When $M = K$, the length of CAP is zero and the nodes transmit only in the assigned TDMA slots. In addition to CAP and CFP, an inactivity period can also be introduced in the superframe as in the IEEE 802.15.4 MAC. Note that with duty cycling and multiple coordinators, this model can be extended to multihop networks. However, in this work, we focus only on single-hop networks and consider only the active period in a superframe t which starts at $(T_{sf} + T_{beacon})t$.

2.3.2 Traffic Model

In this section, we explain the traffic model for a node. Each node has a packet buffer. The maximum length of the buffer for node n is denoted by $B_{max,n}$. As described by Shrestha et al. [39], we consider the batch Poisson process as the packet arrival model for a node. The packets arrived before the start of superframe t keep waiting until they are placed in the packet buffer at the end of superframe $t-1$. The packets are discarded if the packet buffer is full. The arrival time and the number of packets of the j^{th} batch at node n are denoted by $Y_{n,j}$ and $Z_{n,j}$, respectively. For node n, the inter

arrival time between batches, $Y_{n,j+1} - Y_{n,j}$, is exponentially distributed with mean $1/\lambda_n$. The number of packets in each batch, $Z_{n,j}$, is identically and independently distributed. The pmf of $Z_{n,j}$ is denoted by f_n^Z.

We define $X_{n,\Gamma}$ as the number of arrived packets at node n during a time interval the length of which is Γ. Since the packet arrival model is a batch Poisson process, $X_{n,\Gamma}$ follows the compound Poisson distribution [40]. Therefore, the characteristic function of $X_{n,\Gamma}$ for $\tau \in \mathbb{R}$ is given as

$$\varphi_{n,\Gamma}^X(\tau) = \mathbb{E}[\exp(i\tau X_{n,\Gamma})] = \exp\{\lambda_n \Gamma(\varphi_n^Z(\tau) - 1)\} \tag{2.1}$$

where $\varphi_n^Z(\tau)$ is the characteristic function of $Z_{n,j}$ such that $\varphi_n^Z(\tau) = \mathbb{E}[\exp(i\tau Z_{n,j})] = \sum_z \exp(i\tau z) f_n^Z(z)$. The pmf of $X_{n,\Gamma}$, denoted by $f_{n,\Gamma}^X$, can be derived from $\varphi_{n,\Gamma}^X$ by using the inverse formula for the characteristic function.

2.3.3 Operation of Nodes

We define $\pi_{N,K,M}^*$ as the transmission policy for each node when the network size is N, the superframe length is K slots, and the length of CFP is M slots ($T_{cap} = MT_{slot}$UBP). Then length of CAP is $K - M$ slots ($T_{cap} = (K - M)T_{slot}$ UBP). The policy can be determined by solving the MDP problem to be described later in this chapter. The policy $\pi_{N,K,M}^*$ maps the current state (i.e., the current buffer level B) to an action A (i.e. $B \rightarrow A$). According to the policy, in each superframe, based on its current packet buffer level, a node selects an action out of the following four actions: *defer transmission* (a_1), *transmit packet during CAP* (a_2), *transmit packet during CFP* (a_3), and *transmit packet during both CAP and CFP* (a_4).

2.3.3.1 MDCA scheme

In this scheme, the coordinator divides the superframe into a fixed-size CFP (M slots) and a fixed-size CAP ($K - M$ slots). Each node receives a beacon at the beginning of the superframe t and obtains the information such as the network size N, the length of CAP ($K - M$ slots), and the length of CFP (M slots). Note that some or all of the M slots in CFP might be occupied or empty. From this information, each node distributedly determines the policy $\pi_{N,K,M}^*$. Let $G_{t,n}$ denote a TDMA slot indicator for node n in superframe t. If node n is allocated a slot in superframe t, we have

$G_{t,n} = 1$; and otherwise $G_{t,n} = 0$. According to the policy $\pi^*_{N,K,M}$ and the TDMA slot indicator $G_{t,n}$, node n performs the following operations (i.e., $(B, G) \rightarrow A$).

If $A_{t,n} = a_1$ (defer transmission) and $G_{t,n} = 0$, node n does nothing but waits for the next beacon frame. If $A_{t,n} = a_2$ (transmit packet during CAP) and $G_{t,n} = 0$, node n tries to transmit packets by using slotted CSMA/CA during the CAP in superframe t. If there is not enough time to transmit a packet during the current CAP, node n waits until the next beacon frame. If it has no packet to transmit, it does not need to receive any unwanted packet until the superframe period ends. In the case that $A_{t,n} = a_1$ (defer transmission) or $A_{t,n} = a_2$ (transmit packet during CAP) when $G_{t,n} = 1$, node n has to empty the slot by sending a packet with the TDMA slot de-allocation request bit set during allocated time slot in CFP.

If $A_{t,n} = a_3$ (transmit packet during CFP) and $G_{t,n} = 1$, it transmits only in the assigned TDMA slot. If no TDMA slot has been assigned to node n ($G_{t,n} = 0$), in the case that $A_{t,n} = a_3$, node n sets the TDMA slot request bit in the data packet and transmits the packet by using the slotted CSMA/CA in the CAP. If at least one TDMA slot among M slots is available, the coordinator assigns a TDMA slot to node n and notifies node n of the assigned slot number in the acknowledgment packet. If node n is notified of the assigned TDMA slot in the acknowledgment packet, the node halts the transmission during the CAP and resumes the transmission in the assigned slot during CFP in the same superframe. Otherwise, the node continues to transmit by using the slotted CSMA/CA scheme as long as there is enough time left in the CAP.

If $A_{t,n} = a_4$ (transmit packet during both CAP and CFP), $G_{t,n} = 1$ and $B_{t,n} = b$, node n attempts to transmit $\max(b - \eta, 0)$ packets using CSMA/CA during CAP and transmits $\min(\eta, b)$ packets during the assigned TDMA slot in the CFP. If a slot has not been assigned ($G_{t,n} = 0$), node n follows the similar procedure as described for action $A_{t,n} = a_3$ to send the TDMA slot request.

Note that the MDCA scheme requires contention period long enough to send the request successfully. If T_{tx} denotes the packet transmission time including acknowledgment, inter frame space, and propagation time, then contention period of at least NT_{tx} would be desirable for the MDCA scheme. To prevent the starvation of other nodes in accessing the TDMA slots, a node leaves the assigned TDMA slot after

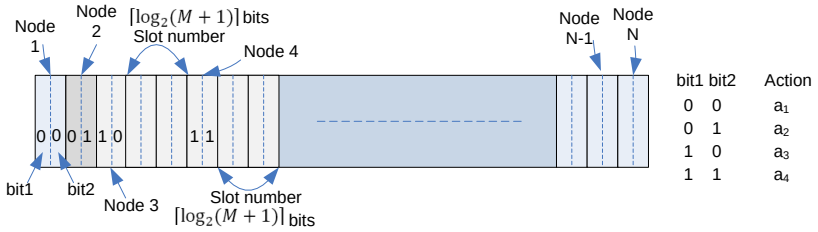

Figure 2.2. *Format of actions and TDMA slot numbers of N nodes in the MCCA scheme.*

using it for a predefined number (ϱ) of consecutive superframes. Since the policy is developed offline, complexity is not a big issue for the nodes.

2.3.3.2 MCCA scheme

In this scheme, the coordinator divides the superframe into a CFP the length of which is $M(0 \leq M \leq M_{max})$ slots, and a CAP the length of which is $K - M$ slots. Note that M slots are allocated to the needy nodes according to a policy and M_{max} is the maximum number of slots available for CFP in this case. With the MCCA scheme, it is assumed that the coordinator has the information of packet arrival rates and buffer levels of all the nodes associated with it. The information of the packet arrival rate can be sent to the coordinator during the node association phase. The coordinator receives the value of the buffer level each time a data packet is received from the node because the information of buffer level is piggybacked by the data packet. For given K and M, the coordinator determines the transmission policy $\pi^*_{N,K,M}$ for each node to reduce the overall energy consumption. For observed buffer level $\mathbf{B}_t$ of N nodes, the coordinator then broadcasts the policy (i.e., action to be taken by each node ($\mathbf{B} \rightarrow \mathbf{A}$)) through the beacon frame. The beacon frame includes the list of actions of N nodes in a format shown in Figure 2.2. The actions a_3 and a_4 are followed by the TDMA slot numbers. Although this scheme can provide a better performance than the MDCA scheme, the complexity grows exponentially with the network size. Therefore, for this approach, we propose an approximate solution to find the transmission policies.

2.3.4 Beacon Loss and Change in Network Size

When a node misses the beacon frame in a superframe t, in the case of MDCA scheme, the node calculates the lengths of the CAP and CFP from the last received beacon frame and uses the CSMA/CA scheme to transmit packets during the CAP. If collision occurs more than once, the node waits for the next beacon frame. The node also uses the slotted CSMA/CA to transmit packets during the assigned TDMA slot in the CFP if the node has not sent any de-allocation request in the last superframe. In case of a collision, the node waits for the next beacon frame. However, with the MCCA scheme, since the node will miss the transmission policy broadcast from the coordinator, it will attempt to access the channel during the CAP. This might cause increased congestion during the CAP and/or wastage of the TDMA slot in superframe t in case the policy has been changed. Throughout this chapter we assume that there is no beacon loss in the network.

When a node joins or leaves the network (e.g., network consisting of energy harvesting sensor nodes or mobile nodes), the network coordinator updates the size of network N. For example, a node can be considered dead if the coordinator does not receive any packets from the node for a predefined number of consecutive superframes. The new node sends the association request to the coordinator using slotted CSMA/CA during CAP. In the MDCA scheme, a node determines the policy $\pi^*_{N,K,M}$ based on N. Note that N is obtained through the beacon frame. In the case of the MCCA scheme, the coordinator takes into account the current network size N to determine the transmission policy.

2.3.5 An Analytical Model of Slotted CSMA/CA

In the design of MDCA and MCCA schemes, the throughput in saturation mode is taken into account because each node assumes that the other $N-1$ nodes have packets to transmit during the superframe period. Therefore, in this section, we calculate the throughput (Φ_{cap}) of the nodes during CAP by including the probability of channel outage (Θ) which induces congestion in the network [24]. Each node in the network uses slotted CSMA/CA as defined in the IEEE 802.15.4 standard-based MAC protocol [6] during the CAP. The parameters, namely, α (i.e., the probability of channel being idle during first carrier sensing), β (i.e., the probability of the channel

being idle during second carrier sensing given that the channel was idle during first carrier sensing), and Φ_{cap} (i.e., MAC throughput) depend on the congestion in the network (e.g., the number of nodes N in the network and the CAP length which is T_{cap} UBP). We refer to [41], [42] for the details of solving a discrete-time Markov chain model and finding the parameters in the saturation mode (i.e., when all the nodes have packets to transmit). We consider retransmission due to collision same as retransmission due to outage. Taking the effects of both collision and channel outage into account, the probability of error ($\widetilde{P}_c$) is defined as follows:

$$\widetilde{P}_c = P_c(1 - \Theta) + \Theta \tag{2.2}$$

We solve the discrete-time Markov chain model using the probability of collision in (2.2). We define $\hat{P}_{cs}$ as the virtual probability of carrier-sensing due to outage probability as follows:

$$\hat{P}_{cs} = 1 - (1 - \widetilde{P}_c)^{\frac{1}{N-1}}. \tag{2.3}$$

Then, the MAC goodput (κ) is expressed in terms of $\hat{P}_{cs}$ as

$$\kappa = \alpha\beta P_{cs}(1 - \hat{P}_{cs})^{N-1} \tag{2.4}$$

where the probability of carrier-sensing (P_{cs}) is determined by solving the discrete-time Markov chain model. As defined by Park et al. [42], the probability of packets being discarded due to the limit on the maximum number of backoff ($P_{discard}$) is given as

$$P_{discard} = \phi^{m+1} \frac{1 - (\widetilde{P}_c(1 - \phi^{m+1}))^{W+1}}{1 - \widetilde{P}_c(1 - \phi^{m+1})} \tag{2.5}$$

in which m is the maximum number of backoffs allowed for a transmission, W is the maximum number of retransmissions allowed before a packet is dropped, and $\phi = (1 - \alpha\beta)(1 - P_d)$ is the probability of going to another backoff stage due to channel being busy given that the packet is not deferred. A packet is deferred when there is not enough time left in the current superframe to transmit a packet. The probability that transmission of a packet is deferred is $P_d = \frac{T_{tx}}{T_{cap}}$, where T_{tx} is the packet length (in time) including acknowledgment wait time and propagation time.

The probability of packet dropping due to maximum number of retransmission (P_{drop}) is simply $P_{drop} = \widetilde{P}_c^{W+1}$. Then the MAC throughput Φ_{cap} is estimated as

$$\Phi_{cap} = \frac{\kappa}{(1 - P_{discard})(1 - P_{drop})} T_{cap} \tag{2.6}$$

where T_{cap} is the contention access period in terms of number of backoff units.

By MATLAB simulations, we observe the variation in throughput of the hybrid MAC in the beacon-enabled mode with respect to the probability of channel outage. In these simulations, superframe length of $T_{sf} = 384$ unit backoff period (UBP), and zero inactive and contention-free periods. We consider packet length $T_{tx} = 10$ UBP including acknowledgment wait time and propagation time. We assume that the nodes start random backoff before starting carrier sensing. In the simulation, to determine Φ_{cap}, we count the average number of packets per superframe that the nodes accept at the MAC layer. Then we calculate goodput $\kappa = \Phi_{cap}(1 - P_{discard})(1 - P_{drop})/T_{sf}$, which is marked as 'Estimated' in Figure 2.3. To estimate goodput κ directly, we also count the average number of packets transmitted successfully, which is marked as 'Simulation' in the figure. Figure 2.3 shows that the results on estimated and the analytical throughput during CAP follow the simulation results. The small gap in the curves is due to the deferred transmissions. Note that lower the number of nodes, higher the packet arrival rate in the saturation region and higher is the probability of deferred transmission of each node.

In the case of heterogeneous nodes (i.e., when the traffic and the MAC parameters are non-identical for the different nodes), we calculate the values of $P_{cs,n}$, α_n, and β_n, $\forall n \in \{1, 2, \cdots, N\}$ for the IEEE 802.15.4 MAC using a discrete-time Markov chain model. For the details of the model and the derivations, which are not provided in this chapter, we refer to [41], [24], and [43]. The probability of collision $P_{c,n} = 1 - \prod_{\substack{j=1 \\ j \neq n}}^{N} (1 - P_{cs,j})$ is the probability that at least one among $N - 1$ nodes starts carrier sensing in the CAP. The throughput, when N nodes are active, is given as $\Phi_{n|N} = \alpha_n \beta_n P_{cs,n} \prod_{\substack{j=1 \\ j \neq n}}^{N} (1 - P_{cs,j})$.

2.3.6 Compatibility to the IEEE 802.15.4 Standard

The superframe structure for the proposed models is similar to the standard IEEE 802.15.4 superframe structure [6] as shown in Figure 2.1. The IEEE 802.15.4 standard

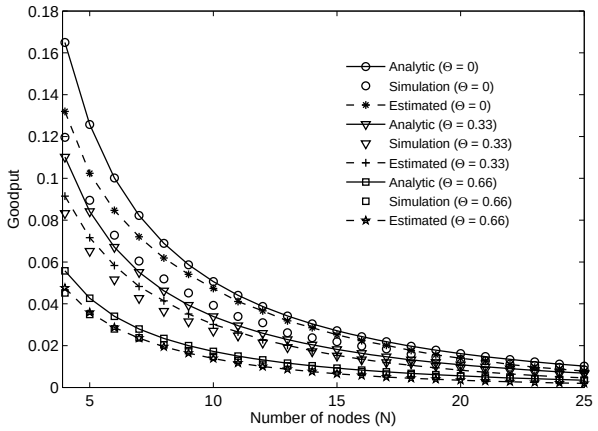

Figure 2.3. *Saturation throughput for different values of channel outage probabilities.*

MAC can be considered to be a special case of the proposed models (i.e., $M = 7$ and each node is allowed to use a slot at maximum in a superframe). The coordinator can assign an index number ($n = 1, 2, \cdots, N$) to the associated node. In the MCCA scheme, the guaranteed time slot (GTS) list field of the beacon frame in the IEEE 802.15.4 can be modified to include the actions and assigned TDMA slot numbers in a format shown in Figure 2.2.

In the MDCA scheme, we assume that each packet contains two bits of overhead. The first bit is set if a TDMA slot request is sent and the second bit is set if a TDMA slot de-allocation request is sent. This modification removes the burden of sending separate packet for the TDMA slot request and de-allocation requests. Similarly, the acknowledgment packet consists of few bits ($\lceil \log_2(M+1) \rceil$ bits) of overhead to notify the assigned TDMA slot number. After receiving a TDMA slot request, the coordinator allocates a TDMA slot to a node in a first-come first-served (FCFS) fashion. Note that in the standard, the guaranteed time slot (GTS) is used for time-critical data transmission. In our case, the purpose of using TDMA slots is to reduce network congestion during CAP. Therefore, the proposed MDCA scheme would be compatible to the IEEE 802.15.4 standard MAC if the standard protocol is enhanced to decode the overhead bits in data packet as the GTS request and the GTS-deallocation request, and the overhead bits in acknowledgment packet as notification

of TDMA slot allocation.

2.4 MDP-Based Distributed Channel Access (MDCA) Model

In this section, we want to determine which action is best when a node has packet buffer level b under condition that number of nodes in the network is N, the length of CAP is $K - M$ slots and the length of CFP is M. We call this as a policy $\pi_{N,K,M}$ of a node. We define a set of actions that a node takes in each superframe as $\Lambda = \{a_1, a_2, a_3, a_4\}$, where

- a_1: go to low power mode (no transmission)
- a_2: transmit data packets during CAP
- a_3: transmit data packets during CFP
- a_4: transmit data packets during CAP and CFP.

Let state of node n at superframe t is defined as $S_{t,n} = B_{t,n}$, where $B_{t,n}$ is the buffer state. The buffer state $B_{t,n}$ is defined as the number of packets in the buffer of node n at superframe t, such that $B_{t,n} \in \{0, 1, \ldots, B_{max}\}$, where B_{max} is the the maximum value of the buffer state. New packets are discarded if the buffer is full. At each buffer state of node n at superframe t, node n takes one of the actions denoted as $A_{t,n} \in \Lambda$. To realize it, we assume that M slots are randomly assigned to N nodes. Note that if all nodes take action a_2, the CAP becomes congested while CFP remains unoccupied. Similarly, if all nodes take action a_3, the CAP remains unoccupied whereas the TDMA slots in CFP become congested given $M < N$. To balance the use of CAP and CFP, we formulate the problem of decision making on packet transmissions during CAP or CFP or both, or no transmission at all by using an infinite-horizon Markov Decision Process (MDP). An MDP is described by its states, actions, reward, and transition probabilities.

For distributed channel access, a node assumes that other nodes also have packets to transmit and will compete to get access to the channel during CAP. Therefore, α, β, P_c, and Φ_{cap} are estimated analytically for given T_{cap} and N in the saturated mode (i.e., a node assumes that all other nodes in the network have packets to send) [41].

We develop the transmission policy for the nodes for given T_{cap}, N, and packet arrival rate λ at the saturation region by solving the infinite-horizon MDP problem.

In the MDCA scheme, we focus on the operation of one node. Therefore, we omit the node index n from all the notations. For example, the buffer state is denoted by B_t instead of $B_{t,n}$.

2.4.1 Reward

Let $R_{s,a}$ be the reward that a node receives for taking action $A_t = a$ at state $S_t = s$ at a superframe t. If a node defers the transmission, it saves energy but its buffer level may remain the same or increase. When the node transmits during both CAP and CFP, its throughput increases but it consumes a significant amount of energy. The reward function considers both the benefit and the cost of using the access method. We want to develop a policy which reduces the energy consumption without degrading throughput performance. For this purpose, we define the expected reward for taking action a at state s as

$$R_{s,a} = \frac{\mu_{s,a} - s}{\max(s,1)} - \frac{\Xi_{s,a}}{\Xi_{max}} + C_{s,a} \tag{2.7}$$

where $\mu_{s,a}$, $\Xi_{s,a}$ and $C_{s,a}$ are the MAC throughput (number of packets retrieved out of the MAC buffer), energy consumed and bandwidth cost, respectively, for taking action a at state s and Ξ_{max} is maximum energy consumed. Note that, the purpose of relative throughput with respect to buffer level is to discourage the nodes refraining from transmission to save energy. The reason of using the ratio in the reward function is to normalize the values with the highest value being zero.

Let Ξ_x denote the energy required to transmit a packet and let Ξ_c denote the energy required to perform carrier sensing. The total amount of energy required to transmit a packet during the CAP is given by

$$\Xi_p = \frac{1 - P_c^{W+1}}{1 - P_c}\Xi_x + \frac{1 - P_c^{W+1}}{1 - P_c}\frac{1 - \phi^{m+1}}{1 - \phi}\Xi_c \tag{2.8}$$

where $\phi = (1 - \alpha\beta)(1 - P_d)$ is the probability of going to another backoff stage with P_d being the probability of transmission being deferred, m is the maximum number of backoffs allowed, and W is the number of retransmissions allowed. The amount of

energy consumed for taking action a at state s is

$$\Xi_{s,a} = \begin{cases} \min(\kappa, s)\Xi_p, \text{if } \ a = a_2 \\ \min(\eta, s) \times (2\Xi_x), \text{if } \ a = a_3 \\ \min(\kappa, \max(s-\eta, 0))\Xi_p + \min(\eta, s) \times (2\Xi_x), \text{ if } \ a = a_4 \\ 0, \text{otherwise} \end{cases}$$

where κ is the goodput expressed in number of packets per superframe. The MAC throughput depends on action a taken at state s and is expressed as

$$\mu_{s,a} = \begin{cases} \min(\Phi_{cap}, s), \text{if } \ a = a_2 \\ \min(\eta, s), \text{if } \ a = a_3 \\ \min(\Phi_{cap}, \max(s-\eta, 0)) + \min(\eta, s), \text{if } \ a = a_4 \\ 0, \text{otherwise.} \end{cases}$$

In the above equation, for the purpose of calculation of relative energy, we set $\Xi_{max} = s\Xi_p$. The bandwidth cost $C_{s,a}$ is high when a node occupies a TDMA slot during CFP even when it has no packet to transmit (i.e., $s = 0$). We define $C_{s,a}$ as follows:

$$C_{s,a} = \begin{cases} -1, & \text{if } \ s = 0 \ \text{ and } \ a \in \{a_3, a_4\} \\ -0.5, & \text{if } \ s = 1 \ \text{ and } \ a \in \{a_3, a_4\} \\ 0, & \text{otherwise.} \end{cases}$$

2.4.2 State Transition Probability

When a node is in state $s = b$ during superframe t, the probability of going to state $s' = b'$, when action a is taken, is given by

$$\Pr[S_{t+1} = s' | S_t = s, A_t = a] = \Pr[B_{t+1} = b' | B_t = b, A_t = a]. \tag{2.9}$$

When action a is taken, the probability that the buffer state changes from b to b' is given by the probability of arrival of $x = \lceil b' - b + \mu_{s,a} \rceil$ packets at the beginning of superframe $t + 1$, i.e., the buffer state transition probability

$$\begin{aligned} \Pr[B_{t+1} = b' | B_t = b, A_t = a] &= \Pr\left[\text{arrival of } x \text{ packets}\right] \\ &= \begin{cases} f_\Gamma^X(x), & \text{if } \ x \geq 0 \\ 0, & \text{otherwise} \end{cases} \end{aligned}$$

where $\Gamma = T_{sf} + T_{beacon}$ and f_{Γ}^{X} is the probability mass function of number of packet arrivals X_{Γ}. Similarly, when the next buffer state is B_{max}, $x = \lceil B_{max} - b + \mu_{s,a} \rceil$, and

$$\begin{aligned} \Pr[B_{t+1} = B_{max} | B_t = b, A_t = a] &= \Pr\left[\text{number of packet arrivals} \geq x\right] \\ &= 1 - \sum_{h=0}^{x-1} f_{\Gamma}^{X}(h). \end{aligned}$$

2.4.3 MDP Solution

Let π_s^* be the policy that maps a state s into an action a and V be the value function corresponding to the total expected discounted reward over an infinite horizon. The objective is to maximize the total expected reward. The optimal value function V^* is expressed by the Bellman optimality equation [17] as follows:

$$V_s^* = \max_{a \in \Lambda} \left(R_{s,a} + \gamma \sum_{s' \in \Upsilon} \Pr[S_{t+1} = s' | S_t = s, A_t = a] V_{s'}^* \right) \tag{2.10}$$

for all $s \in \Upsilon$, where Υ is the set of all possible states, $R_{s,a}$ is the expected value of the reward, and $\gamma \in [0, 1)$ is the discount rate. The Bellman equation can be solved by the value iteration method to find V^* [17]. The optimal policy π_s^* for all $s \in \Upsilon$, is given by, $\pi_s^* =$

$$\arg\max_{a \in \Lambda} \left(R_{s,a} + \gamma \sum_{s' \in \Upsilon} \Pr[S_{t+1} = s' | S_t = s, A_t = a] V_{s'}^* \right).$$

The value iteration method requires $(|\Lambda|\,|\Upsilon|^2)$ computations per iteration [44]. Note that the policy iteration method requires fewer number of iterations to find the optimal policy. However, it requires more computations per iteration than the value iteration method. As described by Puterman [17], the value iteration method converges to the optimal solution in a finite number of iterations at a rate of γ if the stopping criterion is $\epsilon \frac{(1-\gamma)}{2\gamma}$ for $\epsilon > 0$.

2.5 MDP-Based Centralized Channel Access (MCCA) Model

2.5.1 MDP Formulation

With the MDCA method, the nodes are unaware of the actions of the other nodes. This suggests that the method can be improved by using a centralized approach. In this section, we present a method in which the coordinator determines the policy based on the buffer status of all the nodes.

We assume that the coordinator has the knowledge of the packet arrival distribution of all the nodes. In this method, the buffer level represents the state of a node. The state of the network is defined as $\mathbf{S}_t = \mathbf{B}_t$, where $\mathbf{B}_t = (B_{t,1}, B_{t,2}, \cdots, B_{t,N})$ denotes the joint buffer state of N nodes during a superframe t and $B_{t,n} \in \{0, 1, \cdots, B_{max}\}$ is the buffer state for node n. Let $\mathbf{A}_t = (A_{t,1}, A_{t,2}, \cdots, A_{t,N})$ denote the joint actions of N nodes, where $A_{t,n} \in \{a_1, a_2, a_3, a_4\}$. Given any state $\mathbf{b} = (b_1, \cdots, b_N)$ and action $\mathbf{a} = (\bar{a}_1, \cdots, \bar{a}_N)$, let $\mathbf{b}' = (b'_1, \cdots, b'_N)$ denote the next joint state. We define the joint reward as $\mathbf{R}_{\mathbf{b},\mathbf{a}} = \sum_{n=1}^{N} R_{b_n,\mathbf{a}}$, where $R_{b_n,\mathbf{a}}$ is the reward for node n. Similar to the MDCA scheme, the reward is given by

$$R_{b_n,\mathbf{a}} = \frac{\mu_{b_n,\mathbf{a}} - b_n}{\lambda} - \frac{\Xi_{b_n,\mathbf{a}}}{\Xi_m} \tag{2.11}$$

where λ is the average number of packet arrivals per superframe duration, $\Xi_m = \Xi_x \eta T_{cap}/T_{slot}$ and $\mu_{b_n,\mathbf{a}}$ is the MAC throughput of the node n when the joint action by all the nodes in the network is $\mathbf{a}$. The transition probability is defined as $\Pr[\mathbf{S}_{t+1} = \mathbf{b}'|\mathbf{S}_t = \mathbf{b}, \mathbf{A}_t = \mathbf{a}] = \prod_{n=1}^{N} \Pr[B_{t+1,n} = b'_i|B_{t,n} = b_n, \mathbf{A}_t = \mathbf{a}]$. Similar to (2.9), the probability that a node n goes to buffer state b'_n from state b_n is given by

$$\Pr[B_{t+1,n} = b'_n|B_{t,n} = b_n, \mathbf{A}_t = \mathbf{a}] = \Pr\left[\text{arrival of } x_n \text{ packets}\right]$$

where $x_n = b'_n - b_n + \mu_{b_n,\mathbf{a}}$.

The coordinator solves the MDP problem and determines the optimal policy for each state. During a superframe, the coordinator observes the buffer level of all nodes to determine the state and broadcast the optimal policy. A node can piggyback the information of buffer level to the coordinator while transmitting data packets. However, this method is not accurate when a node is not able to transmit any packet

successfully during a superframe and packet arrival rate is not deterministic. Specially when packet arrival takes place at the beginning of the superframe, the piggybacked information of the buffer level would be inaccurate. For this reason, the coordinator has to take into account the time of receiving the buffer level information and the average number of packet arrivals during a superframe period.

For each node, the coordinator has to keep the latest buffer level report as well as the index of the frame in which the latest buffer level report was received. In frame t, the coordinator maintains the buffer level information for node n in the form of the tuple $\mathbf{G}_{t,n} = (Q_{t,n}, F_{t,n})$, where $F_{t,n}$ is the number of superframes which have passed after the latest report was received and $Q_{t,n}$ is the buffer level in the latest report of the node n. The coordinator estimates the average buffer level of node n as

$$\bar{Q}_{t,n} = Q_{t,n} + \lfloor \lambda_n F_{t,n} \rfloor . \tag{2.12}$$

The buffer state of a node n is determined as $B_{t,n} = \bar{Q}_{t,n}$ if $\bar{Q}_{t,n} < B_{max}$, otherwise $B_{t,n} = B_{max}$.

2.5.2 Complexity of Solving the MDP Problem

The coordinator finds the optimal policy $\pi^*_{\mathbf{S}}$ for any state $\mathbf{S}$ by solving the Markov decision problem. The coordinator sends the policy information to the nodes through the beacon frame. However, the complexity is huge because of the large dimensions of state and action. For a network of size N, the value iteration method has a computational complexity of $\mathcal{O}(4^N(B_{max}+1)^N)$. Therefore, finding an optimal solution is not practical. We propose an approximate solution in the next section.

2.5.3 Approximate Solution

This solution (the procedure of which is described in **Algorithm 1**) is based on the assumption that nodes with higher buffer occupancy level are unlikely to defer their transmissions and are highly likely to use a TDMA slot in CFP. In the literature, the longest queue first (LQF) scheduling scheme during CFP has been shown to be throughput maximal [33]. Also, instead of letting all the nodes to compete during CAP, some nodes can be put into the low-power mode so that congestion is reduced

during CAP and throughput is improved. In this section, we present a solution which combines the merits of the LQF scheduling scheme and a congestion reduction scheme. In the latter scheme, $N' \leq N$ nodes are allowed to transmit during the CAP such that for given system parameters the saturation throughput is maximized. If M nodes are allocated TDMA slots, then the remaining $N - N' - M$ nodes with relatively lower buffer occupancy levels are put into low power mode (or no transmission mode).

Algorithm 1 Approximate solution for centralized MDP

1: Input: Buffer level at all the nodes $\mathbf{q} = (q_1, q_2, \cdots, q_N)$, number of slots in CFP M
2: Output: $\mathbf{a}$
3: Sort nodes $\mathbf{d} = \{1, 2, \cdots, N\}$ such that $q_n \geq q_{n+1}, \quad \forall n \in \mathbf{d}$
4: for each element $\mathbf{d}_g \in \{\emptyset, \{1\}, \{1,2\}, \cdots, \{1, 2, \cdots, M\}\}$ do
5: for each element $\mathbf{d}_{dg} \in \{\emptyset, \{j\}, \{j, j+1\}, \cdots, \{j, j+1, \cdots, M\}\}$, for $j = |\mathbf{d}_g| + 1$ do
6: for each element $\mathbf{d}_d \in \{\{j, j+1\}, \{j, j+1, j+2\}, \cdots, \{j, j+1, j+2, \cdots, N\}\}$, for $j = |\mathbf{d}_g| + 1$ do
7: Calculate utility $\mathbf{u}_{\mathbf{d}_g, \mathbf{d}_{dg}, \mathbf{d}_d, \mathbf{d}_s} = \sum_{n=1}^{N} (\frac{\mu_n - q_n}{\lambda} - \frac{\Xi_n}{\Xi_{max}})$ where
8: $\mu_n = \min(q_n, \eta)$ and $\Xi_n = \mu_n \Xi_x$ for $n \in \mathbf{d}_g$
9: $\mu_n = \min(q_n, \eta) + \min(\Phi_{cap}, \max(0, q_n - \eta)$ and
$\Xi_n = \min(q_n, \eta)\Xi_x + \min(\kappa, \max(0, q_n - \eta)\Xi_p$ for $n \in \mathbf{d}_{dg}$
10: $\mu_n = \min(\Phi_{cap}, q_n)$ and $\Xi_n = \min(\kappa, q_n)\Xi_p$ for $n \in \mathbf{d}_d$, $n \notin \mathbf{d}_{dg}$
11: $\mu_n = 0$, $\Xi_n = 0$, $\mathbf{d}_s \leftarrow n$ otherwise
12: where throughput Φ_{cap}, κ are calculated for given $|\mathbf{d}_d|$ and M
13: end for
14: end for
15: end for
16: Find $\mathbf{a} = \{\mathbf{d}_g, \mathbf{d}_{dg}, \mathbf{d}_d, \mathbf{d}_s\}$ for $\max \mathbf{u}_{\mathbf{d}_g, \mathbf{d}_{dg}, \mathbf{d}_d, \mathbf{d}_s}$

The coordinator observes the buffer level $\bar{Q}(t, n)$ of the nodes $n \in N$ at the beginning of the superframe t. Note that from (2.12), $\bar{Q}(t, n)$ might be higher than B_{max}. It sorts the nodes in the descending order of their buffer levels. It calculates the utility function (defined in step 7 in **Algorithm 1**) for every combination of the

actions provided that only the first M nodes are allowed to use TDMA slots. The utility function is the same as the reward function presented earlier. The coordinator determines the set of best actions of all the nodes $\mathbf{a}$ that gives the maximum value of the utility function and sends it through the beacon frame. It can memorize the best action vector $\mathbf{a}$ for the given state $\mathbf{S}$ to use it next time. In the algorithm, $\mathbf{d}_s, \mathbf{d}_d, \mathbf{d}_g$, and $\mathbf{d}_{dg}$ are the sets of nodes taking the actions a_1, a_2, a_3, and a_4, respectively.

Let $\mathcal{A}$ be the set of all possible action vectors and $\mathbf{U}$ be the set of all possible utility functions. **Algorithm 1** has a computational complexity of $\mathcal{O}(N\log N + |\mathcal{A}|)$, where $|\mathcal{A}|$ depends on the number of utility functions to be computed at a state $\mathbf{S}$, and is given by

$$\begin{aligned} |\mathcal{A}| &= |\mathbf{U}| \\ &= \sum_{n=1}^{|\mathbf{D}_g|} \sum_{j=1}^{|\mathbf{D}_{dg}|+1-n} \sum_{h=2}^{N+1-n} 1 \\ &= \sum_{n=1}^{|\mathbf{D}_g|} (|\mathbf{D}_{dg}| + 1 - n)(N - n) \end{aligned} \tag{2.13}$$

where $\mathbf{D}_g$ and $\mathbf{D}_{dg}$ are the sets of all possible elements $\mathbf{d}_g$ and $\mathbf{d}_{dg}$, respectively. Suppose $M = 7$, then $|\mathbf{D}_g| = |\mathbf{D}_{dg}| = 8$ and $|\mathcal{A}| = 36N - 120$. The coordinator determines the policy for the nodes at the beginning of each superframe.

2.6 Extension of the Models Considering Channel Fading

In this section, we present a methodology for the calculation of the parameters $(\alpha_n, \beta_n, P_{c,n}\ \forall n \in \{1, 2, \cdots, N\})$ considering channel fading. The key idea to extend the MDP-based models presented earlier by considering the presence of channel fading is to determine the correct parameters and the throughput (Φ_{cap}). It is assumed that channel fading remains the same during packet transmission time.

Due to signal attenuation in the channel, the transmission range is reduced and so is the carrier-sensing range. Due to the reduced transmission range, the network suffers from outage as well as hidden node collision problem. When the received signal level falls below the receiver threshold, the transmission suffers outage because

the receiver cannot decode the signal successfully. For short-range networks such as personal-area networks [24], signal attenuation can be modeled by using distance-dependent attenuation along with log-normal shadowing. If Ω_{tx} is the transmit power in dB, $\ell(\nu_n)$ is the loss (in dB) for transmission from a node n to the coordinator with separation of ν_n, and ζ is the shadowing component with zero mean and standard deviation of σ (e.g., 4.4 dB) [45], then the received power (in dB) is: $\Omega_{rx} = \Omega_{tx} - \ell(\nu_n) - \zeta$. The probability that the received power is less than the receiver threshold ψ dB (i.e., outage probability) is given by

$$\begin{aligned} \Theta_n &= \Pr[\Omega_{rx} < \psi] \\ &= 1 - \frac{1}{2}\text{erfc}\left(-\frac{\Omega_{tx} - \ell(\nu_n) - \psi}{\sqrt{2}\sigma}\right) \end{aligned} \tag{2.14}$$

where erfc() is the complementary error function. An example of the propagation model for signal attenuation [24] that can be considered is $\ell(\nu_n) = 27.6\log(\nu_n[mm]) + 46.5\log(2400[\text{MHz}]) - 157$.

Let ν_{nj} be the distance between node n and node j and ξ be the carrier-sensing threshold in dB. The channel fading of the links $n, j \in N$ are independent. Even though there is no outage in the link between a node and the coordinator, it is probable that the node is hidden to other nodes in the different links. Then, the probability that node n and node j are hidden to each other is

$$H_{n,j} = 1 - \frac{1}{2}\text{erfc}\left(-\frac{\Omega_{tx} - \ell(\nu_{nj}) - \xi}{\sqrt{2}\sigma}\right).$$

Let Ψ_n be the set of $|\Psi_n|$ nodes which are hidden to node n such that $H_{n,j} \neq 0,\ \forall j \in \Psi_n$. When a node n transmits during CAP, the hidden node collision probability is estimated by the probability of channel being busy during first carrier sensing $P_{b,\Psi_n \cup \{n\}} = (1 - \alpha_{n/\Psi_n \cup \{n\}})$ when at least one node from Ψ_n is transmitting among the nodes in the set $\Psi_n \cup \{n\}$ [43]. We denote by $\alpha_{n/\Psi_n \cup \{n\}}$ the probability of channel being idle in the first carrier sensing for node n given the nodes in the set $\Psi_n \cup \{n\}$.

The hidden node collision probability for node n is estimated as

$$H_n = \sum_{j=1}^{|\Psi_n|_1} H_{n,j} \prod_{\substack{h=1 \\ h\neq j}}^{|\Psi_n|} (1-H_{n,h}) P_{b,\{n,j\}} + \tag{2.15}$$

$$\sum_{j=1}^{|\Psi_n|_1} \sum_{\substack{r=1 \\ r\neq j}}^{|\Psi_n|_2} H_{n,j} H_{n,r} \prod_{\substack{h=1 \\ h\neq j,r}}^{|\Psi_n|} (1-H_{n,h}) P_{b,\{n,j,r\}} +$$

$$\cdots + \sum_{j=1}^{|\Psi_n|_1} \sum_{\substack{r=1 \\ r\neq j}}^{|\Psi_i|_2} \cdots \sum_{\substack{l=1 \\ l\neq jr}}^{|\Psi_n|_{|\Psi_n|}} H_{n,j} H_{n,r} \cdots H_{n,l} \prod_{\substack{h=1 \\ h\neq j,\cdots,l}}^{|\Psi_i|} (1-H_{n,h}) P_{b,\{n,j,r,\cdots,l\}} \tag{2.16}$$

For example, if $\Psi_1 = \{3,4\}$, then $H_1 = H_{1,3}(1-H_{1,4})P_{b,13} + H_{1,4}(1-H_{1,3})P_{b,14} + H_{1,3}H_{1,4}P_{b,134}$. As in (2.2), when both the channel fading and hidden node collision are taken into account, the probability of error is calculated as $\hat{P}_{c,n} = (P_{c,n}(1-H_n)+H_n)(1-\Theta_n)+\Theta_n$. In a similar way, we derive $\alpha_{n/\mathbf{d}}$, where $\mathbf{d} = \{1,2,\cdots,N\}$ is the set of N nodes, as follows:

$$\alpha_{n/\mathbf{d}} = \prod_{h=1}^{|\Psi_i|} (1-H_{n,h}) \alpha_{n/\mathbf{d}} + \sum_{j=1}^{|\Psi_n|_1} H_{n,j} \prod_{\substack{h=1 \\ h\neq j}}^{|\Psi_n|} (1-H_{n,h}) \alpha_{n/\mathbf{d}\setminus\{j\}}$$

$$+ \sum_{j=1}^{|\Psi_n|_1} \sum_{\substack{r=1 \\ r\neq j}}^{|\Psi_n|_2} H_{n,j} H_{n,r} \prod_{\substack{h=1 \\ h\neq j,r}}^{|\Psi_n|} (1-H_{n,h}) \alpha_{n/\mathbf{d}\setminus\{j\}\cup\{r\}}$$

$$+ \cdots + \sum_{j=1}^{|\Psi_n|_1} \sum_{\substack{r=1 \\ r\neq j}}^{|\Psi_n|_2} \cdots \sum_{\substack{l=1 \\ l\neq j,r}}^{|\Psi_n|_{|\Psi_n|}} H_{n,j} H_{n,r} \cdots H_{n,l}$$

$$\prod_{\substack{h=1 \\ h\neq j,\cdots,l}}^{|\Psi_i|} (1-H_{n,h}) \alpha_{n/\mathbf{d}\setminus\{j\}\cup\{r\}\cdots\cup\{l\}}. \tag{2.17}$$

Similarly, we derive $\beta_{n/\mathbf{d}}$ for node n. Even though the nodes are homogeneous, their positions lead to heterogeneity in the network. Given $\mathbf{P}_{cs} = \{P_{cs,1},\cdots,P_{cs,N}\}$, we calculate and update $P_{c,n}, \alpha_n, \beta_n, \ \forall n \in \mathbf{d}$ by solving the Markov chain model (see [24] and [43] for the details of the Markov chain model) until $|\mathbf{P}_{cs}^{c+1} - \mathbf{P}_{cs}^{c}| < \delta$ after c iterations, δ is a small positive number. After determining the new parameters considering channel fading, we calculate the CAP throughput $\Phi_{cap,n}$. We also calculate the CFP throughput as $(1-\Theta_n)\min(\eta, b_n)$, where b_n is the buffer level of node n.

However, if each node is considered to be within the carrier-sensing range of the other nodes when the statistical variation in the channel propagation condition is not considered, carrier sensing range is at least double the transmission range and all the links between nodes in the network suffer same channel fading, there will be no effect of hidden node collision on the packet reception at the coordinator. This is because, when the probability of channel outage is zero, the hidden node collision probability also becomes zero. Hidden node collision will occur when there is outage at the coordinator. In this case, the probability of channel outage is sufficient to update the collision probability, i.e., $\hat{P}_{c,n} = (P_{c,n}(1 - \Theta_n) + \Theta_n)$.

2.7 Performance Evaluation

2.7.1 Performance Metrics and Simulation Parameters

For performance evaluation, we simulate the proposed channel access schemes in MATLAB. We consider packet delivery ratio (PDR), end to end delay, and power consumption rate as the performance metrics. The packet delivery ratio (PDR) is defined as the ratio of the number of packets successfully transmitted and number of packets generated by the nodes during the simulation run time. The end to end delay is measured from the time a packet is generated until it is successfully transmitted. The average energy consumed by nodes (including the coordinator) per successfully transmitted packet in the network is considered as the energy consumption rate metric. For performance evaluation, we use the power consumption values for an IEEE 802.15.4 transceiver as follows [46]: power consumption in sleep mode, transmit mode, receive mode, and idle mode is 36 μW, 31.32 mW, 33.84 mW, and 766.8 μW, respectively.

We consider a star network topology consisting of a coordinator and $N = 20$ nodes placed in a circle with a transmission range of 10m and a carrier sensing range of 20m. Each node is within the carrier sensing range of other nodes when channel fading is not considered. Each node transmits packets to the coordinator located at the centre. We assume that the hybrid MAC protocol operates with a physical data rate of 250 Kbps. The smallest unit of time, i.e., the unit backoff period (UBP), is 320μs. Unless otherwise specified, we assume that there is no packet loss due to channel fading. We

set the discount factor γ to 0.9. For the performance evaluation purpose, we set Ξ_x to 1, and Ξ_c to 0.1. We consider the buffer size of $B_{max} = 5$. The newly arrived packets are dropped if the buffer is full. We assume a fixed batch size of length one.

Unless otherwise specified, we consider the physical packet size of 6 UBP (i.e., 60 bytes long), the acknowledgment packet size of 1 UBP and inter-frame space of 1 UBP. Since a packet has to be transmitted at the boundary of the UBP, a successful packet transmission time including propagation time, inter frame space (IFS) and acknowledgment would be $T_{tx} = 10$ UBP. We also consider the beacon frame length to be 4 UBP. We assume that a node can transmit $\eta = 2$ packets per slot duration. To achieve this, we set $K = 16$, $M = 7$ (similar to the superframe structure of the IEEE 802.15.4 MAC standard). The superframe duration is $T_{sf} = 384$ UBP and the length of a slot is $T_{slot} = 24$ UBP. To prevent starvation of nodes from accessing the TDMA slots, we set $\varrho = 18$. In the figures, we define the offered traffic as $\frac{N\lambda T_{tx}}{T_{sf}+T_{beacon}}$. We run the simulations for 5000 beacon intervals.

2.7.2 Simulation Results

In this section, we present the performance evaluation results for the MDCA and MCCA schemes. The superframe is divided into $K = 16$ slots. For slotted CSMA/CA, during contention period ($K - M$ slots), the set of contention window size is $cw \in [8, 16, 32, 32, \cdots]$. Also, the nodes do not drop packets due to limits on the maximum number of backoffs and retransmissions allowed. Note that acknowledgment is also required for the packets that are transmitted during the allocated TDMA slots.

2.7.2.1 Comparison

In the MDCA scheme, the transmission policy is not developed by the coordinator and is completely distributed. Therefore, we compare the MDCA scheme with the slotted CSMA/CA scheme with default parameters of the IEEE 802.15.4 MAC in beacon enabled mode with no CFP (i.e., $M = 0$) and the Contention Control Scheme (CCS) proposed by Francesco et al. [47]. The assumed MAC parameters for CSMA/CA are: $MACMaxBE = 5$, $MACMinBE = 3$, backoff limit $m = 4$, limit on the number of retransmissions $W = 3$. The contention control scheme (CCS) proposed by Francesco et al. [47] tunes the protocol parameters such as contention window

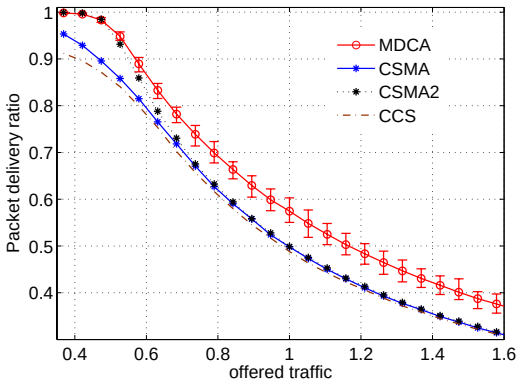

Figure 2.4. *Packet delivery ratio for different distributed schemes (for $N = 20, M = 7, \eta = 2$). The error bar shows maximum and minimum values.*

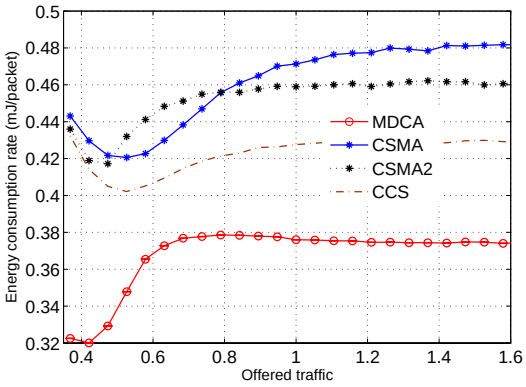

Figure 2.5. *Energy consumption rate for different schemes (for $N = 20, M = 7, \eta = 2$).*

based on the required delivery ratio. The parameters for CCS are taken from Table I in [47]. Note that MDCA is an improved version of our previous work [18] which is hard to realize because each node requires high computational effort to solve MDP. On the other hand, the MDP problem can be solved offline in the proposed MDCA scheme. For this reason, we do not include the scheme proposed by Shrestha et al. [18] in the comparison.

The MCCA scheme is compared with an existing centralized scheme called the Adaptive CSMA/TDMA Hybrid Channel Access (AHCA) scheme [31]. The AHCA scheme is similar to Longest Queue First (LQF) scheme and queue length-aware CSMA/TDMA Hybrid Channel Access (QLHCA) scheme proposed by Zhuo et al. [32] under the system model of the proposed scheme.

2.7.2.2 Performance of the MDCA scheme

Figures 2.4–2.9 show the performance of the MDCA scheme. For comparison, we also consider the CSMA/CA protocol with no packet drops due to the backoff limit or the retransmissions limit. This is indicated as CSMA2 in the figures. Figure 2.4 shows the packet delivery ratio (PDR) for different schemes. In the low congestion regime, the MDCA scheme shows similar performance to the CSMA2 scheme. When

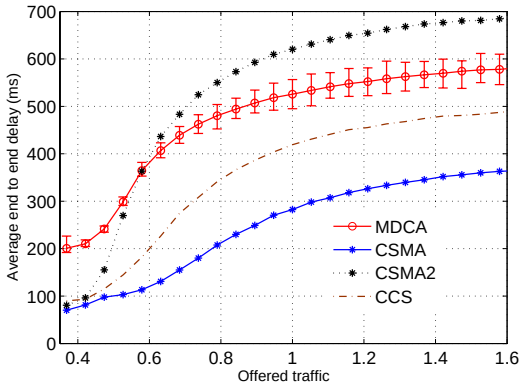

Figure 2.6. *Average end to end delay for different schemes (for $N = 20, M = 7, \eta = 2$).*

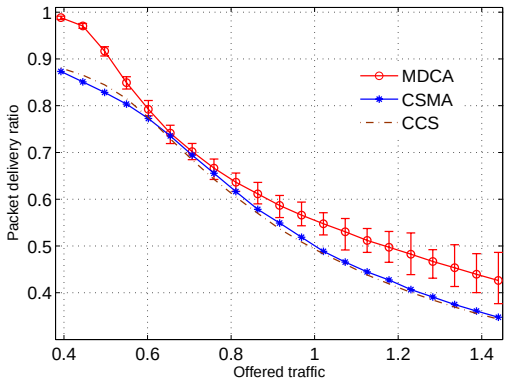

Figure 2.7. *Packet delivery ratio for different schemes (for $N = 20, M = 7, \eta = 4$).*

the MDCA scheme detects congestion, it starts using the TDMA slots during CFP according to the policy π^*. The use of CFP boosts the PDR of the nodes. As shown in Figure 2.5, energy efficiency in terms of consumed energy per successfully transmitted packet per node in the network is also improved. The reason behind this is that transmitting packets during CFP avoids wasting energy in carrier sensing and retransmissions. As shown in Figure 2.6, the price that the nodes have to pay for the improved PDR and energy efficiency is the increased end-to-end delay. One reason of this increased delay is, no packets are dropped because of limits of in number of backoffs or retransmissions. Another reason is, when a node transmits during an assigned TDMA slot, it has to wait during CAP. The CSMA/CA scheme shows the lowest end to end delay when dropping of packets is allowed during contention period. Tuning the MAC parameters would show better performance in low congestion region where CAP is long enough to transmit all packets using the CSMA/CA scheme [47]. However, we consider the superframe to be 384 UBP long and a packet to be 6 UBP long. The performance of the CCS scheme is similar to the performance of CSMA/CA scheme because the nodes in the CCS scheme do not get enough time to converge while tuning the MAC parameters to best in a distributed fashion.

Figures 2.7–2.9 show the results for the scenario when η is changed to 4. To achieve this, we double the CAP and the superframe period. With $K = 16$, the

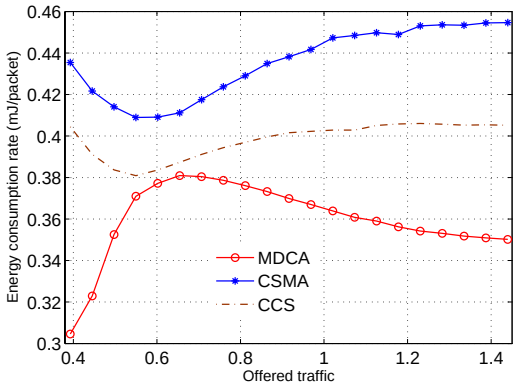

Figure 2.8. *Energy consumption rate for different schemes (for $N = 20, M = 7, \eta = 4$).*

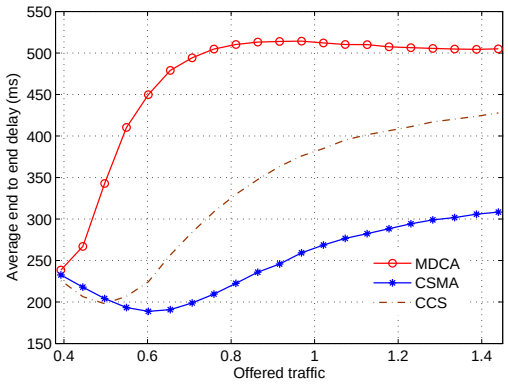

Figure 2.9. *Average end to end delay for different schemes (for $N = 20, M = 7, \eta = 4$).*

slot size is $T_{slot} = 48$ UBP. The proposed MDCA scheme has similar performance as in the case of $\eta = 2$. However, as shown in Figure 2.7, the bandwidth utilization becomes worse as the slot size becomes larger. As the nodes with buffer level less than η packets start using the TDMA slot, the packet delivery ratio does not improve because of bandwidth under-utilization. Therefore, a smaller slot size is desirable for the MDCA scheme.

2.7.2.3 Performance of the MCCA scheme

Figures 2.10–2.15 show the performance results for the MCCA scheme. It is observed that both the MCCA and AHCA schemes have similar performances in terms of PDR and end-to-end delay. Figures 2.11 and 2.14 show that the MCCA scheme consumes less energy to transmit a packet successfully to the coordinator. This is due to the fact that, instead of letting all the nodes compete during CAP as in the AHCA scheme, the coordinator in the MCCA scheme schedules some nodes to go into the low-power mode (defer transmission) to maximize the total CAP throughput. However, this requires the coordinator to perform more computations to find out the list of the nodes that either transmit through CFP and CAP or defer transmissions.

By observing these figures we conclude that the MCCA scheme achieves a better performance than the other. However, if the coordinator does not have capability of

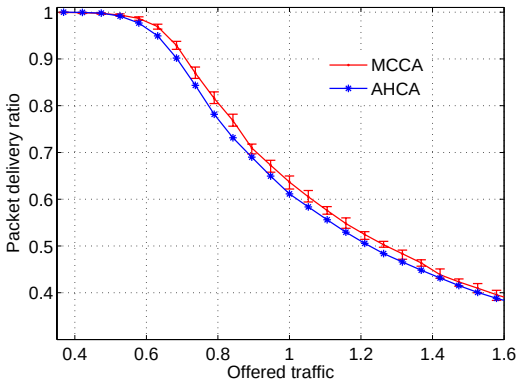

Figure 2.10. *Packet delivery ratio for different schemes (for* $N = 20, M = 7, \eta = 2$*).*

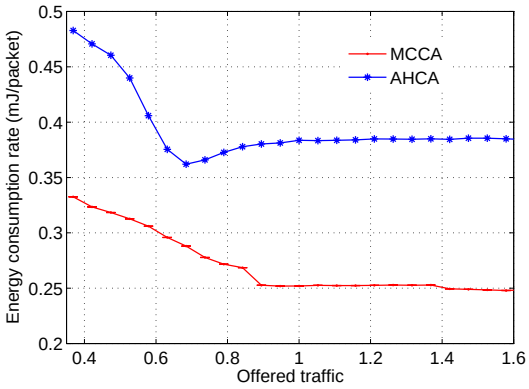

Figure 2.11. *Energy consumption rate for different schemes (for* $N = 20, M = 7, \eta = 2$*).*

processing the information of the traffic loads of all nodes, then the proposed MDCA scheme would be more desirable.

2.7.2.4 Effect of number of time slots on the performance of MCCA scheme

We vary the number of TDMA slots (M) in the superframe. Note that the higher the value of M, the smaller is the contention period. Also, $M = K$ means there is no contention period. For hybrid MAC, we need $M < K$. Figures 2.16 and 2.17 show that, for both the MCCA and AHCA schemes, with increasing M the nodes achieve a better performance. This is because of increased number of successful transmissions during CFP. At a lower traffic load, the proposed MCCA scheme has better PDR than AHCA scheme because of better utilization of bandwidth. Also, as shown in Figure 2.17, sleep scheduling in the proposed MCCA scheme reduces the energy consumption.

2.7.2.5 Effect of probability of outage on the performance of MDCA and MCCA schemes

We vary the probability that the packet is not received correctly at the coordinator (i.e., outage probability). In the simulation, $\Theta = 0.05$ means 5 out of 100 packets

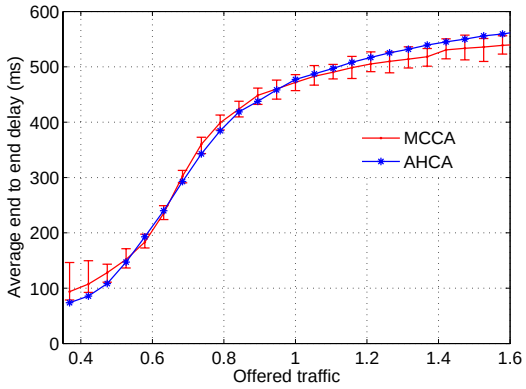

Figure 2.12. *Average end to end delay for different schemes (for $N = 20, M = 7, \eta = 2$).*

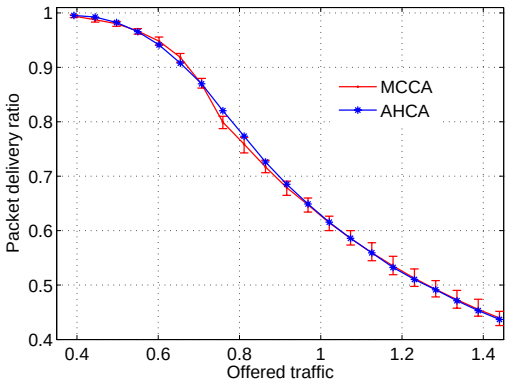

Figure 2.13. *Packet delivery ratio for different schemes (for $N = 20, M = 7, \eta = 4$).*

received by the coordinator from a node are erroneous. We assume that all the links between the nodes and the coordinator go into fading at the same time so that the hidden node collision does not have any adverse effect ($H = 0$). Figure 2.18 indicates that channel outage degrades the performance of the nodes because of increased congestion. The performance of the CSMA/CA scheme with $\Theta = 0.05$ is worse than the performance of MDCA scheme with $\Theta = 0.1$. This shows that when the network gets congested (because of increased traffic load and/or channel fading), the hybrid scheme performs better than the CSMA/CA scheme.

2.7.2.6 Effect of network size on the performance of MDCA and MCCA schemes

We vary the number of nodes (N) in the network. The packet arrival rate of a node is considered to be $\lambda = \frac{T_{sf}+T_{beacon}}{T_{tx}N}$. The packet rate is enough to push the nodes into congestion region. Figure 2.19 shows a comparison among different schemes in terms of the packet delivery ratio. Since the traffic in the network is inversely proportional to the network size N, the packet delivery ratio per node is almost flat for the CSMA/CA, CCS, and centralized schemes. However, the performance of the nodes in the MDCA scheme is dependent on the bandwidth utilization. The nodes require a sufficiently long contention period to transmit the TDMA slot reservation request

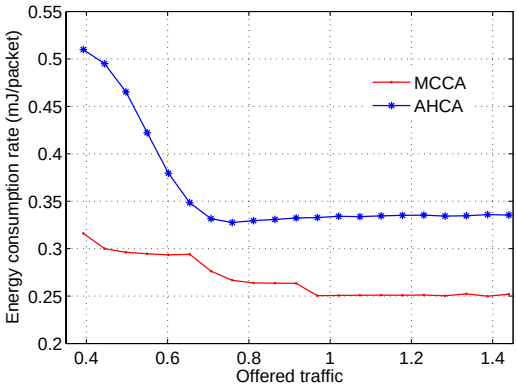

Figure 2.14. *Energy consumption rate for different schemes (for $N = 20, M = 7, \eta = 4$).*

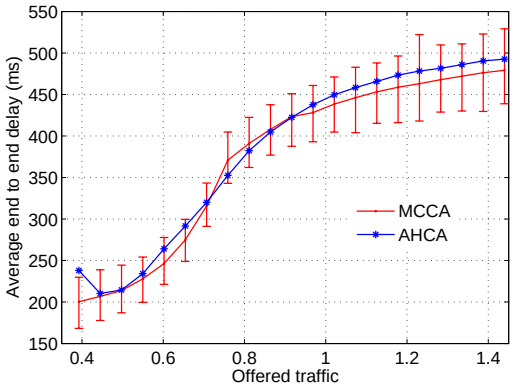

Figure 2.15. *Average end to end delay for different schemes (for $N = 20, M = 7, \eta = 4$).*

successfully. For a higher number of nodes N, the contention period becomes more congested. Eventually, the number of successful requests for TDMA slots decreases and the bandwidth utilization becomes worse. This is the reason why the performance of the MDCA scheme degrades as the network size (N) increases. Therefore, for an efficient operation of the MDCA scheme, the contention period and the number of TDMAs slot need to selected appropriately.

As shown in Figure 2.20, the energy consumption rate grows almost linearly in all the schemes except the MCCA scheme. The reason for linear increase is that the throughput of a node saturates for higher network size but the energy consumption increases due to higher number of retransmissions and carrier sensing. However, in the MCCA scheme, scheduling of the nodes to go into low power mode makes the ratio of energy consumption to the throughput remain at almost the same level. The tradeoff between the average end to end delay and energy consumption is shown in Figure 2.21.

2.7.2.7 Performances of MDCA and MCCA schemes under heterogeneous traffic

We divide the N nodes into three groups based on their traffic, namely, the low rate group, the medium rate group and the high rate group. The size of each group

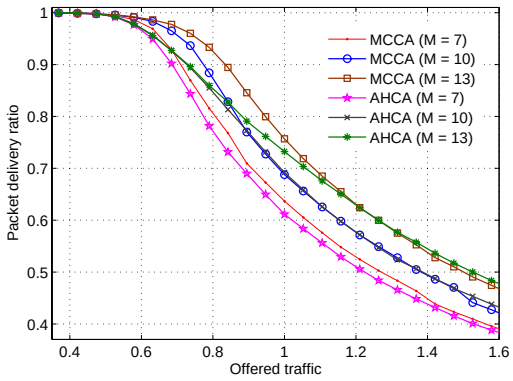

Figure 2.16. *Packet delivery ratio for different values CFP lengths* $M (N = 20, \eta = 2)$.

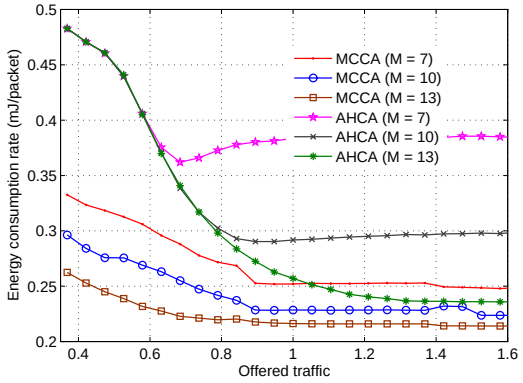

Figure 2.17. *Energy consumption rate for different values CFP lengths* $M (N = 20, \eta = 2)$.

is $N' = N/3$. We investigate the performance of the nodes with heterogeneous traffic in the network. The nodes in the three groups have packet arrival rates of $\lambda_{low} = 0.15\frac{T_{sf}+T_{beacon}}{N'T_{tx}}$, $\lambda_{medium} = 0.30\frac{T_{sf}+T_{beacon}}{N'T_{tx}}$, and $\lambda_{high} = 0.55\frac{T_{sf}+T_{beacon}}{N'T_{tx}}$, respectively. Figures 2.22–2.24 show that the MDCA scheme performs better than the CSMA/CA scheme in the heterogeneous traffic scenario as well. As the lower rate nodes mostly transmit during CAP, they have higher energy consumption rate. Even though the offered traffic rates of the nodes are heterogeneous, the transmission policy $\pi*$ developed for the saturation region in the proposed schemes works well. Similarly, the MCCA scheme is better for higher rate nodes because they mostly use the slots during CFP.

2.8 Chapter Summary

We have proposed two MDP-based channel access schemes, namely, the MDCA and MCCA schemes, to improve the performance of hybrid CSMA/CA and TDMA-based single hop wireless networks (e.g., IEEE 802.15.4-based networks). These models are useful to cope with congestion in the network which may result due to increased traffic load and/or channel fading. We have extended the models to consider channel fading and hidden node collisions. The performance evaluation results have shown that the

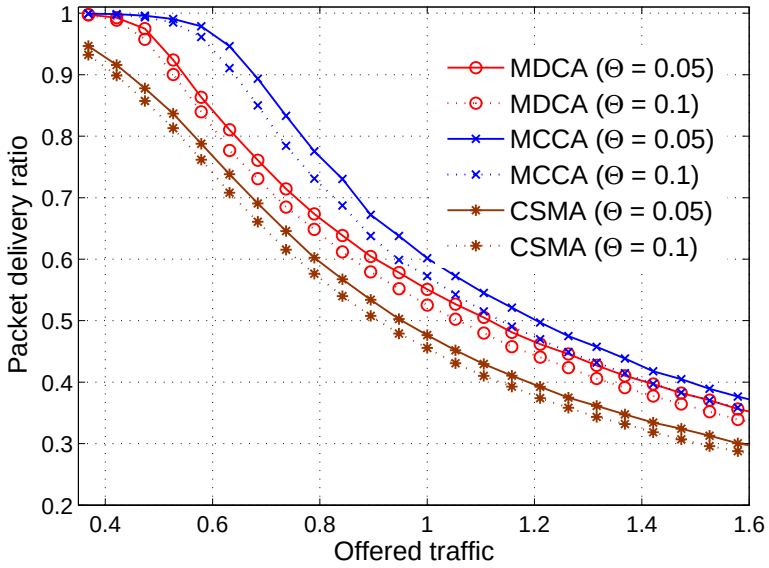

Figure 2.18. *Packet delivery ratio for different values of outage probabilities ($N = 20, M = 7, \eta = 2$).*

proposed MDCA scheme improves network performance by detecting congestion in an intelligent way. The results show that the MCCA scheme is superior but it requires information of packet arrival rate and instantaneous buffer level at all the network nodes. The proposed MCCA scheme is better than the existing hybrid CSMA/TDMA scheme in terms of energy consumption but it requires more computational effort. The proposed MDCA scheme is better (compared to the traditional schemes) when the information of traffic of all the nodes is unknown to the coordinator. Also, the MDCA scheme requires shorter beacon frame because it does not contain information on the actions and the assignment of TDMA slots to the nodes. The MDCA scheme can be enhanced by using the de-centralized partially observable Markov decision process (DecPOMDP) modeling approach. This is left for our future work.

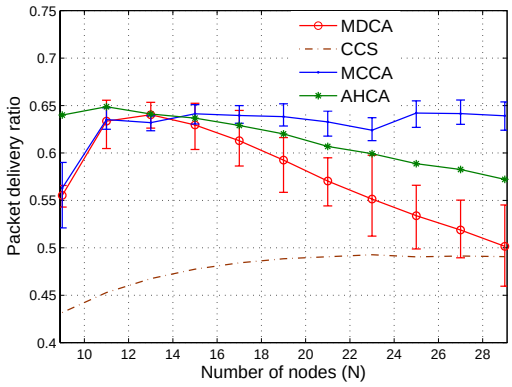

Figure 2.19. *Packet delivery ratio for different network size (for $M = 7, \eta = 2$).*

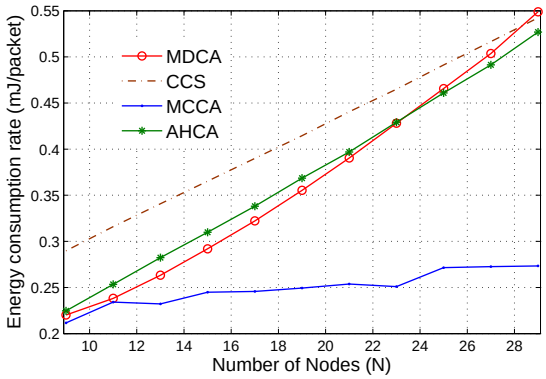

Figure 2.20. *Energy consumption rate for different network size (for $M = 7, \eta = 2$).*

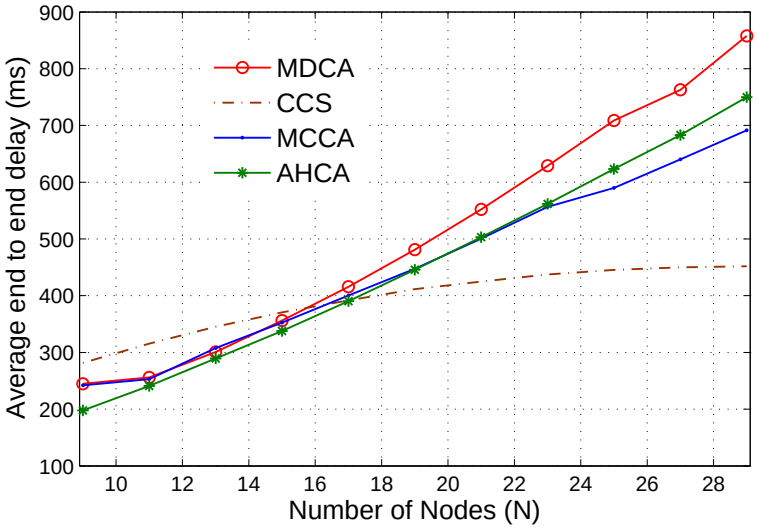

Figure 2.21. *Average end to end delay for different network size (for $M = 7, \eta = 2$).*

Table 2.1. *List of notations*

Notation	Meaning
N	Number of nodes
$A_{t,n}$	Action of node n at superframe t
Λ	Set of all possible actions
$S_{t,n}$	State of node n at superframe t
$B_{t,n}$	Buffer state of node n at superframe t
$\mathbf{B}_t = (B_{t,1}, B_{t,2}, \cdots, B_{t,N})$	Joint buffer state of N nodes
$B_{max,n}$	Maximum value of the buffer state of node n
$R_{s,a}$	Reward when action a is taken at state s
γ	Discount factor
λ	Average packet arrival rate
P_c	Probability of collision
T_{sf}	Length of a superframe
T_{cap}	Length of CAP
T_{cfp}	Length of CFP
T_{slot}	Length of a slot
$\alpha_{n\|N}$	Probability of channel being idle during first carrier sensing for node n given N competing nodes during CAP
$\beta_{n\|N}$	Probability of channel being idle during second carrier sensing for node n given N competing nodes during CAP and the channel was idle during first carrier sensing
$\Phi_{n\|N}$	Throughput of a node n given N competing nodes during CAP
Φ_{cap}	Total number of packets retrieved out of MAC buffer during CAP
κ	Total number of packets successfully transmitted to the coordinator during CAP
η	Number of packets that can be transmitted in a slot duration
Θ	Probability of outage
H	Hidden node collision probability
Ψ_n	Set of nodes which are hidden to node n

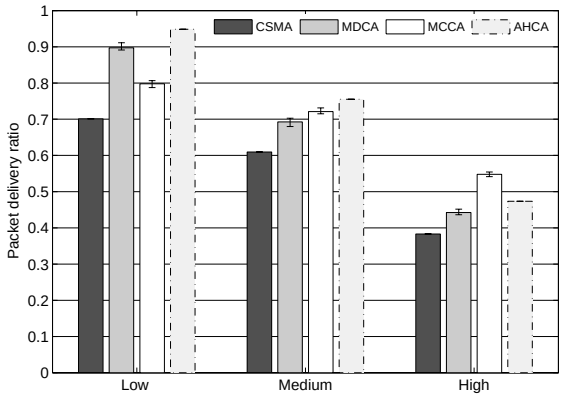

Figure 2.22. *Packet delivery ratio for different groups (for $N' = 6$ nodes, $M = 7, \eta = 2$).*

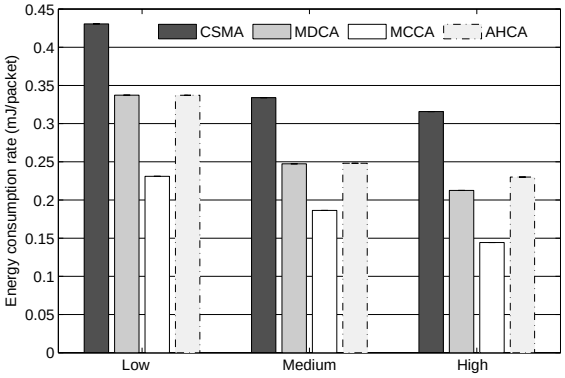

Figure 2.23. *Average energy consumption rate for different groups (for $N' = 6$ nodes, $M = 7, \eta = 2$).*

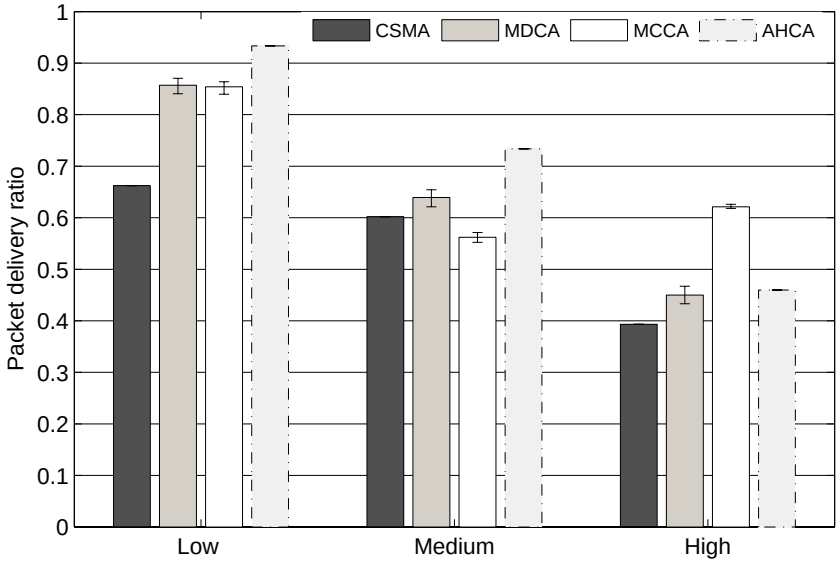

Figure 2.24. *Packet delivery ratio for different groups (for $N' = 7$ nodes, $M = 7, \eta = 2$).*

Chapter 3

Analytical Modeling of Guaranteed Time Slot Transmission by Heterogeneous Devices

3.1 Introduction

The applications of different wireless technology for telemedicine and electronic health (e-Health) services have been studied in recent literature [48]-[51]. Wireless personal area networks (WPANs) such as ZigBee networks can be used to develop an easy-to-install home health monitoring platform [51]. In a WPAN, many low power and low data rate devices communicate with a coordinator. How often they get chance to access the channel and how long it takes to transmit their packets depend on their data rate, packet size, and the type of the medium access control (MAC) protocol used. Most of the time, these devices operate under non-saturated mode as the devices may not always have packets to transmit (e.g., low data rate applications). In WPANs such as wireless body area sensor networks (WBASNs), devices are mostly non-identical in terms of data rate or packet size or both. For example, an electrocardiogram sensor may require a data rate of 2.5 kbps while a 3-axis accelerometer may require a data rate of 1 kbps depending on the application.

The IEEE 802.15.4 MAC [6] is one of the most popular medium access protocols for low power operation in WPANs. It supports guaranteed time slot (GTS) allocation for time-critical data transmissions in the beacon-enabled mode. GTS allocation can improve the reliability of data transmission due to scheduled transmission and also

save the energy which would otherwise be spent for carrier sensing. This mode has the complexity of performing clear channel assessment (CCA) twice for CSMA/CA operation. Further, CCA is performed right after the backoff counter reaches zero. For this reason, the analysis of contention-based access in IEEE 802.15.4 in the beacon-enabled mode is different from that of IEEE 802.11 DCF (Distributed Coordination Function). Also, transmissions during contention-free period (CFP) add complexity to the system since the length of CFP is not fixed in the superframe [25, 52]. The length of the CFP depends on the demand for GTS generated by the applications at the devices. IEEE 802.15.4 MAC is also more flexible compared to traditional time division multiple access (TDMA) MAC because it can transmit by using contention-based access and using GTS (TDMA slot) dynamically. This results in optimum use of bandwidth whether the traffic demand is low or high.

Analysis and optimization of different wireless systems for e-Health applications is a challenging research problem. Discrete-time Markov chain models are widely used to analyze transmission mechanisms in wireless networks. Such a model can describe the exact behavior of a transmission mechanism although the scalability problem may arise when the dimension of the model increases. This chapter presents a four dimensional discrete-time Markov chain model for the operation of IEEE 802.15.4 MAC in the beacon-enabled mode which takes into account the protocol parameters such as active and inactive period, variable backoff window size, deferred transmissions due to insufficient space in contention access period (CAP), non-saturated mode, and GTS transmission mode. In a network of heterogeneous devices, all of the devices may not require to transmit using GTS. For example, temperature sensors in a WBASN may not be as critical as blood pressure sensors to use GTS-based transmission. The temperature sensors have low data rate requirements in the network, and therefore, would waste bandwidth if they use GTS. A temperature sensor may transmit a data packet directly instead of transmitting a request packet first for GTS allocation. In the analytical model we have to consider heterogeneous GTS transmission rates.

The major contribution of this chapter is the modeling of channel access by heterogeneous devices during both CAP and CFP in an IEEE 802.15.4-based single hop WPAN. The usefulness of the developed model lies in the fact that, based on this model, the *utilization factor* can be analyzed for each of the devices in a heterogeneous

traffic scenario. The utilization factor is the ratio of packet arrival rate to MAC layer service rate. For a general traffic scenario, the queueing delay depends on the probability of the MAC layer queue being empty at any arbitrary time. This probability can be calculated from the utilization factor of the device. A low utilization factor indicates that the device in the network has small MAC buffer size and low MAC queueing delay. The model is useful to avoid buffer instability for the devices (i.e., when utilization factor becomes higher than one).

To this end, the model is enhanced with a wireless propagation model in a typical body area sensor network, and the performance of the MAC protocol is evaluated in a wheelchair body area network scenario. A wheelchair is a mobility assistive equipment (MAE) used for the patients with mobility impairment for rehabilitation purposes (Figure 3.1). In a power wheelchair, the bulky and uncomfortable wired devices and circuits can be replaced by wireless devices. To facilitate mobility, positioning, support, and adaptations to temporary and permanent conditions, data collection is an important functionality in such a power wheelchair. For this, different types of sensors can be used to collect data on ambient temperature, temperature in the drive control interface (e.g., joystick), distance, velocity, acceleration, position, motor current [53] (Figure 3.2). For temperature sensors (core, location and ambient), data with 1 degree celsius resolution can be taken at 5 seconds of interval. Similarly, accelerometer is needed to capture the forward distance, velocity and acceleration. The sample of data may be required to take at the interval of 1 second with the resolution of 0.01 m/s^2. Pressure array sensors are used to measure the pressure ulcer. The reading sample of the sensor may be needed at the interval of 0.25 second using 16×16 sensor grid. Force sensors are required to monitor parts, joints and tire pressure of the wheelchair. Data may be taken at the interval of 0.25 second when the wheelchair is active. Further, the different sensor devices may have different data sensing and analog to digital conversion capacities. The sensors typically used in a power wheelchair and the corresponding data rates are shown in Table 3.1. Depending on the positions of the sensor devices, wireless propagation (e.g., shadowing) may significantly affect the transmission performance. The proposed analytical model will be useful for proper dimensioning of a wheelchair body area network.

The rest of the chapter is organized as follows. Section 3.2 reviews the related

Figure 3.1. *A power wheelchair (modified from various sources in the internet).*

Table 3.1. *Sensors in a wheelchair body area network [53]*

Description	Designation	Packet rate	Payload size
Force sensor	N1 to N8	10	8 (byte)
Pressure array	N9 to N10	23	90
core temperature	N11	0.5	8
Driving location temperature	N12	0.5	8
Ambient temperature	N13	0.5	8
Accelerometer	N14	5	8
Gyroscope	N15	5	8
Heart rate	N16	0.5	8
Current sensor	N17	16	8
EGC	N18	25	90

work. Section 3.3 describes the system model and assumptions. The discrete-time Markov chain model for the IEEE 802.15.4 MAC is presented in Section 3.4. Section 3.5 analyzes the MAC service time. Section 3.6 presents the effect of a wireless propagation model. Section 3.7 presents representative numerical results based on the analysis and simulations. Finally, Section 3.8 draws the conclusion.

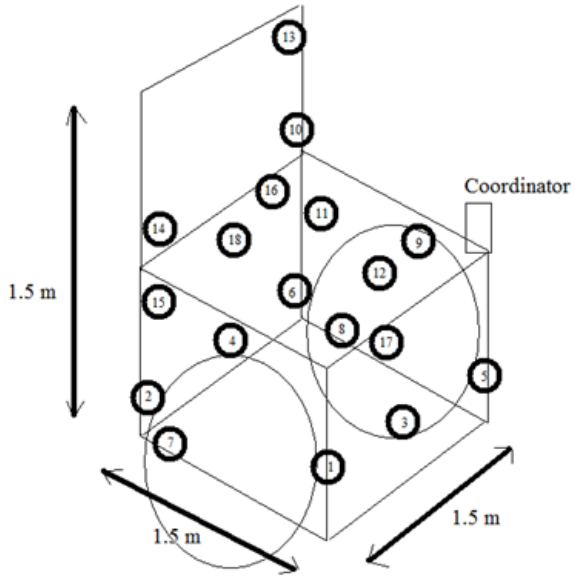

Figure 3.2. *Three dimensional sensor deployment in a wheelchair body area network. Note that the human body is invisible here.*

3.2 Related Work

The performance analysis of IEEE 802.15.4 in contention access is similar to that of IEEE 802.11 except that IEEE 802.15.4 starts carrier sensing when backoff counter reaches zero and performs CCA twice before transmission. In the literature, the performance of the IEEE 802.11 DCF under non-saturated mode with heterogeneous traffic are analyzed in some work [54, 55, 56]. The model presented by Malone et al. [54] is an extension of the model presented by Bianchi [57] for the IEEE 802.11 DCF under non-saturated and heterogeneous traffic conditions. The authors validated the model by considering two classes of service. Stations in the same class have the same packet arrival rate. The model relates the unfairness in bandwidth usage to the quality-of-service performance. Engelstad and Osterbo [55] used a discrete-time Markov chain model to estimate the utilization factor, delay and throughput for different traffic classes in the IEEE 802.11e-based wireless local area networks (LANs). They used the Arbitration Inter-Frame Space (AIFS) value to predict the

starvation point of each access category which occurs when the utilization factor exceeds one. Tickoo and Sikdar [56] presented non-Markov model analysis to estimate the service time distribution for both homogeneous and heterogeneous traffics in the IEEE 802.11-based wireless LANs.

For the saturated mode of operation, the Markov model becomes independent of traffic intensity. Even a low traffic intensity may drive the network into a saturated condition when the network is large, while a high traffic intensity would be required to drive the network into saturated mode when the network is small. Therefore, this mode may not be useful for realistic evaluation of the IEEE 802.15.4 networks. There are quite a few research works on the analysis of IEEE 802.15.4 MAC in saturated mode with homogeneous traffic. Motivated by the Bianchi model [57], the model proposed by Pollin et al. [58] is one of the early works which calculates the probabilities for the channel to be busy during first and second carrier sensing in the IEEE 802.15.4-based networks. Patro et al. [41] claimed their model to be an improved version of that in [58]. Tao et al. [59] showed that the number of carrier sensing in slotted CSMA/CA IEEE 802.15.4 MAC can be reduced to one without degrading the performance. Lee et al. citelee provided an embedded Markov model to calculate the theoretical limit of throughput. Yet another embedded Markov model for saturated mode presented by He et al. [61] introduced a secondary two dimensional Markov chain to model the backoff stages. To model the IEEE 802.15.4 MAC protocol, the model by Gao et al. [62] used backoff analysis.

An analytical model was presented by Mišić and Mišić [63] for the IEEE 802.15.4 MAC under non-saturated condition and heterogeneous traffic, but provided no simulation or experimental results. There are some service differentiation models for the IEEE 802.15.4 MAC in the literature. Kim et al. [64] considered service differentiation in terms of backoff exponent and contention window instead of the data rate. An embedded Markov model was presented by Ndhi et al. [65] with service differentiation based on the number of CCAs performed for class 1 and class 2 stations. Examples of work which deal with the IEEE 802.15.4 MAC in the beacon-enabled mode under non-saturated condition in a homogeneous traffic scenario include [66], [67], [42]. The model presented by Jung et al. [66] assumed that new packets are not allowed in the buffer while the MAC layer is busy in transmitting. The model is compli-

cated to extend for non-identical devices. The model in [67] was not validated. Park et al. [42] assumed a fixed idle state probability for the analysis of non-saturated mode. The probability generating function of service time was estimated but the effect of the probability of deferred transmissions was not considered. Therefore, it can not model the congestion due to smaller size of contention period in slotted IEEE 802.15.4 MAC. The idle state behavior of a device was tuned, however, the details of the tuning process were not provided. In addition, all of the above models considered contention-based transmissions only.

Park et al. [52] used a Markov model to analyze the GTS request and data transmission during CFP only. The work presented by Sheu et al. [25] provided an analysis for channel access during CAP and CFP. However, the purpose of the CFP transmission was to retransmit the packet that is not successful in CAP to cope up with hidden node collisions. Buratti [68] provided analytical model for CAP and CFP transmissions. But they assumed that device has only a packet to transmit in a superframe upon reception of query from the coordinator. However, all of these models assume homogeneous stations in the network. The purpose of this chapter is to extend the traditional analysis of channel access for identical devices in the network to a general case where the devices have different arrival rates and/or different packet lengths. Also, the devices can transmit data packets using CSMA/CA during CAP or using GTS during CFP or both. Application of this model is demonstrated for a wheelchair body area sensor network taking signal attenuation due to shadowing into account.

3.3 System Model and Assumptions

A star network based on the IEEE 802.15.4 MAC in the beacon-enabled mode is considered with N non-identical devices and a single coordinator. Each device is within the sensing range of the other devices in the network (e.g., a WBASN). The devices use slotted CSMA/CA for contention-based transmissions but transmits using GTS in the contention-free period. To transmit packets during CFP, the device has to transmit a GTS request successfully during CAP. We consider only the uplink GTS transmissions. The details of the protocol are provided in [6].

Table 3.2. *MAC parameters for a device (default unit is minimum backoff interval)*

SDS	superframe active period in seconds
SD	superframe active period in backoffs
$B_{data,n}$	Packet length including header for device n
B_{ack}	Acknowledgment length
B_{tack}	Time to receive acknowledgment
$B_{t,n}$	Total backoffs to transmit a packet for device n
B_{CAP}	CAP length
$B_{CFP,n}$	CFP length for device n
B_{inact}	Inactive period in the superframe
$R_{eq,n}$	GTS request rate of device n
b_n	Average bandwidth per request for device n
SL_n	Number of packets allowed to transmit through GTS per superframe for device n
$P_{g,n}$	Probability of GTS allocation for device n
$P_{d,n}$	Probability of deferred transmission for device n

We assume a general traffic scenario where a device, indexed by n, has an average packet arrival rate of λ_n. We assume that each device needs to transmit at a constant rate some of the packets generated by its application by using GTS. The assumption is reasonable because the coordinator may need to collect data packets from the sensors (e.g., ECG sensors) at a guaranteed rate through GTS transmission. A device sends requests to the coordinator to transmit packets during the CFP at the rate $R_{eq,n}$. The MAC parameters for a device are shown in Table II. Let b_n denote the bandwidth (number of packets) to be served per request. To analyze the CFP transmissions, it is necessary to know the average length of CFP in the superframe. For this purpose, we modify the GTS allocation scheme in the standard [30]. Data packets can be used for sending GTS requests by adding few bits when the request rate is lower than the packet arrival rate. The request overhead includes one bit for characteristic type and five bits for number of requested packets. This will reduce the congestion caused by separate request packets. We assume that the application can generate packets and the MAC layer buffer can accept packets from the application while the MAC layer

is busy in handling a packet for transmission. *Note that this assumption also makes the developed analytical model in this chapter different from the other models in the literature.*

The coordinator allocates GTS for every successful GTS request and performs allocation of time slots before transmission of the beacon frame. Since the coordinator ensures that the minimum CAP length is not shorter than $aMinCAPLength$ (= 22 backoff periods) and the number of GTS slots does not exceed seven, some requests may not be served in the current superframe. In this case, the coordinator stores the requests and serves them in the coming superframe(s). Then, at the steady state condition, the average CFP period for device n can be estimated as $B_{CFP,n} = R_{eq,n} \times b_n \times B_{data,n} \times SDS$ assuming all the requests are successful (see Table II for the notations). This assumption is reasonable for the steady state case because, unless a packet is successfully transmitted during CAP, the request header is added to a packet being transmitted. This requires that the request rate satisfies the condition $\frac{b_n R_{eq,n}}{SL_n} < \lfloor \frac{1}{SDS} \rfloor$, where SL_n is the number of packets that device n is allowed to transmit through GTS per superframe. In the ideal case, the number of the superframes per second required to transmit the requested packet through GTS is $\frac{b_n R_{eq,n}}{SL_n}$. Therefore, the packet arrival rate satisfying the following condition should be enough to carry the overhead for the GTS request:

$$\begin{aligned} \lambda_n &\geq b_n R_{eq,n} + \frac{b_n R_{eq,n}}{SL_n} \\ &\geq \frac{1 + SL_n}{SL_n} b_n R_{eq,n}. \end{aligned} \tag{3.1}$$

The probability of GTS allocation is estimated as $P_{g,n} = \frac{B_{CFP,n}}{SD}$ and the number of devices N in the network is limited by

$$\sum_{n=1}^{N} R_{eq,n} b_n B_{data,n} SDS \leq SD - aMinCapLength. \tag{3.2}$$

A device, which has already sent a successful GTS request, can still access the CAP unless the coordinator allocates the GTS slot (with probability $P_{g,n}$). Note that the above modifications make the GTS slot allocation more dynamic and efficient when compared to the scheme specified in the standard [30]. A device may defer transmission until the next superframe because of insufficient time in CAP. Then

the probability of deferred transmission is given by $P_{d,n} = \frac{B_{t,n}}{B_{CAP}}$, where $B_{t,n}$ is the total packet transmission time including inter frame space, acknowledgment, and turn-around time.

3.4 Markov Chain Model

In the GTS allocation scheme, the coordinator places a GTS list in the beacon frame at the beginning of each superframe. If a device is in the GTS list, it stops transmission during CAP and transmits using GTS; otherwise, it uses the CSMA/CA scheme to transmit data during CAP. Therefore, whenever a packet is deferred with probability $P_{d,n}$, device n waits until the next beacon frame. Then, if it is allocated a GTS slot with probability $P_{g,n}$, it does nothing during CAP and transmits its data packet during the CFP period; otherwise, it performs a deferred transmission during CAP. The device waits for the next beacon frame after transmitting during its allocated GTS. But after transmitting the packet during CAP, the device goes to the idle state if it does not have any more packet in the buffer to transmit. If it has, it will start CSMA/CA. If the CAP length is not enough for packet transmission or CAP is over for this superframe, the device defers its transmission. The entire procedure is shown in Figure 3.3. Being in the idle state, a device can receive beacon frame at the beginning of the superframe but we assume that the device does not receive any GTS allocation. For this, the data rate is required to be higher than the request rate such that the device does not go to idle state after sending GTS request.

Based on the above assumptions, a discrete-time Markov chain model (as shown in Figure 3.4) is developed for the heterogeneous traffic case. Since deferred transmission occurs at the beginning of the superframe when no device starts transmission, we assume that the probability of channel being idle is approximately one for deferred transmissions. Unlike the assumption made in the model in [66], we assume that a packet transmission fails after a maximum number of backoffs. We define $\pi_{0,n}$ as the probability of buffer being empty after packet departure and $P_{0,n}$ as the probability that buffer is empty at any arbitrary time for device n. Let $s(t)_n$ denote the backoff state at time t, $b(t)_n \in [0, W_i - 1]$ be the size of the random backoff window, $w(t)_n$ be the number of left CCA, and $r(t)_n$ be the retransmission state. Then, the steady

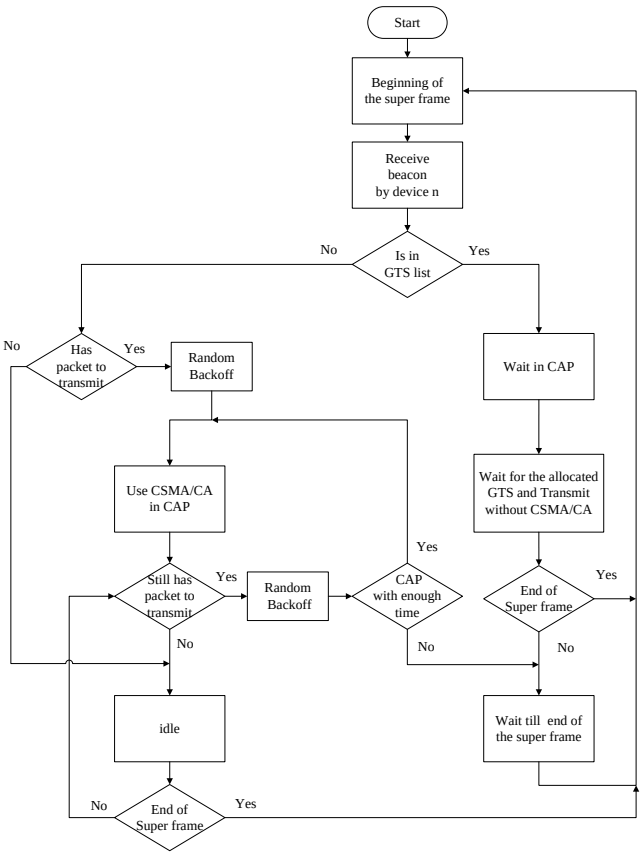

Figure 3.3. *Flowchart of the proposed CAP and CFP transmission scheme. Note that the details of CSMA/CA are not shown here.*

state probability can be represented as

$$x_{i,j,l,k,n} = \lim_{t\to\infty} P\{s(t)_n = i, b(t)_n = j, w(t)_n = l, r(t)_n = k\}$$

for $i = 0, \cdots, m, \quad j = 0, \cdots, W_i - 1,\ l = [1, 2],\ k = 0, \cdots, R,$ where m is the limit on number of backoffs and R is the limit on number of retransmissions. Since $macMinBE = 3$ and $MaxMinBE = 5$, we have $W_i = [8, 16, 32, 32, \cdots]$.

At steady state, assume that $x_{idle,n}$ is the idle state, $x_{T^d_{i,k},n}$ and $x_{T^{nd}_{i,k},n}$ are the deferred and non-deferred states, and $x_{D_i,k,n}$ is the waiting state due to deferred packet. Let $x_{T^g,n}, x_{G^b,n}$, and $x_{G^a,n}$ denote, respectively, the transmission state in CFP, the waiting state before transmitting in CFP, and the waiting state after CFP transmission. $T_{XS,n}$ and $T_{XC,n}$ are successful packet transmission and collision packet transmission states. α_n is the probability that the channel is idle at first CCA, and

β_n is the probability that the channel is idle at second CCA given first CCA is successful. $P_{c,n}^{nd}$ and $P_{c,n}^{d}$ denote the probability of collision for non-deferred and deferred transmissions, respectively. α_n, β_n, $P_{c,n}^{nd}$, and $P_{c,n}^{d}$ are assumed to be independent of backoff stages and retransmission stages. Owing to the chain regularities, we have

$$x_{i,j,2,k,n} = \frac{W_i - j}{W_i} x_{i,0,2,k,n}. \tag{3.3}$$

Let $C_{0,n} = \alpha_n \beta_n$. From Figure 3.4, the steady state probabilities can be derived as follows:

$$\begin{aligned} x_{i+1,0,2,k,n} &= (1 - C_{0,n})(1 - P_{d,n}) x_{i,0,2,k,n} \\ &= C_{1,n} x_{i,0,2,k,n} \end{aligned} \tag{3.4}$$

$$\begin{aligned} x_{0,0,2,k+1,n} &= (P_{c,n}^{nd} C_{0,n}(1 - P_{d,n}) + P_{c,n}^{d}(1 - P_{g,n}) P_{d,n}) \sum_{i=0}^{m} C_{1,n}^{i} x_{0,0,2,k,n} \\ &= C_{2,n} x_{0,0,2,k,n} \end{aligned} \tag{3.5}$$

$$x_{T^g,n} = \frac{P_{g,n} P_{d,n}}{1 - P_{g,n}} \sum_{i=0}^{m} \sum_{k=0}^{R} x_{i,0,2,k,n} \tag{3.6}$$

$$x_{G^b,n} = x_{G^a,n} = x_{T^g,n}. \tag{3.7}$$

The idle state is expressed as

$$x_{idle,n} = \frac{\pi_0}{1 - P_{0,n}} \left(\sum_{k=0}^{R} T_{XS,k,n} + (1 - P_{g,n}) x_{T^g,n} + C_{1,n}^{m+1} \sum_{k=0}^{R} x_{0,0,2,k,n} + C_{2,n} x_{0,0,2,R,n} \right).$$

The value of $x_{0,0,2,0,n}$ can be determined by normalizing all the states of the Markov chain. While normalizing, we have to multiply $x_{D_{i,k},n}$ by the term $\frac{B_{data,n}-1}{2}$ due to deferred backoff which is uniform in the range $[0, B_{data,n} - 1]$. Similarly, GTS transmission and waiting stages during CFP contribute toward $B_{CFP} = \sum_{n=1}^{N} B_{CFP,n}$. Therefore, from the GTS states together, total addition of $(1 + B_{CFP}) x_{T^g,n}$ is required in the normalization. The idle state is tuned as $x_{idle,n} / \sum_{n=1}^{N} \lambda_n$ assuming that the device stays idle for $1 / \sum_{n=1}^{N} \lambda_n$ backoff periods on average. Similarly, $T_{xs,n}$ and $T_{xc,n}$ are tuned as $B_{t,n} T_{xs,n}$ and $(B_{data,n} + B_{tack}) T_{xc,n}$, respectively, assuming constant packet length for each device n. The stationary probabilities $\tau_{nd,n}$ and $\tau_{d,n}$ that the device

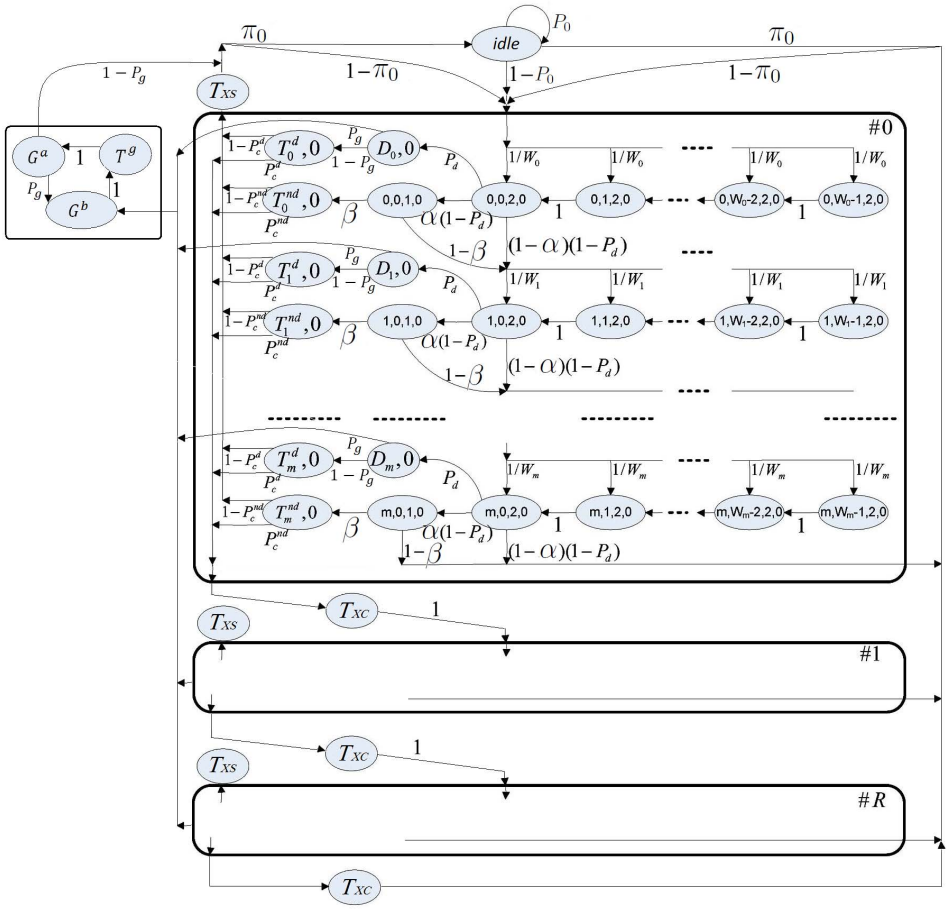

Figure 3.4. *Discrete-time Markov chain model for device n with CAP and CFP transmission using the IEEE 802.15.4 MAC (modified from [66]). Note that subscript n is omitted here.*

carries out non-deferred and deferred transmissions are given as

$$\tau_{nd,n} = \sum_{i=0}^{m} \sum_{k=0}^{R} x_{T_{i,k}^{nd},n} \ , \quad \tau_{d,n} = \sum_{i=0}^{m} \sum_{k=0}^{R} x_{T_{i,k}^{d},n}. \tag{3.8}$$

Then the stationary probability that the device carries out transmission is $\tau_n = \tau_{nd,n} + \tau_{d,n}$. The collision probabilities $P_{c,n}^{nd}$ and $P_{c,n}^{d}$ for non-deferred and deferred transmissions are expressed as the probability that at least one device transmits

among $(N-1)$ devices:

$$\begin{aligned} P_{c,n}^{nd} &= 1-\prod_{\substack{j=1\\ j\neq n}}^{N}(1-\frac{\tau_{nd,j}}{C_{0,j}}) \\ P_{c,n}^{d} &= 1-\prod_{\substack{j=1\\ j\neq n}}^{N}(1-P_{dtx,j}) \\ P_{c,n} &= P_{c,n}^{nd}\frac{\tau_{nd,n}}{\tau_{d,n}+\tau_{nd,n}}+P_{c,n}^{d}\frac{\tau_{d,n}}{\tau_{d,n}+\tau_{nd,n}} \end{aligned} \tag{3.9}$$

where $\frac{\tau_{nd,n}}{C_{0,n}}$ is the probability that device n starts carrier sensing in CAP and $P_{dtx,n}$ is the probability that device n defers transmission in CAP. See [66] for the derivation of $P_{dtx,n}$. Note that there is no collision during CFP. It is worth noting that under the condition that all the transmission probability values are positive and less than or equal to one, we obtain unique solutions for probability of collisions.

We refer to [58] and [41] for the derivation of α_n and β_n. The probability that a device is in carrier sensing stage is $P_{cs,n}=\sum_{i=0}^{m}\sum_{k=0}^{R}x_{i,0,2,k,n}$. The probability that the channel is idle during first CCA accounting for the effect of data and acknowledgment transmissions is

$$\alpha_n = 1-[B_{data,n}(1-\prod_{\substack{j=1\\ j\neq n}}^{N}(1-P_{cs,j}))\frac{\sum_{\substack{h=1\\ h\neq n}}^{N}S_h}{N-1}+B_{ack}\sum_{h=1}^{N}P_{cs,h}S_h\prod_{\substack{j=1\\ j\neq h}}^{N}(1-P_{cs,j})] \tag{3.10}$$

where $S_h=\alpha_h\beta_h(1-P_{d,h})-P_{d,h}(1-P_{g,h})$ is the probability that the channel will be free during carrier sensing period for device h. This equation approximates α_n assuming that device h finds channel busy when at least one device among $(N-1)$ devices starts carrier sensing and any one of them finds the channel to be free during first and second sensing periods. We can also estimate α_n accurately by considering every possible combination of 2 different devices to $(N-1)$ different devices that are successful in carrier sensing among $(N-1)$ different devices. Macro et al. [69] also follow this method. However, when the number of nodes increases, this accurate calculation requires huge computational effort which is undesirable. It is also affected by the transmissions of acknowledgments after successful data transmissions. Although β_n will not be affected by the deferred transmissions, it is affected by the acknowledgment

transmissions. Therefore, the probability that the channel is idle during the second CCA given that the first CCA is idle is given by

$$\beta_n = 1 - \frac{1 - \prod_{\substack{j=1 \\ j \neq n}}^{N}(1 - P_{cs,j})}{2 - \prod_{j=1}^{N}(1 - P_{cs,j})} - B_{ack} \sum_{\substack{h=1 \\ h \neq n}}^{N} P_{cs,h} S_h \prod_{\substack{j=1 \\ j \neq h}}^{N}(1 - P_{cs,j}). \quad (3.11)$$

Equations (3.10) and (3.11) give $2N$ equations with $2N$ unknowns (i.e., α_n and β_n for $n = 1 \ldots N$). For a particular value of P_{cs}, the unknowns can be solved by using numerical methods. The solution gives unique values of α_n and β_n. The proof of uniqueness is shown in the Appendix A.

3.5 Analysis of MAC Layer Service Time

The MAC layer service time depends on the packet transmission time, average sensing time before transmission of packet, collided packet transmission time, average backoff window and average backoffs due to busy channel from the transmissions of other devices. If node n is in the R^{th} retransmission stage in the Markov chain, the average number of backoffs is estimated as

$$z_n = (1 - C_{1,n})\frac{w_0}{2} + (1 - C_{1,n})C_{1,n}\frac{w_1}{2} + \cdots + (1 - C_{1,n})C_{1,n}^{m-1}\frac{w_{m-1}}{2} + C_{1,n}^{m}\frac{w_m}{2} \quad (3.12)$$

where $C_{1,n}$ is the probability of going to another backoff stage. For R retransmission planes, considering all the possibilities of backoffs in the Markov chain, total backoff TB_n for device n can be expressed as

$$TB_n = z_n[(1 - C_{3,n}) \sum_{k=0}^{R-1} ((m+1)C_{3,n})^k + ((m+1)C_{3,n})^R] \quad (3.13)$$

where $C_{3,n} = P_{c,n}^{nd} C_{0,n}(1 - P_{d,n}) + P_{c,n}^{d}(1 - P_{g,n})P_{d,n}$ is the probability that transmission occurs with collision from one of the $(m+1)$ backoff stages. The derivation of (3.13) is shown in Appendix B.

Let t_s denote the CCA time, the default value of which is 8 symbol periods. Then, the average channel sensing time due to busy channel at a stage of backoff and retransmission is given by

$$t_{sc,n} = (1 - \alpha_n)t_s + 2\alpha_n(1 - \beta_n)t_s. \quad (3.14)$$

Similar to (3.12), at state R^{th} retransmission plane, the average sensing time is

$$st_n = (1-C_{1,n})t_{sc,n} + (1-C_{1,n})C_{1,n}2t_{sc,n} + \cdots + (1-C_{1,n})C_{1,n}^{m-1}mt_{sc,n} + C_{1,n}^{m}(m+1)t_{sc,n}.$$

The calculation of total sensing time $T_{sense,n}$ is similar to that in (3.13) which can be expressed as

$$T_{sense,n} = st_n[(1-C_{3,n})\sum_{k=0}^{R-1}((m+1)C_{3,n})^k + ((m+1)C_{3,n})^R].$$

Assuming that a device n takes j backoffs with probability $x_{i,j,2,k,n}$ when it is in i^{th} backoff stage and k^{th} retransmission stage, the average backoff window can be estimated as

$$\begin{aligned}\bar{\omega}_n &= \sum_{k=0}^{R}\sum_{i=0}^{m}\sum_{j=0}^{w_i-1} jx_{i,j,2,k,n} \\ &= \frac{1}{6}\sum_{k=0}^{R} C_{2,n}^{k}\sum_{i=0}^{m}(w_i^2-1)C_{1,n}^{i}x_{0,0,2,0,n}. \end{aligned} \tag{3.15}$$

Assuming that device n goes to another retransmission stage with probability $C_{2,n}$, the average packet collision transmission time can be calculated as follows:

$$T_{coll,n} = \sum_{k=1}^{R+1} kC_{2,n}^{k}(pkt + B_{tack}). \tag{3.16}$$

The total average service time can be estimated as

$$\begin{aligned}T_{s,n} &= B_{t,n} + T_{sense,n} + T_{coll,n} + \bar{\omega}_n + TB_n \\ &\quad + P_{d,n}(1-P_{g,n})(B_{CFP} + B_{t,n} + B_{inact}) \\ &\quad + P_{g,n}SD + \frac{P_{d,n}P_{g,n}(B_{CAP} + B_{CFP} + B_{inact})}{R_{eq,n}}. \end{aligned} \tag{3.17}$$

In (3.17), $B_{CFP} + B_{t,n} + B_{inact}$ backoffs add to the MAC service time due to the deferred transmissions. When GTS is allocated with probability $P_{g,n}$, the service time includes $\frac{B_{CAP}+B_{CFP}+B_{inact}}{R_{eq,n}}$ since the device has to wait during inactive period and during CFP before GTS transmissions. The division by R_{eq} indicates service time calculation per request basis. If the device is allocated GTS at the beginning of an arbitrary superframe, $P_{g,n} \times SD$ contributes to the average service time. We

Table 3.3. *Convergence of the algorithm (data rate = 12 kbps, for GTS request rate = 1/sec)*

No. of nodes	10	11	12	13	14	15	16	17	18	19	20	21
No. of iterations (no GTS)	8	12	11	11	10	10	10	9	9	9	9	8
No. of iterations (with GTS)	11	11	11	10	10	9	9	9	9	8	8	8

assume that the buffer is large enough so that the packet blocking probability is zero. In this case, the channel utilization is

$$\rho_n = \min(1, \lambda_n T_{s,n}) \tag{3.18}$$

and the probability that the buffer will be empty [67] is

$$\pi_{0,n} = P_{0,n} = 1 - \rho_n. \tag{3.19}$$

Finally, all the parameters are estimated by iteratively solving the equations (3.8), (3.9),(3.10), (3.11), (3.17), and (3.19). The procedure can be summarized as follows:

1. Initialize $P_{c,n}$, α_n, β_n, $P_{0,n}$ and $\pi_{0,n}$ for $\forall n \in N$.
2. Solve the Markov chain model to find $x_{0,0,2,0,n}$ for $\forall n \in N$.
3. Given $x_{0,0,2,0,n}$, calculate the new values of τ_n^d, τ_n^{nd} and $P_{c,n}$ for $\forall n \in N$.
4. Update α_n, β_n for $\forall n \in N$.
5. Calculate new values of $P_{0,n}$ and $\pi_{0,n}$ for $\forall n \in N$. If they converge with a tolerance (e.g., 10^{-5}), stop; otherwise, go to step 2.

The numerical result shows good convergence of the algorithm. The table 3.3 shows number of iterations required to converge with tolerance 10^{-5} for different network size.

3.6 Wireless Propagation Model and Outage Probability

Due to channel fading, when the received signal level falls below the receiver sensitivity, the receiver is not able to correctly decode the received signal and it is said

to be in outage. In this case, the transmission is unsuccessful and the transmitter may need to retransmit the packet. For example, in a WBASN, signal received by the coordinator from the bio-sensor devices at different parts of the body may experience high attenuation (e.g., due to shadowing). The propagation model for the body surface to body surface communication can be expressed as [45]

$$PL = PL(d) + S \tag{3.20}$$

where $PL(d)$ is path-loss at distance d and S is the attenuation due to shadowing which follows a log normal distribution with $S \sim N(0, \sigma[dB])$. That is,

$$P(S) = \frac{1}{\sqrt{2}S\sigma\pi} e^{-\frac{(10log_{10}(S))^2}{2\sigma^2}}. \tag{3.21}$$

If P_t is the transmit power in dB and $PL_n(d) + S$ is the loss (in dB) for transmission from device n to the coordinator, then the received power is $R_{x,n} = P_t - PL_n(d) - S$ dB. The probability that the received power is less than the threshold Ω dB (i.e., outage probability) is given by

$$\begin{aligned} P_{out,n} &= Pr(R_{x,n} < \Omega) \\ &= 1 - \frac{1}{2} erfc\left(-\frac{P_t - PL_n(d) - \Omega}{\sqrt{2}\sigma}\right) \end{aligned} \tag{3.22}$$

where $erfc()$ is the complementary error function.

From the perspective of each sensor device, the packet loss due to receiver outage can be considered to be same as that due to collision. The effect of outage probability on the probability of collision can be understood from Figure 3.5. In the presence of outage probability, C_2 is updated with the value of outage probability. The values of P_c, P_{cs}, α, β and π_0 are estimated by updating them with the value of C_2. The probability that a node goes to the successful packet transmission stage from the carrier sensing stage can be expressed as follows:

$$\begin{aligned} P_{succ} &= [(1 - P_{c,n}^d)(1 - P_{g,n})P_{d,n} + (1 - P_{c,n}^{nd})\alpha_n\beta_n(1 - P_{d,n})] \\ &\quad (1 - P_{out,n})\frac{1 - C_{2,n}^{R+1}}{1 - C_{2,n}}\frac{1 - C_{1,n}^{m+1}}{1 - C_{1,n}} \end{aligned}$$

where the constant C_2 is updated from (3.5) to include the outage probability as

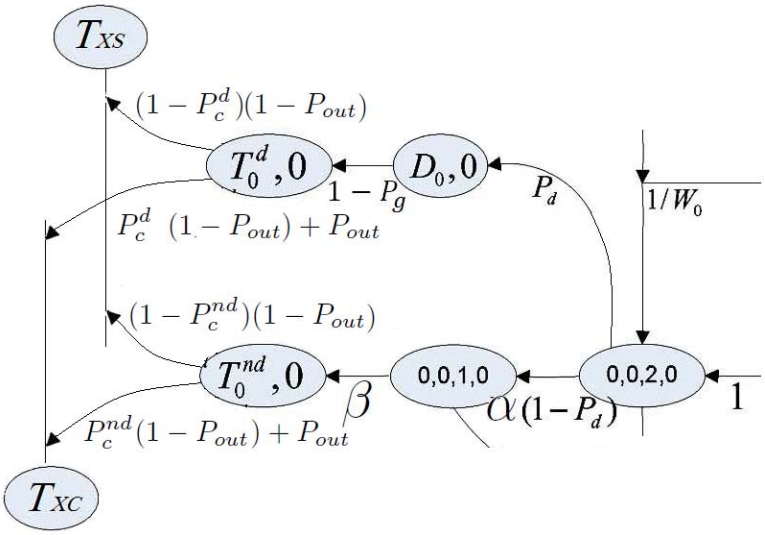

Figure 3.5. *Part of the modified Markov model with the inclusion of outage probability.*

follows:

$$\begin{aligned} C_2 &= \left[\left(P_{c,n}^{nd}(1-P_{out,n})+P_{out,n}\right)C_{0,n}(1-P_{d,n})+\right. \\ &\quad \left.\left(\left(P_{c,n}^{d}(1-P_{out,n})+P_{out,n}\right)(1-P_{g,n})P_{d,n}\right]\sum_{i=0}^{m}C_{1,n}^{i}. \end{aligned} \tag{3.23}$$

Note that the propagation model considered here is a large-scale propagation model (in contrast to small-scale propagation model) to consider the effects of path-loss and shadowing in a wheelchair body area sensor networking scenario. Therefore, this model is not integrated directly with the Markov model, which works at a smaller time-scale the time unit of which is a *UnitBackoffPeriod*.

3.7 Performance Evaluation

Considering different packet arrival rates for the devices in the IEEE 802.15.4 network, the average utilization factor for each device is analyzed with GTS and without GTS transmission mechanisms. Unless otherwise specified, the default parameters for the IEEE 802.15.4 MAC are used [6]. The values of SO and BO are set to 3 resulting

in active period $SD = 7680$ symbols and $B_{inact} = 0$. One unit of backoff period is equal to 20 symbols. Due to backoff boundary, sensing time $t_{sc,n}$ is set to 1 backoff period. The packet size for all devices is set to 10 backoff periods ($27 + 65$ bytes). We ignore the effect of smaller initial backoff window size (8 backoff periods) in the simulation. B_{ack} and B_{tack} are set to 1 and 3 backoff periods, respectively. When $R_{eq,n} = 0$, the system switches to slotted CSMA/CA with no GTS scheme. For the GTS scheme, demand per request b_n is set to 2 packets which is equivalent to the demand of one slot and $SL_n = b_n$. The devices are within the transmission range of the coordinator. MATLAB is used to solve the equations numerically whereas the WPAN module available in the Network Simulator version 2.33 is used to validate the analytical model for average service utilization factor.

3.7.1 Ideal Channel Case

We assume that all the devices are within the transmission range of each other and there is no outage due to channel fading. In the simulations, the MAC service time for a packet is measured from the time when the MAC layer transmitter retrieves the packet from the queue until the packet is freed due to successful transmission or due to maximum backoff or retransmission limit (i.e., the service time does not include the queueing time at the MAC layer queue). Then the utilization factor is calculated by multiplying the service time with packet arrival rate. The network size is varied from 9 nodes to 21 nodes. Three groups of devices (group 1, group 2, group 3) with different data rates but same density are considered. Group 1, group 2, and group 3 represent devices with data rates having Poisson distribution with average of 12, 15, and 20 packets per second, respectively. For the evaluation purpose, the network size and data rates are chosen in a way that the network does not go into extreme under utilization or into saturation. However, same packet size is assumed for all the devices.

Figure 3.6 shows the effect of number of devices on utilization for $R_{eq,n} = 0$ $\forall n \in N$. The analytical results closely follow the simulation results. We observe that the higher data rate devices experience slightly fewer collisions than lower data rate devices and average MAC service times differ slightly for all groups of devices due to same packet size. As expected, the device utilization factor is higher for higher

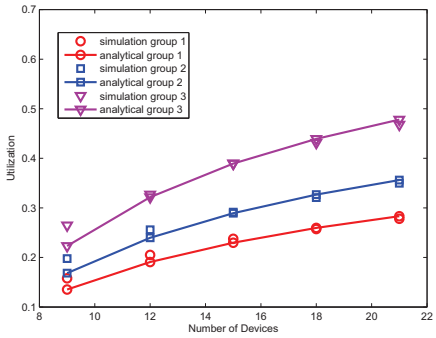

Figure 3.6. *Average channel utilization per device when no GTS is used ($R_{eq,n} = 0$).*

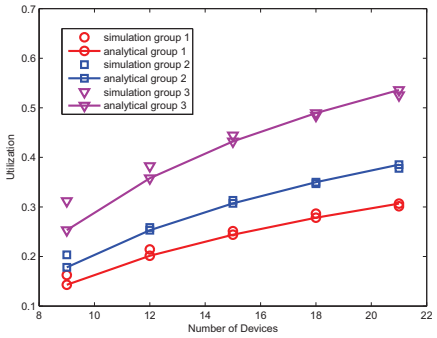

Figure 3.7. *Average channel utilization per device when GTS is used at rate $R_{eq,n} = 1$ only by group 3 devices.*

data rate devices. Figure 3.7 shows the utilization curve for the devices when only group 3 devices request GTS at the rate $R_{eq,n} = 1$, $\forall n \in$ group 3 to transmit data during CFP. Since the CAP period is decreased by a small amount, the utilization is slightly higher for group 1 and group 2 devices whereas group 3 devices have higher utilization due to time spent during CAP while transmitting during CFP. This is a typical scenario in a sensor network. For example, different bio-sensor devices in a wireless body area sensor network have different data rate requirements while all of them may not require to transmit data using GTS.

Figure 3.8 shows the results for GTS scheme (i.e., CAP and CFP transmissions) when devices request to transmit b packets in one second using GTS (i.e., $R_{eq} = 1$). GTS transmission requires no carrier sensing since no other device transmits at the same GTS slot. This saves carrier sensing energy and increase the reliability of packet transmission (i.e., for packets transmitted using GTS). However, waiting time during CAP and smaller contention window for non-GTS packets lead to higher service time for GTS packets.

Figure 3.9 shows the results on utilization when all devices request GTS at the rate $R_{eq} = 2$. For a higher GTS request rate, reduced CAP length incurs congestion and thus results in a higher service time for non-GTS packets. If the allocated slots during CFP are not utilized properly, the service time calculation may not be accurate. This may happen when the device does not have enough packets in its buffer as sought by

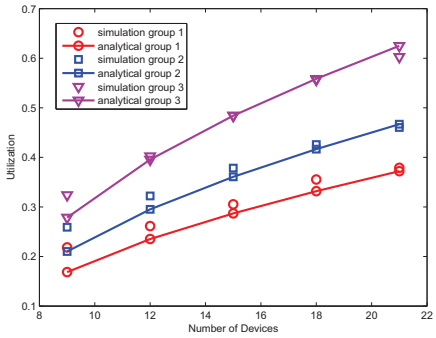

Figure 3.8. *Average channel utilization per device when GTS is used at rate* $R_{eq,n} = 1$ *by all devices.*

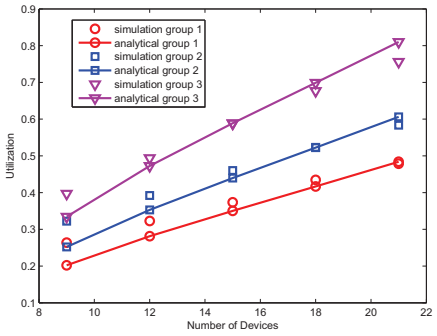

Figure 3.9. *Average channel utilization per device when GTS is used at rate* $R_{eq,n} = 2$ *by all devices.*

GTS allocation during the GTS period in the superframe.

3.7.2 Non-Ideal Channel Case

We consider 18 sensor devices (Table 3.1) deployed in the wheelchair as shown Figure 3.2. We use the following model for signal attenuation [79]:

$$PL_n(d) = 27.6log(d_n[mm]) + 46.5\log(f_n[MHz]) - 157 \tag{3.24}$$

where 150 mm $< d_n <$ 1000 mm and 400 MHz $< f_n <$ 250 GHz. It is reasonable to use high shadowing loss in the human body and wheelchair surface. We use this model for a distance up to 1500 mm (between any sensor and the coordinator) and wireless transmission in the frequency band of 2400 MHz. For all the devices, the path-loss is different because their locations are not the same. Since GTS transmission does not suffer from collisions, the outage probability gives the probability of GTS packet loss assuming that the GTS packets have no retransmission schedule. We study the shadowing effect with only CSMA/CA mechanism. Also, the beacon frame or acknowledgment frame can experience outage. We assume that the coordinator sends those frames with high power (e.g., 10 dBm) to avoid the outage.

Figure 3.10 compares the utilization factor of each device for the ideal channel case and shadowing channel case. For the threshold $\Omega = -90$ dBm, the channel behavior

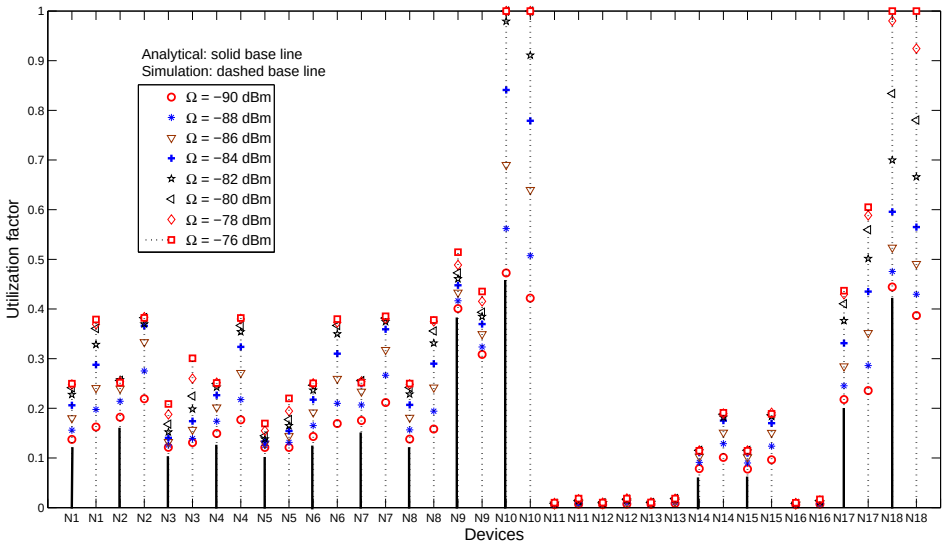

Figure 3.10. *Average utilization factor of the devices for network size of 18 devices.*

is close to that of the ideal case. For high data rate devices suffering from shadowing (e.g., $N10$ and $N18$), the service time is high and the MAC buffer remains in busy state as service utilization becomes high. We have also performed simulations in NS2 with the same scenario to validate the model. As the received power threshold Ω increases, due to the retransmission process, a packet takes longer time to be transmitted out of the MAC layer buffer. Therefore, the utilization factor increases. Apparently, it reduces the probability that a packet goes to successful transmission stage (as shown in Figure 3.11). The devices which are closer to coordinator (e.g., $N5$ and $N9$) experience less shadowing effect for all the given received threshold values. This analysis tells us that we should carefully calculate the positions of the sensor devices in the wheelchair to minimize the shadowing effect.

We can also limit the number of sensor devices to limit the utilization factor, since a higher utilization factor corresponds to a higher delay or a higher probability that the buffer is not empty (which may cause buffer instability). For example, as shown in Figure 3.12, with receiver threshold set to -88 dBm, we can keep the utilization factor of all devices under 0.4 if we remove the devices N1, N2, N3, N4 and N18 from the network.

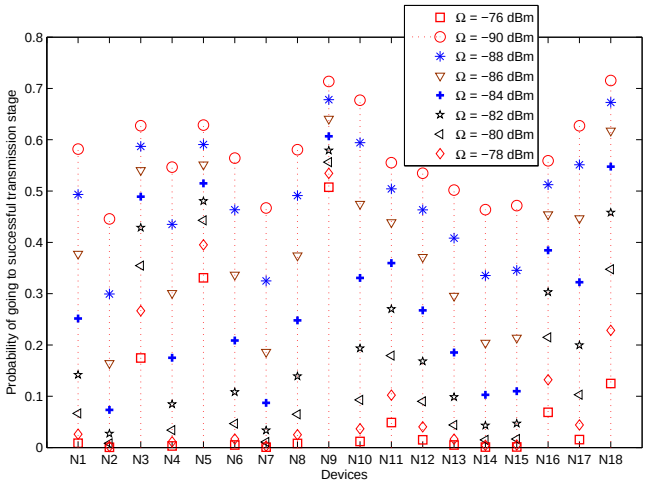

Figure 3.11. *Average probability of going to successful transmission stage from carrier sensing stage.*

Based on the location, we can vary the transmit power of each device in its allowable range to cope up with high signal attenuation. For example, as shown in Figure 3.13, in high shadowing condition where receiver threshold reaches to $\Omega = -76$ dBm, device N10 needs to increase its transmit power by at least 7 dBm to avoid buffer instability. Since device N9 is closer to the controller, increased transmit power does not affect it much. In Figure 3.14, with receiver threshold set to -80 dBm, we analyze the utilization factor of the devices when the superframe duration is changed. For lower values of SO and BO, the protocol has a smaller CAP which results in higher probability of channel being busy and probability of collision which in turn increases the utilization factor. Higher values of SO and BO degrade the performance in case we implement the GTS and inactive period in the superframe. The proposed heterogeneous model helps avoid the buffer instability of non-identical devices in the network.

3.8 Chapter Summary

The average MAC service time has been analyzed for the IEEE 802.15.4-based MAC protocol with heterogeneous devices. The analysis is based on a discrete-time Markov

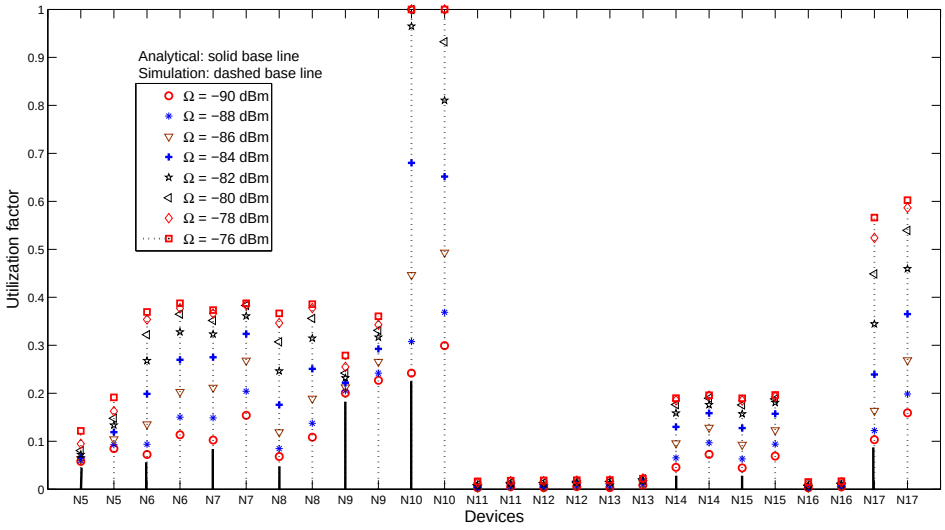

Figure 3.12. *Average utilization factor of the devices for network size of 13 devices.*

chain model which takes into account all the protocol parameters (e.g., active and inactive periods, deferred transmissions) and transmissions during CFP. The standard GTS allocation scheme has been modified and an infinite buffer has been assumed for the derivation of average service time. The numerical and simulation results have shown that the utilization factor is always higher for the higher data rate devices. The MAC service time differs slightly for the heterogeneous devices with same packet size. Further, the utilization with GTS transmission (for all the packets transmitted during both CAP and CFP) is higher than that without GTS scheme. However, note that, the packets for which GTS request is granted, will have bounded service time. The model presented in the chapter will be useful for dimensioning WPANs (e.g., to determine the number of sensors that can be supported in a wireless body area sensor network given the transmission requirements such as the service utilization factor for the different sensors). We have incorporated a wireless propagation model in the analysis and evaluated the performance of the MAC protocol in a wheelchair body area sensor network. High signal attenuation (primarily due to shadowing) in such a body area network can be coped up by proper positioning and power control of the sensor devices which can be verified by the proposed model.

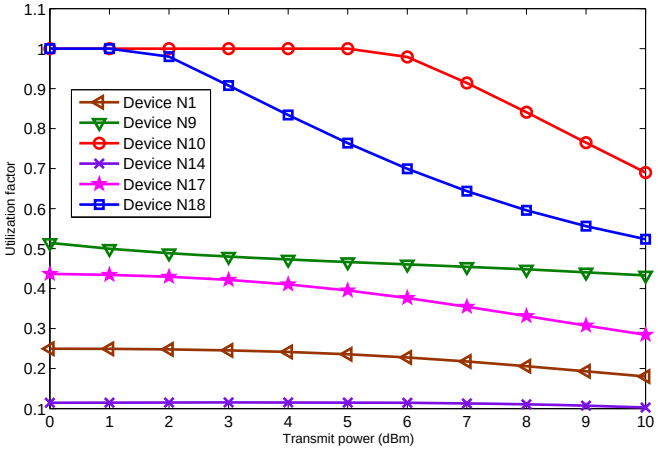

Figure 3.13. *The effect of transmission power over some devices when receiver threshold is at -76 dBm.*

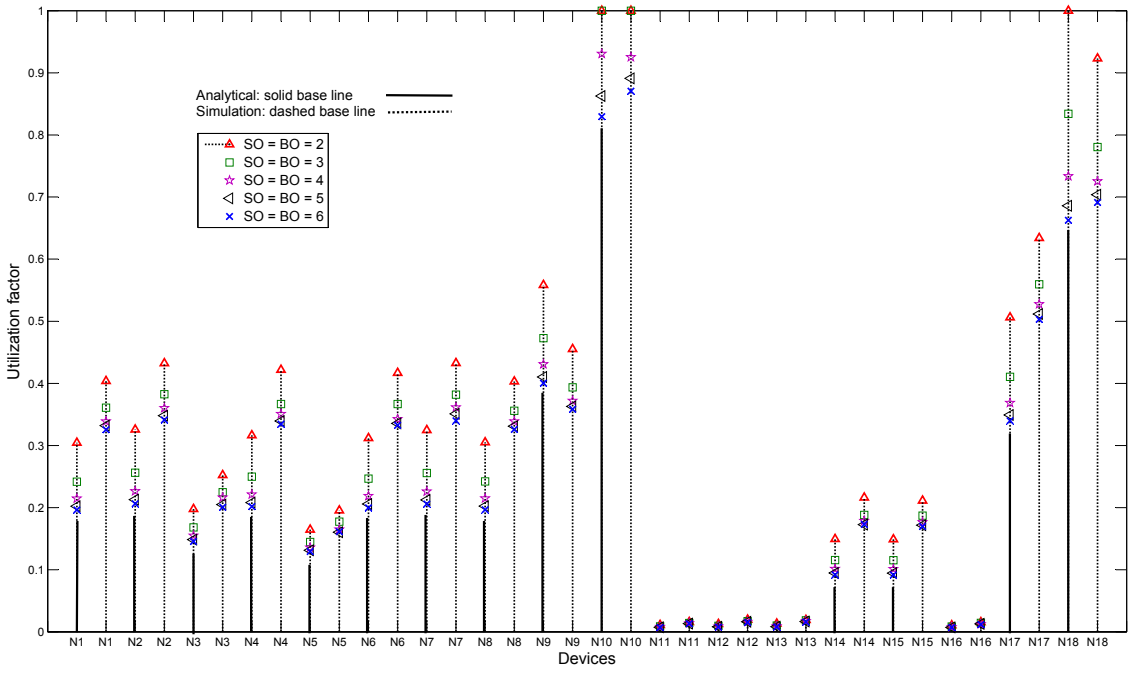

Figure 3.14. *The effect of superframe duration on utilization when receiver threshold is at -80 dBm.*

Chapter 4

An Optimization-Based Guaranteed Time Slot Allocation Scheme

4.1 Introduction

Wireless body area sensor network (WiBASE-Net) [4] is an emerging technology that can be used in medical, entertainment, and fitness applications. In a WiBASE-Net, several wearable or implanted sensor devices, for instance electrocardiogram (ECG) sensor, blood pressure sensor, temperature sensor, respiratory sensor, pulse oximeter, and accelerometer, are deployed throughout the body. A body controller unit (BCU) collects data from the sensor devices and sends it to the medical center. The IEEE 802.15.1 [5] and the IEEE 802.15.4 [6]-based technologies will be suitable for WiBASE-Nets [7].

IEEE 802.15.4 supports not only contention-based access mechanism but also guaranteed time slot (GTS) scheme under beacon-enabled mode for delay-sensitive applications. GTS transmission can avoid packet drop due to collisions in the contention-based protocol (i.e., CSMA/CA), limited number of allowable retransmissions and number of backoffs as specified in the standard. In a medical sensor network, GTS allocation can also reduce the energy consumption of the sensor nodes due to carrier sensing. The IEEE 802.15.4 standard allocates GTS to devices in first-come first-serve (FCFS) fashion. Due to the lack of optimization, this standard allocation results in wastage of bandwidth while serving asymmetric traffic from different sensor devices.

The objective of this chapter is to improve the GTS allocation scheme in the IEEE 802.15.4-based MAC when used for a large number of medical and physical sensor devices deployed in a WiBASE-Net. In such an environment, there are uneven traffic generation rates in the different medical sensors, unequal data rate requirements of the sensor devices as well as unequal packet sizes. To efficiently utilize the GTS, an optimization model based on the knapsack problem [70] is formulated and solved to obtain the optimal GTS allocation for the different devices. This optimization model takes the priority which is based on the packet generation rate of each device into account. Performance evaluation results show that the proposed GTS allocation scheme can improve the utilization of GTS scheme and also enhance the performance of data transmission from sensor devices in a WiBASE-Net when compared to the standard scheme in the IEEE 802.15.4 standard.

In this chapter, we develop an optimization-based scheme to allocate GTS slots to wireless devices with different rate requirements. In this scheme, one GTS request can support the demand of up to $D_{max} = 2^5 = 32$ packets from a device without changing its standard format.

The rest of the chapter is organized as follows. We discuss related work in Section 4.2. In Section 4.3, we present the system model and formulate the knapsack problem. In Section 4.4, we propose the GTS allocation algorithm using the solution of knapsack problem. We evaluate the performance of the proposed algorithm in Section 4.5. Finally Section 4.6 concludes the chapter.

4.2 Related Work

The problem of GTS allocation was addressed in the literature. A GTS allocation and priority updating scheme was presented by Huang et al. [71] taking latency and fairness of data transmission into account. Koubaa et al. [72] proposed i-GAME scheme to improve the GTS utilization. In this scheme, GTS is shared among multiple devices in a round-robin fashion. This scheme allows more than seven devices to use GTS simultaneously. Na et al. [73] proposed the algorithm for GTS allocation during CFP for the IEEE 802.15.4 standard. This allocation is based on the payload, number of requested slots, and the delay constraint for data transmissions. The method to

improve bandwidth utilization of GTS was presented Cheng et al. [74] by dividing the CFP into 16 slots for simultaneous transmissions without any change in the GTS descriptor format. Kumar et al. [75] restructured the GTS characteristic field to accommodate the information about payload demand, delay constraint, and number of periods which can be used to improve bandwidth utilization. However, a device can have only limited choices of payload demand, delay and number of periods due to limited number of bits available in the GTS characteristic field.

GTS allocation schemes were proposed by Koubaa et al. [72] and Na et al. [73] considering the delay-guaranteed service. In these schemes, the information of delay requirements needs to be exchanged with the controller which incurs signaling overhead. The scheme in [73] also has high computational complexity due to the execution of a number of algorithms. The scheme in [72] requires each requesting node to identify flow specification which incurs additional control overhead.

4.3 WiBASE-Net Model and Knapsack Problem Formulation

4.3.1 IEEE 802.15.4-Based WiBASE-Net Model

We consider a WiBASE-Net based on the IEEE 802.15.4 standard (Figure 4.1) using a star network topology. The body controller unit collects data from the different sensors deployed in the body of the subject [4]. These sensor devices can be electrocardiogram (ECG), blood pressure, temperature, and accelerometer for a health care monitoring service [76]. Data from these sensors are collected periodically. However, an emergency data may be generated randomly and need to be transmitted immediately. To support this time-critical data transmission, GTS in the IEEE 802.15.4 standard will be used by setting seventh reserved bit in the characteristic field of the GTS request packet (Figure 4.2). The proposed GTS scheme is used when the reserved seventh bit is reset. The bandwidth demand is considered in terms of the number of packets with the maximum of D_{max} packets.

The generated packets in a sensor device are buffered in a transmission queue. At the beginning of a super-frame, the device checks the buffer state. If the number of

packets in the device transmission buffer is larger than the threshold T_i, device i will send the bandwidth demand information to the coordinator for GTS slot allocation. During the CAP period, the coordinator collects the bandwidth demands from the devices. Then, a fractional knapsack problem [70] is solved by the coordinator to allocate GTS to the requesting devices given their priority. The proposed GTS allocation algorithm (to be presented later in this chapter), which is based on the solution of the knapsack problem, ensures that the radio bandwidth in the GTS is utilized in an optimal manner.

Let $S_{pkt,i}$ denote effective packet length in symbols for device i. We assume that $aMinCAPLength = \ell$ symbols and the length of active period is $SD = (2^{SO} \times aBaseSuperFrameDuration)$. The maximum number of symbols that can be transmitted during CFP is $S_{max} = (SD - \ell)$. The number of symbols per slot duration is $S_{slot} = SD/16$ symbols such that $S_{slot} \geq S_{pkt,i}$. For device i, let K_i denote the buffer threshold parameter. When the instantaneous queue length in the device is larger than threshold $T_i = K_i \frac{S_{slot}}{S_{pkti}}$, the device sends GTS request to the coordinator. The request contains the number of packets in the queue immediately after receiving beacon at the beginning of super frame.

If a device does not send GTS request or misses the beacon frame, it can use slotted CSMA/CA to transmit its data. If the request is unsuccessful, the device waits for the next beacon to send another GTS request. Unlike the standard [6], the device, in order to transmit its data packets, can still compete with other devices during CAP after successful GTS request unless a slot is allocated. For each successful data transmission, the bandwidth demand will be updated accordingly by the coordinator

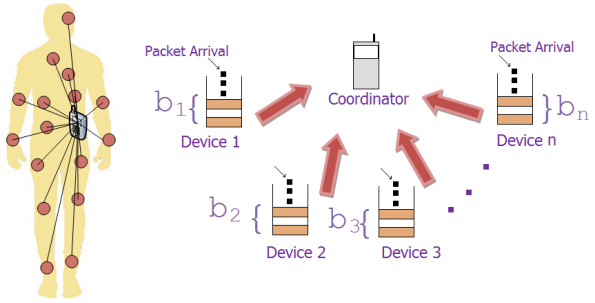

Figure 4.1. *System model of a WiBASE-Net.*

bits: 0–3	4	5	6–7
GTS Length	GTS Direction	Characteristics Type	Reserved

Figure 4.2. *Format of the GTS characteristics field in the IEEE 802.15.4 standard.*

and the device itself. We assume that there is a limit on the transmission delay for a packet in a sensor device. If the packet waiting time exceeds this delay limit, the sensor device simply discards the packet. The coordinator collects all the GTS requests during CAP and solves the knapsack algorithm for GTS allocation before transmitting the beacon frame. It saves the remaining bandwidth that is not allocated for GTS to use in the next super frame.

4.3.2 Knapsack Problem Formulation

Let the set of demands collected and set of remaining bandwidths to be served for n devices from previous $(t-1)^{th}$ super frame be denoted by $\mathbf{b} = \left\{b_1^{t-1}, b_2^{t-1}, \cdots, b_n^{t-1}\right\}$, $b_i^{t-1} \leq D_{max}$, and $\mathbf{r} = \left\{r_1^{t-1}, r_2^{t-1}, \cdots, r_n^{t-1}\right\}$, respectively. Let $\mathbf{p} = \{p_1, p_2, \cdots, p_n\}$ denote the corresponding priority. We assume that the coordinator has the information on priority and $S_{pkt,i}$. For example, these information can be delivered to the coordinator at the time of neighbor discovery or association phase. Let x_i denote the decision variable of the knapsack problem. This x_i is the fraction of bandwidth that will be used by the devices in the upcoming CFP. The knapsack problem can be formulated as follows:

$$\text{maximize:} \quad \sum_{i=1}^{n} p_i x_i \tag{4.1}$$

$$\text{subject to:} \quad \sum_{i=1}^{n} (b_i^{t-1} + r_i^{t-1}) x_i S_{pkt,i} \leq S_{max}$$

$$0 \leq x_i \leq 1.$$

Let x_i^* be the solution of the optimization problem defined in (4.1)-(4.2). The fractional knapsack problem can be solved optimally by a greedy algorithm [70] as given in Algorithm 1. The computational complexity of the fractional knapsack algorithm is $O(n \log n)$ [77].

Algorithm 2 Knapsack algorithm

Input: $\mathbf{p}, \mathbf{m} \leftarrow (\mathbf{b} + \mathbf{r}).\mathbf{S}_{pkt}$ and $\Gamma \leftarrow S_{max}$
Output: $\mathbf{x}$
sort devices $\mathbf{d} = \{d_1, d_2, \cdots, d_n\}$ such that $p_i/m_i \geq p_{i+1}/m_{i+1} \ \ \forall$ device $d_i \in \mathbf{d}$
foreach device $d_i \in \mathbf{d}$ **do** $x_i \leftarrow 0$ **end for**
$i \leftarrow 1$
while $\Gamma > 0$ **do**
    if $m_i < \Gamma$ **then**
        $x_i \leftarrow 1$
        $\Gamma \leftarrow \Gamma - m_i$
    else
        $x_i \leftarrow \Gamma/m_i$
        $\Gamma \leftarrow 0$
    end if
    $i \leftarrow i + 1$
end while

4.4 Proposed Algorithm

The proposed algorithm can be adopted by the IEEE 802.15.4 standard without any modification to the specification. The basic idea is to impose a condition to send a request on the device side and to use knapsack solution to schedule requested devices for GTS on the coordinator side.

Based on the optimal solution x_i^* obtained from Algorithm 1 at the beginning of t^{th}super frame, the total bandwidth that will be allocated to device i in upcoming slots is $b_{new,i}^t = (b_i^{t-1} + r_i^{t-1})x_i^*$. The remaining bandwidth is $r_{new,i}^t = (b_i^{t-1} + r_i^{t-1})(1 - x_i^*)$. Then, the coordinator converts the allocated number of packets to number of slots such that the GTS idle period will be less than 50%. Let S_i^t be the number of slots allocated to serve $b_{new,i}^t$. The number of packets per slot is $P_{slot,i} = \frac{S_{slot}}{S_{pkt,i}}$. The number of allocated GTS slots for device $i = 1, 2, \ldots, 7$ can be obtained from

$$S_i^t = \min\left(\left\lfloor \frac{b_{new,i}^t}{P_{slot,i}} \right\rfloor + \Delta S_i, \left\lfloor \frac{S_{max}}{S_{slot}} \right\rfloor - \sum_{j=0}^{i-1} S_j^t\right) \tag{4.2}$$

where $S_i^t = 0$ for $i = 0$ and $i > 7$; $\Delta S_i = 1$, if $\mathbf{mod}(b_{new,i}^t, P_{slot,i}) > \frac{1}{2}P_{slot,i}$; and $\Delta S_i = 0$ otherwise. The fraction of GTS idle period due to excessive slot allocation is given by

$$GTS_{idle} \leq \frac{\Delta S_i}{2S_i^t}, \quad \forall S_i^t > 0. \tag{4.3}$$

The final remaining bandwidth to be served is obtained as follows:

$$r_i^t = \max(0, r_{new,i}^t + b_{new,i}^t - S_i^t P_{slot,i}). \tag{4.4}$$

$$r_i^t = 0 \text{ for } r_i^t \leq \frac{1}{2}P_{slot,i}. \tag{4.5}$$

The amount of bandwidth that will be served in upcoming slots is $S_i^t P_{slot,i}$. The coordinator places the starting slot and slot length S_i^t in the descriptor for each device i. Then, the coordinator updates the CAP length and transmits in the beacon frame.

Let us assume that each device i maintains the following parameters at the beginning of the t^{th} super frame. R_i^{t-1} is the number of requested packets in previous super frame, B_i^t is the current buffer size (number of packets), S_i^t is the number of slots allocated in current beacon frame, $P_{slot,i}$ is slot size in terms of number of packets, and T_i is the buffer threshold. Assume that each device receives beacon at the beginning of current super frame. Then, it updates the number of requested packets as follows:

$$R_i^t = \max(0, R_i^{t-1} - S_i^t P_{slot,i}). \tag{4.6}$$

Similar to (4.4), condition in (4.5) also applies for R_i^t. The condition for each device i to send a GTS request is $B_i^t - R_i^t - S_i^t P_{slot,i} > T_i$. If device i satisfies the condition, then the bandwidth demand is determined by device i from

$$b_i^t = \min(D_{max}, B_i^t - R_i^t - S_i^t P_{slot,i}). \tag{4.7}$$

If device i transmits GTS request successfully, then it updates the number of requested packets as: $R_i^t = R_i^t + b_i^t$. Otherwise, it resets bandwidth demand $b_i^t = 0$. If $S_i^t = 0$, the device can access CAP. In this case, the device reduces the value of R_i^t (when R_i^t is non-zero) by one with each successful packet transmission during CAP whereas the coordinator reduces the value of $b_i^t + r_i^t$ (when $b_i^t + r_i^t$ is non-zero) by one. In the case that the device misses a beacon, it also misses GTS and has to reset the value of R_i^t. However, the device may obtain GTS information in the next received beacon.

Since the buffer threshold T_i determines the minimum bandwidth to be served per GTS request message, the value of T_i depends on the GTS request rate requirement of the devices. The ideal GTS request rate is $R_{eq,i} = \frac{\lambda_i}{T_i}$, where λ_i is the packet generation rate for device i. Since the maximum request rate is one per beacon interval (BI), the minimum buffer threshold is $T_{min,i} = \lambda_i \times BI$. As $T_i \to \infty$ and $R_{eq,i} \to 0$, the scheme switches to slotted CSMA/CA scheme. To control the number of GTS requests, the buffer threshold is determined from

$$T_i \geq \max\left(\frac{\sum_{j=1}^{q} N_j \lambda_j}{\sum_{j=1}^{q} N_j}, \max\left(T_{min,i}, P_{slot,i}\right)\right) \tag{4.8}$$

where N_j is the number of devices with packet rate λ_j in the network having devices with q different packet rates.

As an example, consider $P_{slot,i} = 2, T_i = 4$ for device $i = 1, 2$. At the beginning of t^{th} super frame, let $B_1^t = 5, R_1^{t-1} = 0, S_1^t = 0, B_2^t = 7, R_2^{t-1} = 0, S_2^t = 0$. From the request condition, the demands are given by: $b_1^t = 5, b_2^t = 7$. Suppose the GTS request is successful for both devices. Then, $R_1^t = 5, R_2^t = 7$. Assume that none of these devices could transmit data packets during CAP. Then, at the start of $(t+1)^{th}$ frame, the coordinator allocates slots $S_1^{t+1} = 2, S_2^{t+1} = 3$. Assuming $r_1^t = 0, r_2^t = 0$, the remaining bandwidths are $r_1^{t+1} = 1, r_2^{t+1} = 1$. If both the devices receive beacon at $(t+1)^{th}$ frame, then $R_1^{t+1} = 1, R_2^{t+1} = 1$. Using (4.5), $r_1^{t+1} = 0, R_1^{t+1} = 0, r_2^{t+1} = 0, R_2^{t+1} = 0$. If there is no packet arrival at this frame then $B_1^{t+1} = 5, B_2^{t+1} = 7$. Since none of the devices satisfies the GTS request condition, $b_1^{t+1} = 0, b_2^{t+1} = 0$. They transmit packets in the allocated slots. If no new packet arrives in the buffer, at the beginning of $(t+2)^{th}$ frame, $B_1^{t+2} = 1, B_2^{t+2} = 1$. Since the devices will not be allocated any slots at this frame, $R_1^{t+2} = 0, R_2^{t+2} = 0$. However, each of the devices can transmit the remaining packet using CAP competing with other devices. Here, device 1 can transmit 4 packets successfully at the cost of 1 GTS request, and thereby, it saves the energy for carrier sensing for transmission of 3 packets while improving GTS utilization.

4.5 Simulation Setup and Performance Evaluation

4.5.1 Simulation Setup

To evaluate the performance, the proposed algorithm is implemented on a WPAN model of the NS2 version 2.33. A star topology with single WPAN coordinator and N devices ($N \in [10, 20]$) deployed in the area of $1000mm \times 1000mm$ is considered. Path loss model for body surface analyzed by Aoyagi et al. [78] and Takada et al. [79] is used. The path loss $G(f, d)$ in dB for body surface to body surface propagation at distance d and frequency $f = 2.4$ GHz can be obtained from

$$G(f, d) = -27.6 \log(d[mm]) - 46.5 \log(f[MHz]) + 157 + W \tag{4.9}$$

where W is the shadowing component following log normal distribution with standard deviation of 4.4 dB. As in the standard [6], typical values for transmit power of 0 dBm and receiver sensitivity of -85 dBm are used.

Impulsive or bursty traffic and constant-bit-rate (CBR) traffic are common traffic models for medical applications [80]. For the simulation period of 500s, each device generates a demand of $(\tau \times \lambda_i)$ packets in burst during a time interval τ, where the time interval is assumed to be exponentially distributed with mean value of $\overline{\tau} = 2$ seconds. The payload size of a packet is assumed to be 70 bytes for all devices. The data rate depends on the sensor type, its application and resolution [80]. Six average data rates $\{12, 9, 7.5, 6, 4.5, 2.5\}$ Kbps are uniformly assigned to devices for performance evaluation purpose.

The values of BO and SO are set to 3. Here, $aMinCAPLength$ is assumed to be $2 \times S_{slot}$ symbols. The transmission delay limit for a newly generated packet at a sensor device is set to 4s. With all signaling (e.g., packet transmission time, propagation delay, and IFS period) and packet headers, a device can transmit 2 ($= \frac{S_{slot}}{S_{pkt,i}}$) packets within a slot duration. For each device, the threshold parameter is set to $K_i = 7$ such that $T_i = K_i \frac{S_{slot}}{S_{pkt,i}}$ satisfies (4.8). The priority of the devices is distributed over the packet rate requirements as follows:

$$p_i = \lambda_i - \lambda_{min} + 1, \quad \text{for } i = 1, 2, \cdots, n. \tag{4.10}$$

For comparison purpose, the GTS allocation scheme defined in the standard (i.e.,

FIFO scheme) is also implemented. The deallocation of GTS is initiated by the device when its queue length is less than half of the threshold for five super frames.

4.5.2 Performance Evaluation

The following performance measures are considered: packet delivery ratio (PDR), packet discard rate, link quality indication (LQI) packet drop rate, average delay, percentage of GTS idle period, and average probability of GTS transmission. PDR is the ratio between the number of packets successfully received by the coordinator and the total packets generated by the devices during the simulation period. Packet discard rate indicates the ratio of packet drops due to packet delay limit (i.e., before transmission) to the total packets generated by application. The LQI measurement [6] indicates the quality of received packets in terms of signal to noise ratio (SNR). This metric is also useful for channel selection and routing in higher layer. The LQI packet drop rate indicates the ratio of received packet drops to the total transmitted packets.

Since the proposed algorithm is focused on reliability of the network, it is compared with the beacon-enabled IEEE 802.15.4 MAC with no CFP and standard GTS scheme. Figure 4.3 shows the effect of number of devices on PDR. The proposed algorithm achieves higher PDR since the algorithm optimizes the utilization of GTS.

An LQI drop occurs when the received SNR is below the threshold (i.e., link quality is bad due to collision). As the number of devices increases, collision and LQI drop increase (Figure 4.4) due to high contention during CAP. In the standard scheme, dedicated slots and deallocation procedure reduce the data transmission during CAP. In proposed scheme, the device can access CAP unless a GTS is allocated even after successful GTS request. For this reason, the devices have more access to CAP and higher LQI drop rate than that in the standard scheme.

Figure 4.5 shows the average packet delay. Delay is measured from the time when the packet is first generated by the application at the transmitter to the time when it is successfully received by the application at the receiver. The delay increases if a device does not receive enough bandwidth during CFP or enough transmission time during CAP because the device has to wait next beacon frame to start the transmission process. In this scenario, the packet delay in the proposed scheme degrades when more than 18 devices request for GTS due to limit on system throughput. Since

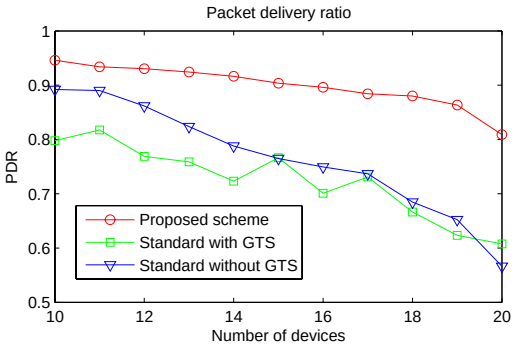

Figure 4.3. *Average packet delivery ratio (PDR).*

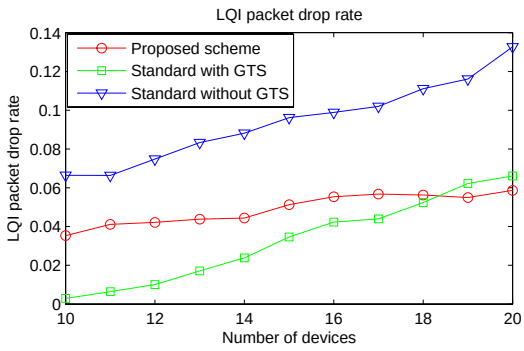

Figure 4.4. *Link quality indication (LQI) packet drop rate.*

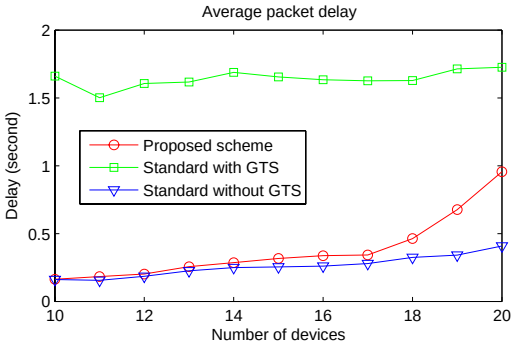

Figure 4.5. *Average packet delay.*

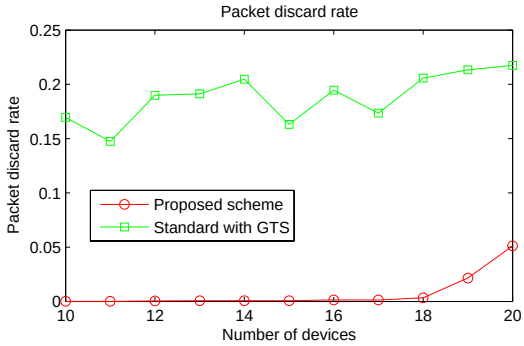

Figure 4.6. *Packet discard rate.*

the sensor devices discard packets for which the transmission delay limit has expired, the packet discard rate (Figure 4.6) also increases. Figures 4.4–4.5 show the tradeoff between delay and LQI packet drop.

Figure 4.7 shows the percentage of idle period in the GTS that is not used for data transmission. This idle period occurs due to excessive GTS allocation, or when the devices are unable to receive beacon frames due to poor channel condition, or due to the difference in packet transmission duration and slot duration. GTS idle period in the proposed scheme occurs only due to the gap in slot duration after transmission of P_{slot} packets and missing of beacons. Clearly, the proposed scheme can effectively minimize this idle period.

Figure 4.8 shows the average probability of GTS transmission for the group of devices with different data rates. The probability is defined as the average ratio of GTS transmissions to total data transmissions for all the devices. Again, the allocation of

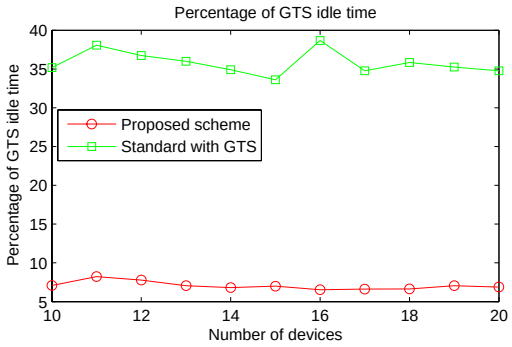

Figure 4.7. *Average percentage of GTS idle period.*

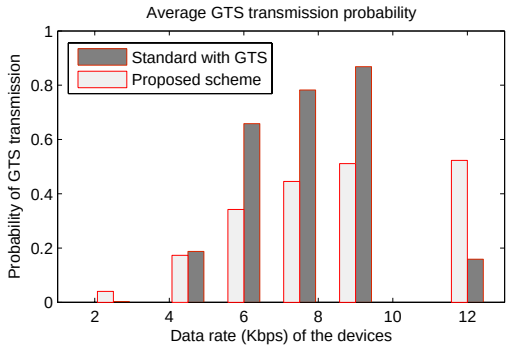

Figure 4.8. *Probability of data transmissions using GTS by the devices with different data rates.*

GTS based on the proposed scheme and that in the standard are considered. The priority of devices is considered to be proportional to the data rates because high priority devices require more bandwidth (i.e., more time slots). Therefore, the probability of GTS transmission is also proportionally distributed over different groups of devices in the proposed scheme. On the other hand, in the standard scheme, GTS transmission is highly unfair for some devices. For GTS allocation, the proposed scheme is observed to be fair among devices.

4.6 Chapter Summary

To efficiently utilize the guaranteed time slots (GTSs) in the IEEE 802.15.4 MAC standard, an optimal GTS allocation scheme has been proposed with its potential application for data collection in a wireless body area sensor network (WiBASE-Net). To allocate GTS to the sensor devices, the priority determined from the data arrival rates at the devices has been taken into account. The GTS allocation problem has been formulated as a knapsack problem and solved to obtain the optimal allocation. Performance evaluation results show that the proposed scheme can significantly improve the packet delivery ratio while decreasing the packet drop rate. Compared to the GTS allocation scheme specified in the standard, the proposed scheme offers higher packet delivery ratio and hence higher bandwidth utilization.

Chapter 5

A Dynamic Time Slot Allocation Scheme

5.1 Introduction

The carrier-sense multiple access (CSMA) protocol is a popular contention-based random access protocol with high flexibility and scalability. However, the CSMA protocol is inefficient in terms of throughput due to wasted time caused by back-off procedure and collisions. Although the time-division multiple access (TDMA) protocol minimizes the wasted time, it also has some inherent disadvantages such as reduced scalability and channel underutilization. A hybrid CSMA/TDMA MAC protocol combines the strengths of both CSMA and TDMA protocols. Such hybrid protocols are adopted by short-range high-rate wireless networks (e.g., IEEE 802.15.3c [81] and IEEE 802.11ad [82]) as well as low-rate wireless personal area networks (e.g., IEEE 802.15.4 [83]).

We consider a network in which a coordinator takes charge of controlling multiple devices. In the existing protocols (e.g., proposed by Koubaa et al. [72] and Pyo and Harada [84]), if a device needs time slots, the device sends a time slot request, which contains the required number of slots, to the coordinator. Then, the coordinator semi-statically allocates slots to the device based on the request from the device. This semi-static request-based time slot allocation can suffer from a channel underutilization problem. Channel underutilization occurs when a device does not have data packets enough to fill up the allocated slots. Since the data traffic arrival process is generally non-deterministic, the channel underutilization problem is inevitable as long as the semi-static time slot allocation is used.

To overcome this channel underutilization problem, we propose a dynamic queue-length-based time slot allocation scheme. In this scheme, each device sends a time slot request containing the report of the current data queue length to the coordinator. However, since no dedicated control channel is set up between a device and the coordinator, the device can send the request only in an intermittent manner. Therefore, the coordinator cannot always maintain the up-to-date queue length information. After the latest queue length report has been received at the coordinator, data packets might have arrived in the queue of the device according to a certain probabilistic traffic arrival pattern. The queue length of each device is uncertain from the point of view of the coordinator. Note that the queue length information can be piggy-backed by the data packet. However, we do not consider this because it requires a modification in the packet frame structure.

The main contribution of this work is that we design a time slot allocation scheme for the hybrid MAC, which maximizes the channel utilization under the *queue length uncertainty*. The proposed scheme calculates the probability mass function (*pmf*) of the distribution of the queue length for each device from the traffic arrival pattern. Based on this *pmf*, the proposed scheme allocates slots to the devices in such a way to maximize the channel utilization. To our knowledge, the problem formulation in this work has not been considered in any previous literature.

The remainder of this chapter is organized as follows. In Section 5.2, we explain the system model. Section 5.3, we formulate and solve the time slot allocation problem. Section 5.4 presents the simulation results for the proposed scheme and this chapter is concluded in Section 5.5.

5.2 System Model and Assumptions

5.2.1 Network Model and Superframe Structure

We assume a wireless network which consists of $N + 1$ nodes (i.e., a coordinator and N devices). The index of the coordinator is $n = 0$ while each device is indexed by $n = 1, \ldots, N$. A link is defined as a unidirectional communication link, which can be set up between the coordinator and a device as well as between two devices.

We consider the frame structure for the hybrid MAC protocol as shown in Fig-

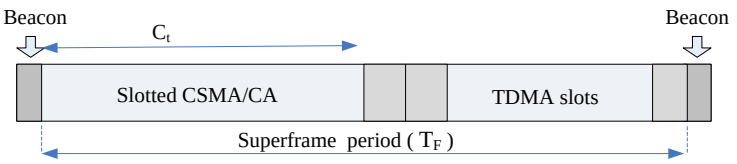

Figure 5.1. *Superframe structure for the considered system model.*

ure 5.1. Each superframe is indexed by t and the length of the superframe excluding the beacon frame is denoted by T_F. A superframe begins with a beacon which is issued by the coordinator. The beacon is followed by the CSMA period, during which the CSMA protocol is used by the coordinator and devices. The TDMA period, which immediately follows the CSMA period, is divided into a number of time slots. The length of a slot is denoted by T_S. We assume that $T_F = \omega T_S$, where ω is the number of slots in a superframe.

We assume that all the data packets have same size and one data packet can be sent during a slot. The size of the request packet is smaller than that of the data packet. The payload of the request packet contains the report of the queue length. Since the data packet sizes of the nodes might not be the same in some applications, frame aggregation can be used to equalize their sizes.

The coordinator allocates slots to each node during a TDMA period on a superframe-by-superframe basis. Let $S_{t,n}$ denote the number of slots allocated to node n in superframe t. Then, the total number of allocated slots in superframe t is $\sum_{n=0}^{N} S_{t,n} \leq s_{max}$ where s_{max} is the maximum number of TDMA slots available for allocation in a superframe. The rest of the superframe is used as the CSMA period, and therefore, the length of the CSMA period in superframe t is $C_t = T_F - T_S \sum_{n=0}^{N} S_{t,n}$. The coordinator decides slot allocation for the TDMA period right before superframe t starts and announces the slot allocation to devices via the beacon.

5.2.2 Data Traffic Model

The queue length of a node is defined as the number of all packets in the transmission queue in that node. Let $Q_{t,n}$ denote the queue length of node n at the beginning of superframe t. The arrived packets wait until the end of the superframe to be placed in the queue. In addition, let $q_n^{\max}$ denote the maximum queue length of node n. The

packets, which have waited until the end of the superframe, are discarded if the queue is full.

We consider the batch Poisson process as the packet arrival model for each node. In this model, a batch, which contains one or more packets, arrives according to the Poisson process. The arrival time and the number of packets of the jth batch at node n are denoted by $X_{n,j}$ and $Y_{n,j}$, respectively. For node n, the inter arrival time between batches, $X_{n,j+1} - X_{n,j}$, is exponentially distributed with mean $1/\lambda_n$. The number of packets in each batch, $Y_{n,j}$, is identically and independently distributed. The pmf of $Y_{n,j}$ is denoted by f_n^Y.

We define $A_{n,\tau}$ as the number of arrived packets at node n during a time interval the length of which is τ. Since the packet arrivals follow a batch Poisson process, $A_{n,\tau}$ follows a compound Poisson distribution [40]. Therefore, the characteristic function of $A_{n,\tau}$ is given as

$$\varphi_{n,\tau}^A(z) = \mathbb{E}[\exp(izA_{n,\tau})] = \exp\{\lambda_n \tau(\varphi_n^Y(z) - 1)\} \tag{5.1}$$

where $\varphi_n^Y(z)$ is the characteristic function of $Y_{n,j}$ such that $\varphi_n^Y(z) = \mathbb{E}[\exp(izY_{n,j})] = \sum_y \exp(izy) f_n^Y(y)$. The pmf of $A_{n,\tau}$, denoted by $f_{n,\tau}^A$, can be derived from $\varphi_{n,\tau}^A$ by means of the inverse formula for the characteristic function.

Note that we can also incorporate a "deterministic arrival process" into our model, in addition to the batch Poisson process. Suppose that node n has deterministic traffic which generates γ_n packets during one superframe. Then, we can roughly calculate the number of arrived packets during τ as $A_{n,\tau} = \gamma_n \tau / T_F$. In this case, the characteristic function of $A_{n,\tau}$ is given as $\varphi_{n,\tau}^A(z) = \exp(iz\gamma_n \tau / T_F)$. Although we can easily consider this deterministic arrival process, we will focus on the batch Poisson process as our main traffic model.

5.2.3 Node Operation

At the start of superframe t, node n finds out the number of slots allocated to it (i.e., $S_{t,n}$) and the length of the CSMA period (i.e., C_t). If the node is a device, it receives the beacon from the coordinator to know such information. If at least one slot is allocated to node n, the node transmits $L_{t,n} = \min\{Q_{t,n}, S_{t,n}\}$ packets through the allocated slots. Note that $(S_{t,n} - Q_{t,n})$ slots are wasted if there are not enough

packets in the queue. In case that there are multiple outgoing links from node n, it is up to node n's decision to select an outgoing link for transmission in each slot.

During the CSMA period, only the nodes with no allocated slot are allowed to attempt to transmit a request packet. Let $\mathcal{B}_t$ denote the set of nodes, which have at least one packet in the queue and have no allocated slot in superframe t. That is, $\mathcal{B}_t = \{n|Q_{t,n} > 0 \text{ and } S_{t,n} = 0\}$. The nodes in $\mathcal{B}_t$ try to send the request packet during the CSMA period, and only a subset of these nodes, denoted by $\mathcal{D}_t$, successfully transmit the packet. Note that in a system with beamforming (e.g., IEEE 802.15.3c), the nodes should direct a beam to the coordinator to send a request packet.

The queue length report is piggybacked by the request packet during the CSMA period to let the coordinator know the queue length. If device n is successful in transmitting the request packet during the CSMA period in superframe t (i.e., $n \in \mathcal{D}_t$), the coordinator becomes aware of the queue length of device n in the superframe t (i.e., $Q_{t,n}$). In superframe t, the coordinator maintains the queue length information for node n in the form of the tuple $\mathbf{V}_{t,n} = (U_{t,n}, J_{t,n})$, where $J_{t,n}$ is the number of superframes which have passed after the latest report was received. We define $U_{t,n}$ as the queue length reported in the latest report during the superframe. It is updated as $U_{t,n} = \max(U_{t-J_{t,n},n} - S_{t-J_{t,n},n}, 0)$. Since the coordinator knows its own queue length without any report, we have $U_{t,n} = Q_{t,n}$ and $J_{t,n} = 0$ for $n = 0$.

5.2.4 Random Access During CSMA Period

In the CSMA period, the carrier-sense multiple access with collision avoidance (CSMA/CA) protocol is used. We can consider two types of the CSMA/CA protocols, which differ in the backoff mechanism. The one is used in the IEEE 802.15.4 networks and the other is used in the IEEE 802.15.3 and IEEE 802.11ad networks. In this chapter, we do not delve into the details of these protocols.

We are interested in the instantaneous throughput of the CSMA/CA protocols for a given condition. Let $\Delta(b, c)$ denote the average number of packets transmitted by the CSMA/CA protocol under the condition that the number of nodes participating in the CSMA period is b and the length of the CSMA period is $c \cdot T_S$. That is,

$$\Delta(b, c) = \mathbb{E}\left[|\mathcal{D}_t| \big| |\mathcal{B}_t| = b,\ C_t = c \cdot T_S\right] \tag{5.2}$$

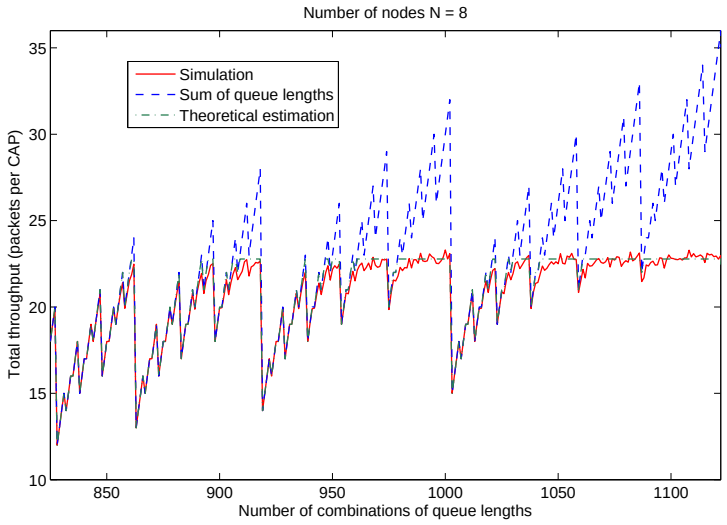

Figure 5.2. *Total average throughput per CAP period for different queue length combinations.*

where $|\cdot|$ denotes the number of the elements in a set.The value of $\Delta_c(\mathbf{b})$ depends on the type of protocol used in the contention period. For example, IEEE 802.15.4 MAC in beacon enabled mode uses slotted CSMA/CA scheme for packet transmissions during contention period. Let $\mu_c(N)$ be the total saturation throughput given number of nodes N and contention period length c then

$$\begin{aligned} \Delta_c(\mathbf{b}) &= \sum_{n=1}^{N} b_n \quad \text{if} \quad \sum_{n=1}^{N} b_n \leq \mu_c(N) \\ &= \mu_c(N) \quad \text{if} \quad b_n \geq \frac{\mu_c(N)}{N} \quad \forall n \in N \end{aligned} \tag{5.3}$$

For rest of queue length combinations, the total throughput can be slightly higher than the saturation throughput (i.e. $\Delta_c(\mathbf{b}) > \mu_c(N)$). For an example, consider $N = 8$, CAP period $c = 384$ unit backoff period and buffer size $Q^{max} = 5$. The saturation throughput is $\mu_c(N) = 22.78$ packets per CAP period. Consider that each node has at least a packet in its buffer, total number of combinations of queue lengths of the nodes (i.e., $\mathbf{b} = (b_1, \cdots, b_N), \forall b_n \in Q^{max}$) is $\binom{N + Q_n^{max}}{N} = 1287$. Each combination represents a vector of queue lengths of all nodes. For the combinations from 1 to 827, we get $\sum_{n=1}^{N} b_n \leq \mu_c(N)$. Therefore, we consider the simulation result of total throughput for the combination from 828 to 1287. In the Figure 5.2, the sum

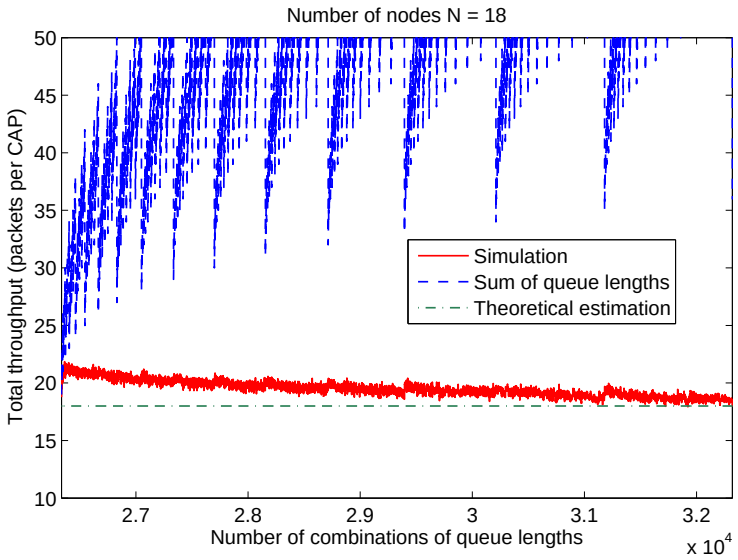

Figure 5.3. *Total average throughput per CAP period for different queue length combinations.*

of queue length represents $\sum_{n=1}^{N} b_n$ for each combination. The theoretical estimation is the value of $\Delta_c(\mathbf{b})$ calculated as $\sum_{n=1}^{N} b_n$ if $\sum_{n=1}^{N} b_n \leq \mu_c(N)$ otherwise $\mu_c(N)$. The Figure 5.2 shows that the total throughput obtained from the simulation follows the theoretically estimated throughput.

Similarly consider the case of $N = 18$, then saturation throughput is $\mu_c(N) = 18$. The Figure 5.3 shows that the theoretical estimation by $\mu_c(N)$ is slightly lower than the actual total average throughput obtained by the simulation. The randomness in the throughput of CSMA/CA is hard to capture especially when some nodes are saturated (i.e., high queue length) and some are not (i.e. low queue length). The Figure 5.3 shows that estimated throughput deviates from the actual throughput obtained by the simulation by 3 packets at maximum in the case $N = 18$. Therefore, the total throughput per CAP ($\Delta_c(\mathbf{b})$) can be estimated by $\mu_c(N)$ with small deviation. We can develop a look-up table by simulation to find more accurate values of $\Delta_c(\mathbf{b})$.

Since throughput is proportionally dependent on the contention period, the total throughput at different CAP length c' can be estimated as

$$\mu_{c'}(N) = \frac{c'}{c}\mu_c(N) \tag{5.4}$$

For CSMA/CA, total number of calculations to find all the combinations of through-

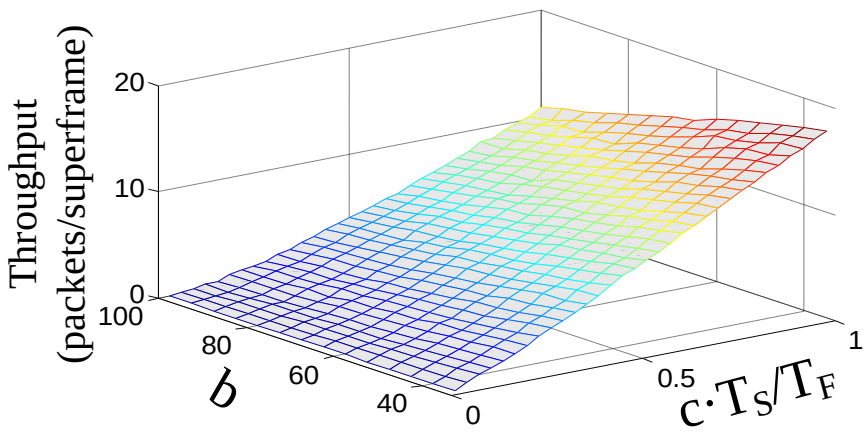

Figure 5.4. *Network throughput of CSMA/CA scheme.*

puts for N competing nodes with maximum queue length Q_n^{max} is $\binom{N+Q_n^{max}}{N} - \binom{N+\mu_c(N)}{N} - \binom{N+Q_n^{max}-\mu_c(N)}{N}$.

The proposed time slot allocation scheme makes use of $\Delta(b,c)$ to decide on slot allocation. Therefore, $\Delta(b,c)$ is calculated offline by simulation or analysis and is loaded in the coordinator in advance. In Figure 5.4, we present an example of $\Delta(b,c)$ for the CSMA/CA protocol used in the IEEE 802.15.4 [83]. Figure 5.4 implies that the values of $\Delta(b,c)$ depend largely on the length of the CSMA period $c \cdot T_S$.

5.3 Dynamic Time Slot Allocation Scheme

5.3.1 Queue Length Distribution

The time slot allocation scheme decides slot allocation based on the queue length information $\mathbf{V}_{t,n} = (U_{t,n}, J_{t,n})$. However, the exact queue length, $Q_{t,n}$, cannot be obtained from this queue length information since new packets may have arrived during $J_{t,n}$ superframes after the latest report came in. Therefore, the proposed scheme derives the distribution of the queue length instead of the exact queue length.

The queue length distribution is defined as the distribution of the queue length conditioned on the queue length information. The pmf of the queue length distribu-

tion of node n, given the queue length information $\mathbf{v} = (u, j)$, is

$$f_n^Q(q|\mathbf{v}) = \Pr[Q_{t,n} = q|\mathbf{V}_{t,n} = \mathbf{v}]. \tag{5.5}$$

No packet has been transmitted after the superframe in which the latest report is received and the number of arrived packets during j superframes is A_{n,jT_F}. Therefore, the queue length $Q_{t,n}$ given $\mathbf{V}_{t,n} = \mathbf{v}$ is $Q_{t,n} = \min\left\{\left(u + A_{n,jT_F}\right), q_n^{\max}\right\}$. Then, we can calculate $f_n^Q(q|\mathbf{v})$ as

$$\begin{aligned} &f_n^Q(q|\mathbf{v}) \\ &= \begin{cases} 0, & \text{for } q = 0, \ldots, u-1 \\ f_{n,jT_F}^A(q-u), & \text{for } q = u, \ldots, q_n^{\max}-1 \\ \sum_{i=q_n^{\max}}^{\infty} f_{n,jT_F}^A(i-u), & \text{for } q = q_n^{\max}. \end{cases} \end{aligned} \tag{5.6}$$

5.3.2 Formulation of a Utilization Maximization Problem

In this section, we formulate a utilization maximization problem in which we maximize the average number of packets transmitted within a superframe by optimally allocating slots to each node given the queue length information.

First, we derive the average number of packets transmitted by node n via the TDMA period when s slots are allocated to the node (i.e., $S_{t,n} = s$) and the queue length information is $\mathbf{V}_{t,n} = \mathbf{v}$, as follows:

$$\begin{aligned} \zeta_n(s, \mathbf{v}) &= \mathbb{E}[L_{t,n}|S_{t,n} = s, \mathbf{V}_{t,n} = \mathbf{v}] \\ &= \sum_{q=0}^{\infty} \min\{q, s\} f_n^Q(q|\mathbf{v}) = \sum_{i=1}^{s} \delta_n(i|\mathbf{v}) \end{aligned} \tag{5.7}$$

where $\delta_n(i|\mathbf{v}) = 1 - \sum_{q=0}^{i-1} f_n^Q(q|\mathbf{v})$. From (5.7), we can see that $\delta_n(i|\mathbf{v})$ is the increase of $\zeta_n(s, \mathbf{v})$ such that $\delta_n(s|\mathbf{v}) = \zeta_n(s, \mathbf{v}) - \zeta_n(s-1, \mathbf{v})$, and $\delta_n(i|\mathbf{v})$ decreases with increasing i. The decreasing nature of $\zeta_n(s, \mathbf{v})$ implies that the efficiency of a slot decreases as more slots are allocated.

Now, we consider the average number of request packets transmitted during the CSMA period provided $S_{t,n}$ and $\mathbf{V}_{t,n}$ $\forall n \in N$. That is,

$$\begin{aligned} \xi(\mathbf{s}, \bar{\mathbf{v}}) &= \mathbb{E}\left[|\mathcal{D}_t| \middle| \mathbf{S}_t = \mathbf{s}, \bar{\mathbf{V}}_t = \bar{\mathbf{v}}\right] \\ &= \sum_{b=0}^{\infty} \Delta(b, \omega - \mathbf{1}^T\mathbf{s}) f^B(b|\mathbf{s}, \bar{\mathbf{v}}) \end{aligned} \tag{5.8}$$

where b is the number of nodes participating in the CSMA period, $\mathbf{S}_t = (S_{t,0}, S_{t,1}, \ldots, S_{t,N})^T$, $\bar{\mathbf{V}}_t = (\mathbf{V}_{t,0}, \mathbf{V}_{t,1}, \ldots, \mathbf{V}_{t,N})^T$, $\mathbf{1}$ is the column vector of all ones, and $f^B(b|\mathbf{s}, \bar{\mathbf{v}})$ is the pmf of the distribution of $|\mathcal{B}_t|$ given that $\mathbf{S}_t = \mathbf{s}$ and $\bar{\mathbf{V}}_t = \bar{\mathbf{v}}$. Then, we have

$$\begin{aligned} f^B(b|\mathbf{s}, \bar{\mathbf{v}}) &= \Pr[|\mathcal{B}_t| = b | \mathbf{S}_t = \mathbf{s}, \bar{\mathbf{V}}_t = \bar{\mathbf{v}}] \\ &= \sum_{\mathbf{x} \in \mathcal{X}(b,\mathbf{s})} \prod_{n \in \mathcal{G}(\mathbf{s})} (x_n + (-1)^{x_n} f_n^Q(0|\mathbf{v})) \end{aligned} \tag{5.9}$$

where $\mathcal{X}(b, \mathbf{s}) = \{(x_0, x_1, \ldots, x_N)^T | \sum_{n=0}^N x_n = b,\ x_n = 0 \text{ for } n \neq \mathcal{G}(\mathbf{s}), \text{ and } x_n \in \{0, 1\} \text{ for all } n\}$ and $\mathcal{G}(\mathbf{s}) = \{n = 0, 1, \ldots, N | s_n = 0\}$.

In the following utilization maximization problem, we aim to maximize the average number of request packets and data packets transmitted via the CSMA and TDMA periods, respectively. Note that maximizing the CSMA throughput helps the coordinator receive the most recent queue length information of more nodes.

$$\text{maximize} \quad \xi(\mathbf{s}, \bar{\mathbf{v}}) + \textstyle\sum_{n=0}^N \zeta_n(s_n, \mathbf{v}_n) \tag{5.10}$$

$$\text{subject to} \quad \textstyle\sum_{n=0}^N s_n \leq s_{\max}. \tag{5.11}$$

In this optimization problem, we find $\mathbf{s} = (s_0, s_1, \ldots, s_N)^T$ to maximize the objective function (5.10).

5.3.3 Greedy Algorithm for Solving Utilization Maximization Problem

We propose a simple suboptimal greedy algorithm to solve the utilization maximization problem in (5.10)–(5.11). In the objective function (5.10), it is difficult to calculate the average number of packets transmitted via the CSMA period, i.e., $\xi(\mathbf{s}, \bar{\mathbf{v}})$. Therefore, we use an approximated $\xi(\mathbf{s}, \bar{\mathbf{v}})$, which is calculated by taking an average of b before substituting b into Δ as

$$\begin{aligned} \widehat{\xi}(\mathbf{s}, \bar{\mathbf{v}}) &= \Delta\big(\textstyle\sum_{b=0}^{\infty} b f^B(b|\mathbf{s}, \bar{\mathbf{v}}), \omega - \mathbf{1}^T\mathbf{s}\big) \\ &= \Delta\big(\textstyle\sum_{n \in \mathcal{G}(\mathbf{s})} (1 - f_n^Q(0|\mathbf{v})), \omega - \mathbf{1}^T\mathbf{s}\big) \end{aligned} \tag{5.12}$$

where $\sum_{n \in \mathcal{G}(\mathbf{s})} (1 - f_n^Q(0|\mathbf{v}))$ is the average number of nodes participating in the CSMA period.

Motivated by the decreasing increment of $\zeta_n(s, \mathbf{v})$, we propose **Algorithm 3** to maximize $\widehat{\xi}(\mathbf{s}, \bar{\mathbf{v}}) + \sum_{n=1}^{N} \zeta_n(s_n, \mathbf{v}_n)$. In each iteration, **Algorithm 3** allocates one slot to node n, for which the increment of $\zeta_n(s, \mathbf{v})$ is the highest. The average number of packets transmitted via the CSMA period $\widehat{\xi}(\mathbf{s}, \bar{\mathbf{v}})$ decreases if one more slot is allocated for the TDMA period. Therefore, a slot is allocated only when the increment of $\zeta_n(s, \mathbf{v})$ exceeds the decrement of $\widehat{\xi}(\mathbf{s}, \bar{\mathbf{v}})$ in this algorithm. In this algorithm, a node attempts to transmit a request packet through the CSMA period only if a slot is not allocated.

Algorithm 3 Utilization maximization algorithm

$b \leftarrow \sum_{n=0}^{N}(1 - f_n^Q(0|\mathbf{v}))$
$c \leftarrow \omega$
$s_n \leftarrow 0$ for $n = 0, 1, \ldots, N$
$\delta_n \leftarrow 1 - f_n^Q(0|\mathbf{v})$ for $n = 0, 1, \ldots, N$
repeat
  $n^* \leftarrow \text{argmax}_{n=0,1,\ldots,N}\, \delta_n$
  $\alpha \leftarrow \delta_{n^*}$
  if $s_{n^*} = 0$ **then**
    $\beta \leftarrow \Delta(b - (1 - f_{n^*}^Q(0|\mathbf{v})), c - 1) - \Delta(b, c)$
  else
    $\beta \leftarrow \Delta(b, c - 1) - \Delta(b, c)$
  end if
  if $\alpha + \beta > 0$ **then**
    if $s_{n^*} = 0$ **then**
      $b \leftarrow b - (1 - f_{n^*}^Q(0|\mathbf{v}))$
    end if
    $c \leftarrow c - 1$
    $s_{n^*} \leftarrow s_{n^*} + 1$
    $\delta_{n^*} \leftarrow \delta_{n^*} - f_n^Q(s_{n^*}|\mathbf{v})$
  end if
until $\mathbf{1}^T\mathbf{s} < s_{\max}$ **and** $\alpha + \beta > 0$
return $\mathbf{s}$

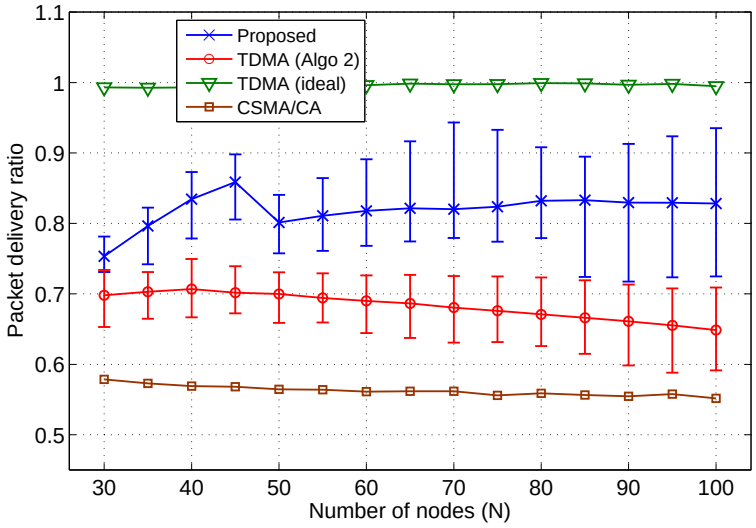

Figure 5.5. *Average packet delivery ratio for different network sizes ($N \geq \omega - 2$). The error bar shows the maximum and minimum values.*

5.4 Performance Evaluation

We assume that there is neither hidden node collision nor packet error. The smallest unit of time, which is called unit backoff period (UBP), is $230\mu s$[6]. We set the beacon length to 4 UBP. The slot length is $T_S = 12$ UBP which is long enough to transmit one packet and receive the acknowledgment. The size of a request packet is 2 UBP. We set $\omega = s_{max} = 32$ and $q_n^{max} = 5$. We assume $\lambda_n = \omega/N$ (packets/superframe) for each node n and there is only one packet in each batch. For slotted CSMA, we set the contention window to $[32, 64, 128, 128, \cdots]$ and we assume there is no packet drop due to the limit on the number of retransmissions or the number of backoffs. We consider uplink communications from the devices to the coordinator. The results are based on the average of four repeated simulations, each of which is 5000 superframes long.

For comparison purpose, we consider a slotted CSMA/CA scheme in which we set $C_t = \omega$. The CSMA/CA is very robust to the changes in traffic and in network size. We also consider a hybrid CSMA/CA-TDMA scheme which uses **Algorithm 4** (denoted as "TDMA (Algo 2)" in Figure 5.5). It differs from the proposed algorithm in that it does not consider the distribution of the queue length. In Figure 5.5, "TDMA

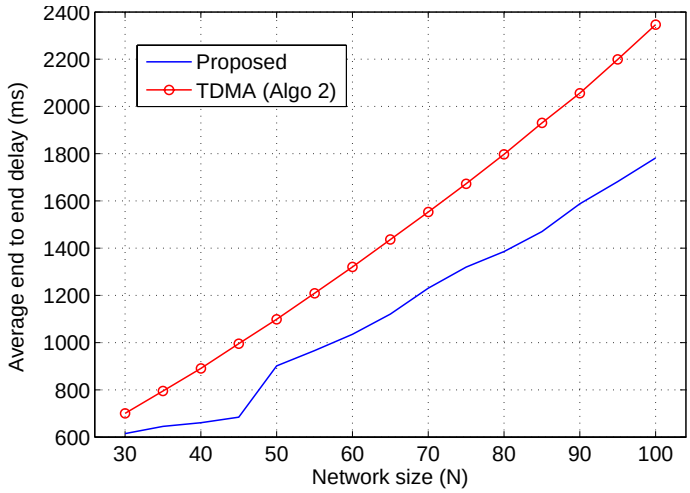

Figure 5.6. *Average end to end delay for different network sizes ($N \geq \omega - 2$).*

Algorithm 4 A dynamic time slot allocation algorithm

1: $s_n \leftarrow 0$ for $n = 0, 1, \ldots, N$
2: $\mathbf{U}_t = (u_{t,1}, \cdots, u_{t,N})$
3: **repeat**
4: $\quad n^* \leftarrow \text{argmax}_{n=0,1,\ldots,N} \mathbf{U}_t$
5: $\quad s_{n^*} \leftarrow s_{n^*} + 1$
6: $\quad u_{t,n^*} = u_{t,n^*} - 1$
7: **until** $\mathbf{1}^T\mathbf{s} < s_{\max}$ **and** $\mathbf{1}^T\mathbf{U}_t > 0$
8: **return** $\mathbf{s}$

(ideal)" represents **Algorithm 4** when the coordinator has the exact information of the queue lengths of the nodes.

Figure 5.5 shows that the proposed scheme (**Algorithm 1**) achieves better throughput than the "TDMA (Algo 2)" for larger networks ($N \geq \omega - 2$) under the uncertainty of queue length in each node. The reason behind this is that the nodes require higher number of time slots than actually requested in the latest report. The proposed algorithm tries to allocate more TDMA slots to the nodes without worsening the channel utilization. However, for a small network size (i.e., $N < \omega$), when the packet arrival rate becomes high (i.e., $\lambda_n = \omega/N$), the nodes have enough packets to fill the slots. In this case, "TDMA (Algo 2)" works well. Figure 5.6 shows that the proposed scheme

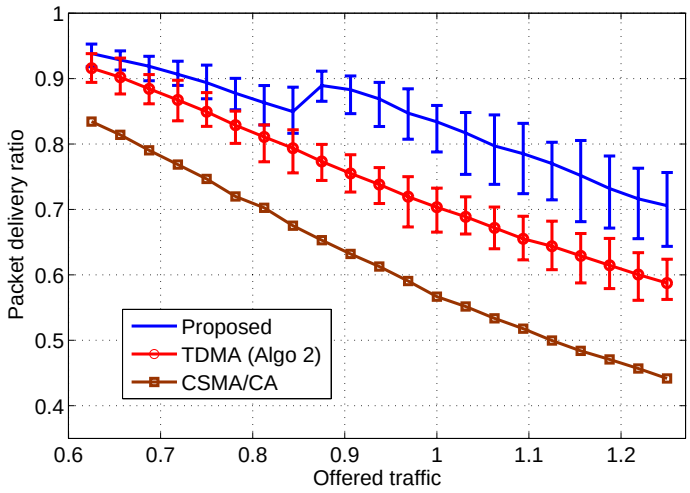

Figure 5.7. *Average packet delivery ratio for different traffic load ($N = 40$).*

also provides better performance in terms of end to end delay than " TDMA (Algo 2)". Similarly when the traffic load is varied for network size, the proposed schemes shows improvement in throughput as shown in Figure 5.7.

5.5 Chapter Summary

In a hybrid CSMA/TDMA MAC protocol under a non-deterministic traffic scenario, a semi-static time slot allocation method underutilizes the bandwidth and cannot satisfy the time slot requests from several devices. We have proposed a queue-length-based dynamic time slot allocation scheme which takes into account the dynamics of a traffic pattern to maximize the utilization. The simulation results show the effectiveness of the proposed scheme. This model is useful for a protocol such as the IEEE 802.15.3c MAC protocol, where time slots are allocated based on the requests from the devices.

Chapter 6

Hidden Node Collision Mitigated Multihop Wireless Sensor Networks

6.1 Introduction

In carrier-sense multiple access with collision avoidance (CSMA/CA)-based multihop wireless networks, the hidden node collision problem may degrade network performance significantly [85]. Two nodes which are out of their carrier sensing range may transmit packets causing collision to a destination node. The request-to-send (RTS)/clear-to-send (CTS)-based handshaking method can mitigate this problem to a large extent. However, it is unable to eliminate the collision completely in the network. There is still chance of collision between RTS message and data message, or CTS message and data message in this handshaking method [86].

The IEEE 802.15.4 standard provides a low data-rate and low-power standard medium access control (MAC) protocol suitable for wireless sensor networks. In the non-beacon-enabled mode, it uses an un-slotted CSMA/CA scheme and it does not require any synchronization among the nodes. In the beacon-enabled mode, it uses slotted CSMA/CA scheme where time is divided into superframes each of which is further divided into sixteen equal slots. The smallest time unit is a backoff unit which is equal to twenty symbols. A coordinator broadcasts a beacon at the beginning of the superframe to synchronize the nodes in the network. A superframe consists of an active period and an inactive period. The active period is divided

into contention access period (CAP) and contention-free period (CFP). During CFP, nodes use guaranteed time slot(s) to transmit their packets without using CSMA/CA. During CAP, nodes transmit packets using CSMA/CA. A node uses random backoff before performing carrier sensing. When the backoff counter reaches zero, it starts clear channel assessment (CCA). If the channel is idle, it goes for a second CCA. The node transmits after the channel is observed to be free in the second CCA; otherwise, it returns to the backoff stage. A node considers a packet transmission to be unsuccessful when the waiting time for acknowledgment expires. In low-power wireless networks such as the IEEE 802.15.4 networks [6], RTS and CTS message consume significant amount of energy which is undesirable. Therefore, 802.15.4 networks are affected significantly by the hidden node collision problem.

In this chapter, we present a cellular-like network model to mitigate the hidden node collision in multihop CSMA/CA networks such as the IEEE 802.15.4-based wireless sensor networks. The proposed model is suitable for high density wireless sensor networks where nodes are vulnerable to hidden node collisions. It does not incur any control overhead. The contributions of the chapter can be summarized as follows:

- Modeling the cellular layout of a multihop wireless sensor networks,
- Analysis of signal-to-interference ratio (SIR) to mitigate hidden node collisions in the network,
- Application of the proposed model to IEEE 802.15.4 MAC-based wireless sensor networks, and
- Estimation of the size of the network based on the proposed model conditioned on the traffic flow capacity.

The rest of the chapter is organized as follows. Section 6.2 reviews the related work. Section 6.3 presents the details of the cellular layout of the network. Section 6.4 presents the application of the model in the IEEE 802.15.4-based wireless sensor networks. Section 6.5 analyzes the capacity of the multihop network based on the proposed model. Section 6.6 presents the performance evaluation results. Finally, Section 6.7 summarizes the chapter.

6.2 Related Work

The hidden node collision problem has been extensively studied in the literatures [87]. A survey of different solutions to hidden node collision problem is presented by Kosek [87]. In single-hop networks, hidden node collision can be avoided by placing nodes within the carrier-sensing range of each other. For multihop networks, some of the common solution approaches to this problem include time-division multiple access (TDMA), cluster formation, and spatial reuse in time or frequency domain [88], [89], [90], directional antenna approach [91], and routing scheme [92]. TDMA [10] is inherently a collision-free transmission method. Although it is suitable for low-density networks, it is not scalable in the network. In multiple cluster networks, the nodes transmit their packets to their cluster head and can avoid the hidden node collision [88]. However, communications among cluster heads bring complexity in the system.

Collisions can be avoided by grouping the hidden and exposed nodes and scheduling their transmissions. In a model proposed by Kobatake and Yamao [89], cluster tree network is divided into subnet groups which are assigned different time slots for transmission to reduce interference. However, the method does not guarantee required signal to interference ratio. The centralized grouping strategy presented Hwang et al. [90] is suitable for single-hop networks. The routing scheme proposed by Parvin and Fujii [92] incurs control overhead in the network whereas the methods based on directional antenna [91] add hardware complexity in the nodes. Interference cancellation methods [93] can also help reduce the hidden node collision at the cost of high processing complexity to retrieve amplitude and phase of the required signal. Another method to mitigate hidden collision is to control the carrier-sensing range [94], [95]. However, a larger carrier-sensing range decreases the spatial reuse and may also suffer hardware limitation. Also, the network requires to minimize the effects of exposed node problem [96], [97].

6.3 A Cellular Layout for CSMA/CA-based Multihop Wireless Sensor Networks

6.3.1 Network Model

We consider a CSMA/CA-based multihop wireless sensor network which is divided into cells (Figure 6.1). Each node transmits its packets to a next hop node in the same cell or different cell using CSMA/CA scheme in the same channel. Let r denote the number of tiers of the cellular structure. The total number of cells in the network is $\sum_{i=0}^{r} 6i + 1$. Let n denote the number of nodes per cell. The network size is given by: $N = n\,(3r^2 + 3r + 1)$.

We also assume that each node is identified by its coordinates (Υ, θ) and each node knows its one-hop neighbors and locations of the nearest co-cells. We assume that nodes collect information of neighbors and co-cells in the network during neighbor discovery phase. The radius of the cell is determined by the transmission range x of the nodes. Note that signal attenuation due to channel fading changes the transmission range x and hence the radius of the cell. We assume channel fading does not vary in the network.

Using the radius and centres of the cells, a node identifies its cell and co-cells. The cells are categorized into seven groups. This is a classical seven frequency reuse planning concept used in cellular system. There exists a unique pattern of numbering the whole network with seven numbers such that each number is reused two cells away as shown in Figure 6.1. We also assume time is divided into superframes and the superframe is further divided into slots. Each type of cell is assigned a time slot and is activated for transmission during the assigned time slot. However nodes can receive packets any time (i.e., can be in low-power listening mode).

6.3.2 Node Mobility

When a new node joins the network, it needs to identify the cell, co-cells and assigned time slot for the cell. For this purpose, we assume that there is some mechanism such as periodic beacon transmission by a node (or the head) of the cell. The node exchanges messages with the neighbors to get their locations. When a node moves, it

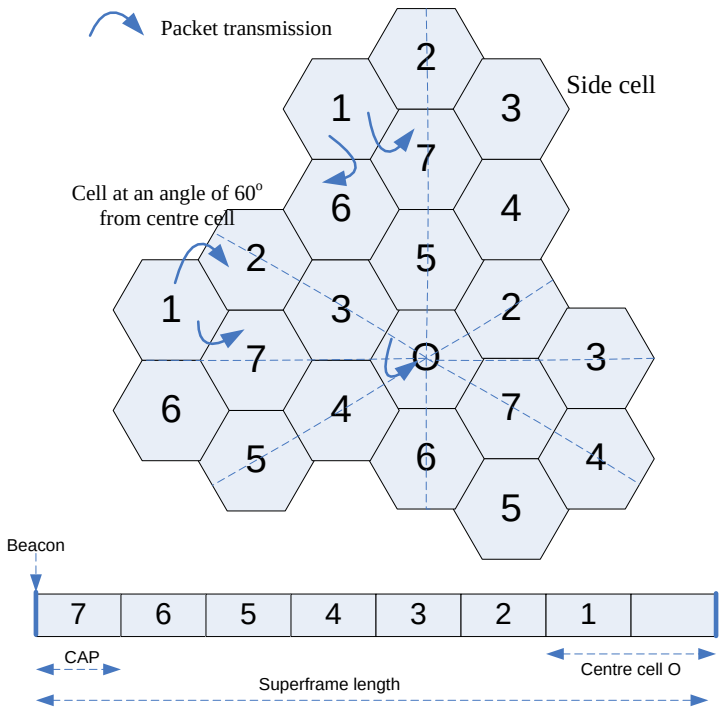

Figure 6.1. *Cellular layout of the network with scheduling of cells.*

has to broadcast its new location to the neighbors. When the node moves to another cell then it will be a newly joined node in the cell. When a node does not receive acknowledgment for the transmitted data from its next hop node for more than ℓ number of times, it considers the node to be dead or inactive. In case a cell head becomes inactive, a node sends a request message with its distance to the centre of the cell to be cell head. A node with shortest distance to the centre of the cell is declared to be cell head. Although the proposed model is valid under node mobility, we do not consider node mobility explicitly in this work.

6.3.3 Hidden Node Collision (HNC) Mitigation

A node wishing to transmit packet to the destination determines the direction of transmission or side of the cell toward which packet would be transmitted. This can be done by calculating the angle that the sender and destination node make with centre of the cell. Among the neighbors toward the desired side of the cell, a node

chooses next hop node if the signal-to-interference ratio (SIR) remains above the desired threshold.

When the next hop node is in the same cell, there will be negligible interference or no hidden collisions. It is because only those nodes in the co-cells which are more than two hop away transmit data at the same time. If next hop node is in another cell, it might be interfered from the acknowledgment transmissions in another cells which are not the co-cells. This is because when a node receives a packet, it has to send an acknowledgment to the sender even if it is not the owner of the portion of CAP.

Since a node wishing to transmit knows the location of the next hop node, it can estimate the worst-case interference at the receiver from the interfering node of the co-cells. A node can calculate the distance of the next hop node from the closest point of the co-cells. Using the distance-dependent path-loss model, the node calculates the received power because transmitting power is assumed to be same for all nodes. Therefore, hidden node collision can be mitigated by selecting the next hop node with acceptable SIR. The details of the next hop selection procedure is explained in the next section.

6.3.4 Selection of Next Hop Nodes

Based on the assumption that each node knows the location (coordinates) of its one hop neighbors and centres of its co-cells, it is possible that each node determines the next hop nodes to transmit packets such that the hidden node collision does not occur. We present a simple distributed algorithm (**Algorithm 1**) to choose the next hop node in the region where SIR of φ is achieved. **Algorithm 1** generates an output *false* if the next hop node $Q(q_1, q_2)$ is in the collision region from the co-cell nodes. Let us first derive the condition to guarantee the SIR.

Let d_{AB} denote distance between point A and point B. As shown in Figure 6.2, a node wishing to transmit has two interfering nodes from two co-cells. Let (p_1, p_2) be the coordinates of the node P wishing to transmit packet to Q. Let (q_1, q_2) be coordinate of the next hop node Q. Let (u_1, u_2) be the location of nearest interfering node U in the co-cell and (r_1, r_2) be the location of interfering node R for Q. Now hidden node collision may occur when node R, the next hop node of node U, sends

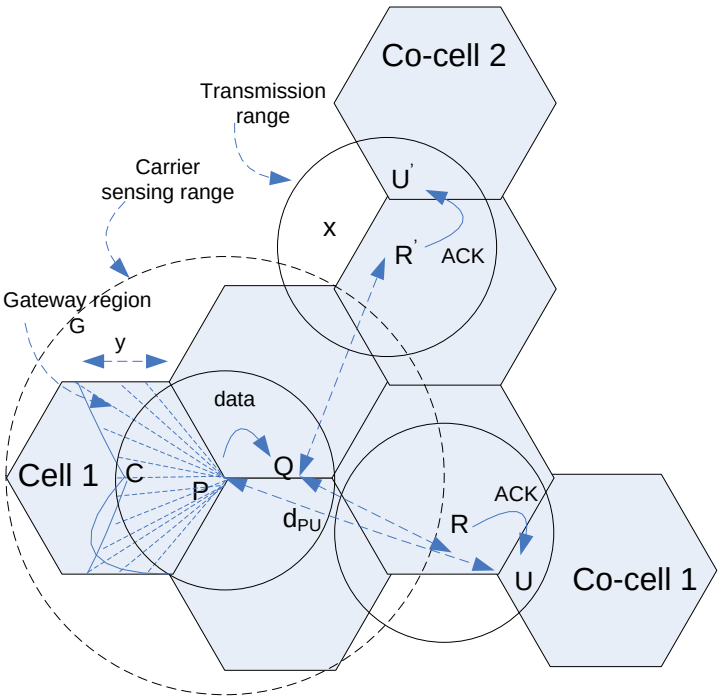

Figure 6.2. *The worst-case interference scenario for receiver Q.*

acknowledgment packet and reduces the SIR at next hop node Q below threshold φ. Similarly, R', the next hop node of U' in another co-cell, affects SIR at Q. We ignore negligible amount of interference from the nodes in the rest of the co-cells in the network since they are out of interference range. Therefore, we consider interference from two co-cells in each side of the cell.

Let x denote transmission range. We consider the following path-loss model: $P_r \propto \frac{P_t}{\mathcal{D}^\gamma}$, where P_r is the received power, P_t is the transmitted power, $\mathcal{D}$ is distance, and γ is path-loss exponent. If φ is the SIR threshold then for a node P at distance d_{PQ} from next hop node Q, we require

$$\frac{d'}{d_{PQ}^\gamma} \geq \varphi \tag{6.1}$$

where $d' = \frac{d_{QR}^\gamma d_{QR'}^\gamma}{d_{QR}^\gamma + d_{QR'}^\gamma}$. This is the worst-case scenario when the nearest nodes R and R' in different cell transmit acknowledgment packets at the same time node Q is receiving packet. It is possible to find the distance d_{QR} accurately by determining the location of the nearest interfering node U in the co-cell. Note that U can be

determined if centre of the co-cell is known. In the neighbor discovery phase, nodes can gather information about the nearest interfering nodes from the co-cells. Gupta and Kumar [98] also introduced the distance and SIR relationship to calculate the network capacity assuming that nodes can transmit ω bits of data per second.

Let P, U, and U' denote the closest nodes at the boundary of the co-cells as shown in the Figure 6.2. From simple geometry, we calculate that $d_{CU} = 3.6055x$, $d_{PU} = 2.645x$. For inter-cell transmissions, we require the carrier sensing range be less than $2.645x$. Considering the worst-case scenario, the maximum distance of next hop node from boundary d is then $d_{PQ} = d_{RU} = d_{R'U'} = d$. From (6.1),

$$d^{\gamma} \leq \frac{(d_{QR}^{\gamma})(d_{QR'}^{\gamma})}{\varphi(d_{QR}^{\gamma} + d_{QR'}^{\gamma})}. \tag{6.2}$$

The node Q in Figure 6.2 receives larger interference from R than R' because $d_{QR} < d_{QR'}$. To find out the closed-form solution at the worst case scenario, we consider $d_{QR} = \min(d_{QR}, d_{QR'})$. From the geometry in Figure 6.2, the minimum value of d_{QR} is taken to be $2.598x - 1.866d$, where d can be expressed as $d \leq \frac{2.598x - 1.866d}{(2\varphi)^{1/\gamma}}$. Considering small margin in SIR, we express d as

$$d \leq \frac{2.598x}{1.866 + (2.5\varphi)^{1/\gamma}}. \tag{6.3}$$

Assume that a source node P and destination node Q are in random positions in the cell. Then we need to find out location of the nearest interfering node U to estimate d_{QR}. In case the location of node U is unknown, transmitting node P has to make sure that condition (6.3) is satisfied to guarantee the required SIR at the node Q (i.e., $d_{PQ} \leq d$). In case the location of node U is known, the condition is given by

$$d_{PQ} \leq \frac{(d_{QU} - d)(d_{QU'} - d)}{(\varphi\left((d_{QU} - d)^{\gamma} + (d_{QU'} - d)^{\gamma}\right))^{1/\gamma}} \tag{6.4}$$

where d is given by (6.3).

Consider, for an example, $\gamma = 2$ for free-space propagation. Then, for an SIR requirement of 6 dB (e.g., in IEEE 802.15.4 with negligibly small noise power), we have $d = 0.51x$. This indicates that there would be no hidden node collision in the multihop CSMA/CA transmission if nodes are close to each other within the distance $0.51x$ when the transmission range is x.

Algorithm 5 Next hop selection

Input: source node $S(s_1, s_2)$**, next hop node** $Q(q_1, q_2)$**, transmission range** x**,** φ**, and** γ.
Output: NextHop
NextHop = false
find $d = \frac{2.598x}{1.866+(2.5\varphi)^{1/\gamma}}$
case 1: UNKNOWN co-cells
  if $d_{SQ} \leq d$ **then**
    NextHop = true
  end if
case 2: KNOWN closest points to co-cells $U(u_1, u_2)$ and $U'(u'_1, u'_2)$
  if $d_{SQ} < \frac{(d_{SU}-d)(d_{SU'}-d)}{(\varphi((d_{SU}-d)^\gamma+(d_{SU'}-d)^\gamma))^{1/\gamma}}$ **then**
    NextHop = true
  end if

We can also consider different propagation models to find out the hidden node collision free region. For example, let the path-loss model be represented by $P_{L,0}^{dB} + 10\gamma \log 10(\frac{d_{PQ}}{d_0}) + S_{PQ}^{dB}$, where $P_{L,0}^{dB}$ is the free-space path-loss at the reference distance d_0 and S_{PQ}^{dB} is a random variable for the link PQ which follows a zero mean log normal distribution with standard deviation of σ_{PQ}^{dB}. Due to the environment conditions, links may have variations in the mean value of random number. In the absolute term, the condition to satisfy the SNR requirement can be calculated as

$$d_{PQ} \leq \frac{(d_{QU} - d)(d_{QU'} - d)(S_{QU}S_{QU'})^{1/\gamma}}{(\varphi S_{PQ}\left((d_{QU} - d)^\gamma S_{QU} + (d_{QU'} - d)^\gamma S_{QU'}\right))^{1/\gamma}}. \tag{6.5}$$

If the variable is constant and same for each link, the condition is similar to (6.4). When fading occurs, interference from co-cell becomes less severe; however, nodes within the same cell become vulnerable to hidden node collisions. In this case, we need to figure out the appropriate size of the cell based on the transmission range and carrier-sensing range in presence of fading. However, we do not consider the variation in the fading in this work.

6.4 Application of the Model to the IEEE 802.15.4-Based Networks

6.4.1 IEEE 802.15.4-Based Multihop Sensor Networks

Assume an IEEE 802.15.4-based wireless sensor network with the beacon-enabled CSMA/CA MAC protocol. In order to start transmission, nodes in the network have to complete the neighbor discovery phase and the synchronization phase [10]. In the neighbor discovery phase, each node gathers information about its one-hop neighbors. This can be done by sending hello message over a time duration. The sink node or main control node at the centre cell has the coordinate $(0, 0)$. It transmits a beacon with the information of cell ID and coordinates of centre points of its six neighbor cells. The coordinates include radius and angle. Each cell calculates the distance from the sink node and determines its cell ID. Each node broadcasts its cell ID and its distance from the centre of its cell. The node having the minimum distance declares itself to be cell-head. This process propagates to the outermost cell until a node at this cell declares itself to be head. Each cell head helps synchronize other nodes in the cell by transmitting information of superframe structure in the beacon frame. However, nodes can transmit data packet to any other node inside or outside the cell.

After the neighbor discovery phase, the cell heads are synchronized with the clock of the sink node at the centre cell in the synchronization phase. However, we assume that nodes do not require association with the cell head.

6.4.2 Scheduling of Cells

Time is divided into superframes. Each superframe is divided into eight equal slots. As shown in Figure 6.1, each cell is assigned a slot. Each cell is activated for data transmission using CSMA/CA in its allocated slot. This implies that this method allows nodes to transmit packets with maximum duty cycle of 0.125, and during the rest of the cycle the nodes receive or goes to low power listening mode. On the other hand, for the centre cell O, two slots are allocated to cope up with high traffic and the transmission duty cycle is 0.25. To increase the spatial reuse, nodes in the co-cells

remain active for transmission. We assume that if the allocated slot of superframe is not for the node, it is allowed to transmit only acknowledgment packet after reception of the data packet.

6.5 Analysis of Network Size

We analyze the average traffic flow per node in a sensor network. Let us consider the case of path-loss exponent $\gamma = 3$. Each node generates data at the allowed maximum rate of λ (e.g., packets per second). We assume IEEE 802.15.4 MAC in the beacon-enabled mode. The nodes transmit with duty cycle of 0.125 except the nodes at the centre cell transmitting with duty cycle of 0.25 as shown in the superframe structure in Figure 6.1. Assuming $\varphi = 6$ dB (SNR requirement is 5 dB for IEEE 802.15.4 at 1% bit error rate [6]), from (6.3) we obtain $d_{PQ} < 0.64x$.

We find that the next hop node Q can be as far as $0.64x$ from the sender P at the border of the cell. As shown in Figure 6.2, nodes in the gateway region (i.e., the region where inter-cell transmission occurs) can transmit packets to next hop nodes in another cell closer to the centre cell. The throughput of the cell is the incoming traffic to the next hop cell. The throughput of the cell depends on the number of gateway nodes in the gateway region. Assuming a node which is $y < x$ (e.g., $y = 0.64x$) distance away from the border of cells can transmit packets to the nodes in the cells closer to sink. The area of gateway region in Figure 6.2 is $\sqrt{3}yx$. Considering uniform distribution of n nodes in a cell, the number of gateway nodes is given as $g = \frac{2y}{3x}n$.

Based on this analysis, our goal is to design a stable CSMA/CA multihop network with tier size r. For this we determine how many tiers (r) exist in the network of cell size n such that nodes nearby or in the centre cell are not over-loaded by the traffic or do not go into saturation. We need to determine the throughput (T) from each cell. In the IEEE 802.15.4 slotted CSMA/CA MAC, T depends on duty cycle, CAP size, superframe duration, number of nodes, and packet arrival rate. To determine the throughput for the IEEE 802.15.4 slotted CSMA/CA MAC, analytical models proposed by Jung et al. [99] and Park et al. [42] can be used. However, in this chapter, we assume that a look-up table is available for throughput with respect to duty cycle (D), number of nodes (n), and packet arrival rate (λ) for given value of

CAP and superframe duration, i.e., $T = f_T(n, \lambda, D)$.

Let us use subscript m to denote the cells aligned with centre cell at an angle of 60^o and k to denote the rest of the side cells. Let us denote by $I(i)$ the incoming traffic to the i^{th} cell and by $T(i)$ the throughput of the cell i. Then in the cell $i = r$, $I_k(r) = I_m(r) = 0$, $T_k(r) = T_m(r) = gf_T(n, \lambda, 0.125)$. We assume that the incoming traffic in the cell is propagated toward the centre cell and traffic per node is approximated as $\lambda + \frac{I(i)}{n}$. Then for $i \in [r-1, 2]$,

$$
\begin{aligned}
I_k(i) &= T_k(i+1) && (6.6)\\
I_m(i) &= T_m(i+1) + T_k(i+1) && (6.7)\\
T_k(i) &= gf_T(n, \lambda + \frac{I_k(i)}{n}, 0.125) && (6.8)\\
T_m(i) &= f_T(n_1, \lambda + \frac{I_m(i)}{n}, 0.125). && (6.9)
\end{aligned}
$$

The cell corresponding to $i = 1$ represents the centre cell. The centre cell is surrounded by six cells. Therefore, $I_k(2)$ and $T_k(2)$ do not exist. Since the nodes in the centre cell have the transmission duty cycle of 0.25,

$$
\begin{aligned}
I_m(1) &= 6T_m(2) && (6.10)\\
T_m(1) &= nf_T(n, \lambda + \frac{I_m(1)}{n}, 0.25).
\end{aligned}
$$

If $r = 1$ then $I_m(1) = 0$. We assume $g > 2$ to maintain connectivity in the network. Let $\lambda_m = \lambda n + I_m(1)$ be the total traffic in the centre cell. Let $\mathcal{F}$ be the flow capacity of the superframe with transmission duty cycle of 0.25. To avoid heavy congestion and packet dropping, we require $\lambda_m \leq \mathcal{F}$. The incoming traffic $I_m(1)$ for the given number of tiers should not go into saturation. The conditions give a stable CSMA/CA multihop network that supports the maximum number of tiers r^*. Note that the higher the number of tiers, the larger is the size of the network.

6.6 Performance Evaluation

We evaluate the performance of the proposed network model by using simulations in MATLAB. We generated a table for average throughput with respect to number of competing nodes, data rate, and duty cycle for the IEEE 802.15.4 MAC standard.

We set the superframe order (SO) and beacon order (BO) to 4. The required duty cycle is achieved by setting contention size accordingly. We set the data packet size to 6 unit backoff period (UBP), RTS/CTS to 2 UBP and acknowledge packet to 1 UBP. We assume that the packet arrivals follow a Poisson distribution. We use the default values for the 802.15.4 parameters. In the first part, we present numerical analysis of network size for the proposed multihop wireless network. In the second part, we present the simulation-based comparison of the proposed cellular-like model with the RTS/CTS (a popular solution to hidden node collision) model and the pure slotted CSMA/CA model.

Figure 6.3 shows numerical analysis of the network size when traffic of nodes is varied. In the network, higher number of tiers (higher number of nodes) exists for low data-rate condition. Figure 6.3 also indicates that when the transmission range (i.e., size of cell n) is reduced, larger number of cells and hence larger network size can be achieved for given n.

For the comparison purpose, we set the transmission range to $x = 10$ and the carrier-sensing range to $2x$. We consider $\varphi = 5$, $\gamma = 2$ at the frequency 2.4 GHz. We deploy the $N = 63$ nodes as shown in Figure 6.4. We assume the N^{th} node in the centre is sink. Each node transmits a packet to the next hop node closer to the sink. We define the packet delivery ratio (PDR) of the network as the ratio of total packets received by the sink to the total number of packets generated by all the nodes.

From Figure 6.5, we see that the RTS/CTS mechanism has slightly better PDR at lower packet rate. When the packet rate increases, RTS/CTS is not able to completely avoid hidden node collision and also suffers from the exposed node problem (i.e., due to the CTS message, nodes outside the carrier-sensing range are required to defer their transmission). Therefore, PDR decreases when the packet rate increases. Slotted CSMA/CA does not have the exposed node problem but is vulnerable to hidden node collisions. The reason that the proposed model has slightly lower PDR at lower packet arrival rate is that nodes transmit with duty cycle of 0.125 while nodes in other model attempt to transmit at any time. Therefore, the proposed model has lower power consumption in the nodes as shown in Figure 6.6. The power consumption curve is almost flat above 1 packet/sec since nodes transmit in their assigned contention period. Note that the proposed model mitigates only hidden

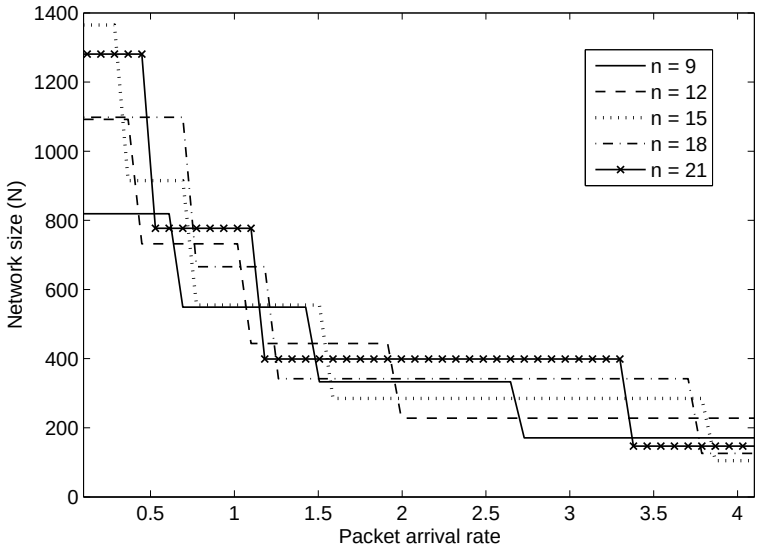

Figure 6.3. *Network size for different traffic load (number of nodes and packet arrival rate).*

node collisions. Therefore, the chance of collisions between nodes in the same cell because of starting carrier sensing at same time remains.

6.7 Chapter Summary

We have proposed a network model to mitigate the hidden node collision problem in multihop CSMA/CA networks such as the IEEE 802.15.4-based networks. A node can be put into one of seven regions and assigned one of seven parts of the CAP in the superframe. Assuming that the location (Υ, θ) is the identity of a node, the nodes can self-organize into the regions during neighbor discovery phase. Based on this model, the distance between a sender and the receiver can be found which guarantees the required SIR at the receiver in the worst-case condition in presence of distance-dependent signal attenuation as well as shadowing. This model will be useful for the design of efficient (in terms of network size and flow capacity) multihop CSMA/CA networks.

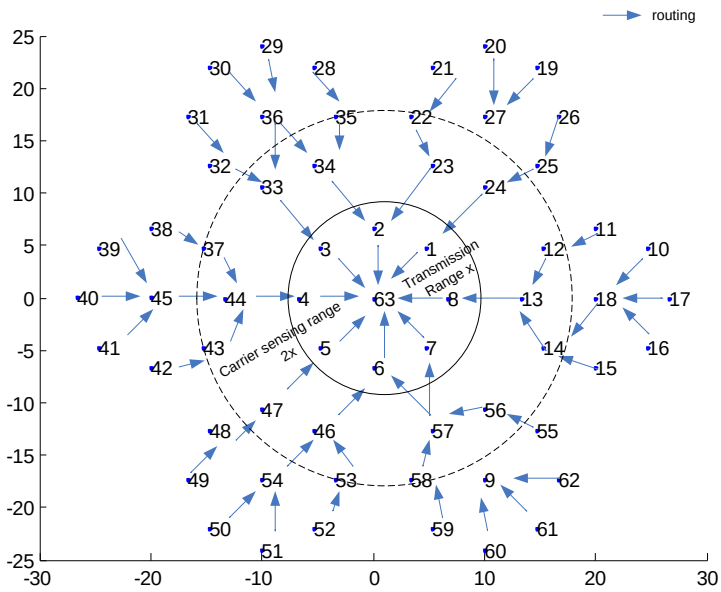

Figure 6.4. *Deployment of nodes in the network (for simulations).*

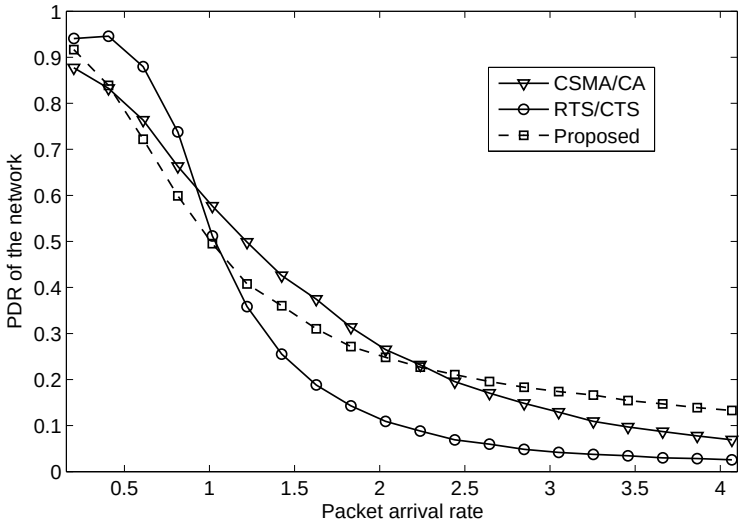

Figure 6.5. *Average packet delivery ratio of the network.*

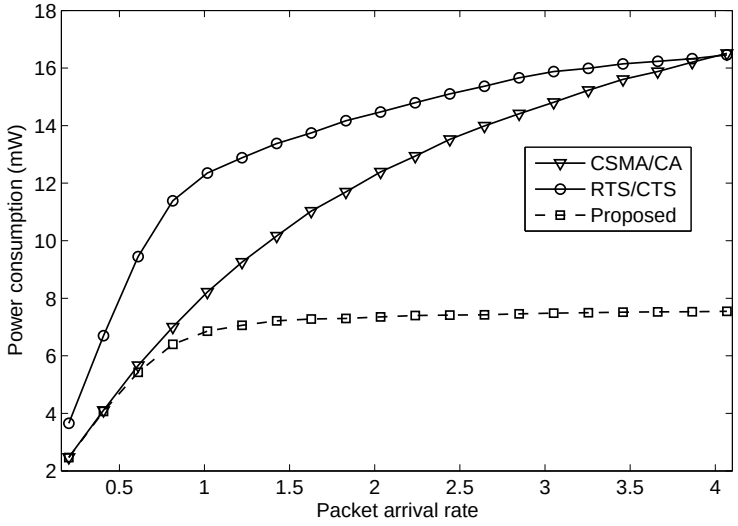

Figure 6.6. *Power consumption per node in the network (assuming power consumption during transmit mode, receive mode, and idle mode to be 31.32 mW, 33.84 mW, and 766.8 μ W, respectively [46]).*

Chapter 7

Summary and Discussions

For wireless sensor networks such as wireless body area networks, hybrid CSMA/CA-TDMA protocols such as the IEEE 802.15.4 MAC protocol is an attractive channel access protocol. It is because the hybrid MAC protocol derives the benefits of both the CSMA/CA MAC and TDMA MAC protocols. However, the hybrid MAC protocols such as the IEEE 802.15.4 MAC protocol in its current state of art does not bring its full benefits to the network. Careful design of such hybrid MAC protocol is necessary to improve both the energy efficiency and packet delivery performance. The TDMA slot allocation algorithm as well as the CSMA/CA and TDMA periods should be adapted with the requirement of the network. Such a hybrid MAC protocol requires a coordinator to handle the devices associated with it. Therefore, the design of such a hybrid MAC protocol should be able to handle multiple coordinators in the network as well. In this work, we have proposed a set of solutions to address the above mentioned problems to improve the performance of a wireless sensor network using hybrid CSMA/CA-TDMA scheme in terms of throughput and energy efficiency.

In this chapter, we summarize the contributions of the thesis in Section 7.1 and outline a few directions for future research work in Section 7.2.

7.1 Summary of Contributions

In **Chapter 2**, we have developed a Markov decision process (MDP)-based Distributed Channel Access (MDCA) scheme which takes buffer status of the devices as an indication of congestion. The policy of the scheme by solving MDP maps the buffer state of the nodes to the best action to be taken. A node develops the transmission policy based on its own buffer status. The proposed distributed scheme

provides a method to change the legacy CSMA/CA channel access scheme to hybrid CSMA/CA-TDMA channel access scheme and improves the performance of the sensor devices in terms of packet delivery ratio and energy consumption rate. Since policy can be developed offline, this scheme is applicable to sensor device with low processing power. We have also developed an MDP-based Centralized Channel Access (MCCA) scheme in which a coordinator develops the transmission policy based on the information of buffer status of all the devices. Such policy of the scheme improves the energy consumption rate compared to the existing hybrid CSMA/CA-TDMA schemes by putting the sensor devices with relatively low buffer levels to low power mode without degrading the throughput and delay performance of the devices in comparison with existing centralized hybrid channel access schemes. The centralized scheme performs better than the distributed scheme because of the knowledge of the traffic loads of all devices in the network. This scheme stands as the benchmark for a hybrid CSMA/CA-TDMA scheme. Since congestion in the network can also result due to channel fading, we have also provided a methodology to take into account the effect of channel fading in the proposed schemes.

In **Chapter 3**, we have developed a Markov chain model to include the contention and contention-free transmission behavior together. The developed model works for heterogeneous sensor devices in non-saturated mode. The Markov chain model is helpful to avoid the buffer instability by calculating service utilization. We have extended the model to incorporate signal attenuation due to log normal shadowing in the body surface. We have validated the analyses by simulations for a wheelchair-based wireless body area sensor network.

In **Chapter 4**, we have proposed a guaranteed time slot (GTS) allocation algorithm based on Knapsack problem. This model allows coordinator to collect sensed data from prioritized sensor devices with improved performance in terms of throughput. The proposed model is also useful in the networks where sensor devices have uneven traffic generation rates and unequal bandwidth requirements as well as unequal packet sizes.

Semi-static slot allocation scheme such as in IEEE 802.15.4 standard and IEEE 802.15.3c standard is not efficient due to wastage of bandwidth. Also TDMA slot allocation requires the coordinator to know the information of traffic loads (e.g., buffer

level) of the devices. However, there is not mechanism to transfer this information to the coordinator. We assume each device sends a slot request with traffic information to the coordinator during CSMA/CA period. By the time coordinator executes the algorithm using received information from the request packet, the queue length might be changed due to certain probabilistic traffic arrival pattern of the devices. In such scenario, we have modeled the probability mass function (pmf) of the distribution of queue length of the devices in **Chapter 5**. We have proposed a dynamic TDMA slot allocation algorithm by solving the utility maximization problem which takes into account the uncertainty in queue length of all devices to allocate slots to the devices.

Hidden terminal collision problem degrades the performance of a CSMA/CA-based networks. The handshake signaling (RTS/CTS) resolves the hidden terminal problem only partially. This signaling is also energy consuming in the network. To address this issue, we have proposed a cellular-like model of a hybrid CSMA/CA-TDMA MAC-based dense multihop wireless sensor networks in **Chapter 6**. The network is divided into cluster of δ cells. The supeframe of the hybrid MAC is also divided into δ slots. The devices in a cell are allocated same time slot. The devices transmit using CSMA/CA technique during their allocated time slots. This model does not require any signaling to mitigate the hidden terminal problem. We have developed the relation of signal-to-interference ratio (SIR) to the separation of devices to design a hidden terminal collisions mitigated network. We have developed an analytical model to estimate the size of the network conditioned on the traffic flow capacity. This model is useful in dimensioning the network.

7.2 Future Work

We have addressed the problem of modeling and analysis of hybrid CSMA/CA-TDMA protocols. Such hybrid MAC protocols are inherently energy efficient because of features like inactive period in the superframe. Also, the devices which are allocated time slots can go to low power mode during CSMA/CA period while the rest go to low power mode during TDMA period. In this research, we have excluded the inactivity period in the analysis. The effect of inactivity period can be analyzed in the future. Also, the end-to-end delay is an important performance metric in wireless sensor

networks. However, there is a tradeoff between end-to-end delay, throughput, and energy efficiency. This research has focused on improving the throughput and energy efficiency performance without considering the end-to-end delay. In the future, such hybrid MAC protocols can be designed to satisfy the quality-of-service (QoS) in terms of delay requirement in the network. The modeling approach developed (except that of **Chapter 6**) can be analyzed in the context of multihop wireless sensor networks.

Several potential extensions of the work presented in this thesis are outlined below.

- In **Chapter 2**, the centralized channel access scheme suffers from high complexity. In the distributed channel access scheme, the Markov decision process (MDP) model can be extended to a de-centralized partially observable Markov decision process (DecPOMDP) model which takes into account the observation of channel condition and traffic condition of the network (e.g., packet loss rate and time slot allocations of other devices) to improve the decision making capability of the devices.
- In **Chapter 3**, the analytical model for the IEEE 802.15.4-based channel access scheme measures the packet service time of the devices. This can be extended to analyze the end to end delay of the network in the context of wireless sensor networks.
- In **Chapter 4**, a knapsack problem has been formulated to prioritize the devices based on their traffic load and allocate the time slot. The devices or their traffic can be prioritize based on the urgency of time to incorporate the QoS in terms of average packet transmission delay.
- In **Chapter 5**, the proposed model makes use of a look-up table for the throughput of devices during CSMA/CA period. The throughput during CSMA/CA period depends on the number of competing devices, length of the CSMA/CA period, length of superframe, packet size and traffic load of the devices. An analytical model of the throughput incorporating all of the above factors can be developed for the proposed model. Then the proposed model can be extended to incorporate quality of service of the network, for example, in terms of guaranteed packet delivery time.
- In **Chapter 6**, to mitigate hidden terminal collision, the burden of over signaling (RTS/CTS messages) reduced by the proposed model is always beneficial for

wireless sensor networks. The proposed model analyzes the worst-case scenario of interference to determine the relation between signal-to-noise ratio (SNR) and separation of the devices. In future, this model can be extended with more realistic channel propagation model (such as log normal shadowing) and average case analysis incorporating proper distribution (e.g., Poisson point process) of the devices in the network.

Bibliography

[1] W. Dargie, C. Poellabauer, *Fundamentals of Wireless Sensor Networks: Theory and Practice*, John Wiley & Sons, Nov 5, 2010.

[2] P. Huang, L. Xiao, S. Soltani, M. W. Mutka, N. Xi, "The Evolution of MAC Protocols in Wireless Sensor Networks: A Survey," *IEEE Communications Surveys & Tutorials*, vol. 15, no. 1, pp. 101–120, First Quarter 2013.

[3] C. T. Cheng, C. K. Tse, F. C. M. Lau, "An Energy-Aware Scheduling Scheme for Wireless Sensor Networks," *IEEE Transactions on Vehicular Technology*, vol. 59, no. 7, pp. 3427–3444, Sept. 2010.

[4] M. A. Hanson, H. C. Powell, A. T. Barth, K. Ringgenberg, B. H. Calhoun, J. H. Aylor, and J. Lach, "Body Area Sensor Networks: Challenges and Opportunities," *IEEE Computer*, vol. 42, no. 1, pp. 58–65, January 2009.

[5] IEEE Standard for Information Technology Part 15.1: Wireless Medium Access Control (MAC) and Physical Layer (PHY) Specifications for Wireless Personal Area Networks (WPANs), *IEEE Standard 802.15.4 Working Group Std.*, 2005.

[6] IEEE Standard for Information Technology Part 15.4: Wireless Medium Access Control (MAC) and Physical Layer (PHY) Specifications for Low-Rate Wireless Personal Area Networks (LR-WPANs), *IEEE Standard 802.15.4 Working Group Std.*, 2006.

[7] J. Espina, T. Falck, and O. Mlhens, "Network Topologies, Communication Protocols, and Standards," *Body Sensor Networks*, Ed. Javier Espina, Springer, London, December 2007.

[8] I. Demirkol, C. Ersoy, F. Alagoz, "MAC Protocols for Wireless Sensor Networks: A Survey," *IEEE Communications Magazine,* vol. 44, no. 4, pp. 115–121, April 2006.

[9] K. Langendoen, G. Halkes, "Energy Efficient Medium Access Control", *Chapter Sensor Networks, Embedded Systems Handbook*, San Francisco, California, USA, CRC press.

[10] I. Rhee, A. Warrier, M. Aia, J. Min, and M. L, Sichitiu, "Z-MAC: A Hybrid MAC for Wireless Sensor Networks," *IEEE/ACM Transactions on Networking,* vol. 16, no. 3, pp. 511–524, June 2008.

[11] IEEE Standard for Information technology–Telecommunications and informa-

tion exchange between systems–Local and metropolitan area networks Specific requirements Part 15.3c: Wireless Medium Access Control (MAC) and Physical Layer (PHY) Specifications for High Rate Wireless Personal Area Networks (WPANs): Amendment 2: Millimeter-wave based Alternative Physical Layer Extension, *IEEE Std 802.15.3c*, 2009.

[12] IEEE Standard for Information technology–Telecommunications and information exchange between systems Local and metropolitan area networks–Specific requirements Part 11: Wireless LAN Medium Access Control (MAC) and Physical Layer (PHY) Specifications, *IEEE Std 802.11*, 2007.

[13] ZigBee, http://www.zigbee.org.

[14] WiFi, http://www.wi-fi.org/discover-and-learn

[15] Wibree, http://www.bluetooth.com/Pages/Low-Energy.aspx.

[16] H. I. Liu and J. D. Wu, "A Hybrid MAC Protocol for HFC Networks," in *Proc. of IEEE ICC'98*. vol. 2, pp. 859–863, Atlanta, 1998.

[17] M. L. Puterman, *Markov Decision Processes: Discrete Stochastic Dynamic Programming*. New Jersey: John Wiley & Sons, Inc., 1998.

[18] B. Shrestha, E. Hossain, K. W. Choi, and S. Camorlinga, "A Markov Decision Process (MDP)-based Congestion-Aware Medium Access Strategy for IEEE 802.15.4," in *Proc. of IEEE Global Communications Conference (Globecom 2011)*, pp. 1–5, Houston, TX, USA, 5-9 December 2011.

[19] A. Ephremides, O. A. Mowafi, "Analysis of a Hybrid Access Scheme for Buffered Users-Probabilistic Time Division," *IEEE Transactions on Software Engineering,* vol. SE-8, no. 1, pp. 52– 61, January 1982.

[20] S. T. Cheng and M. Wu, "Contention-Polling Duality Coordination Function for IEEE 802.11 WLAN Family," *IEEE Transactions on Communications*, vol. 57, no. 3, pp. 779–788, March 2009.

[21] B. Liu, Z. Yan, and C. W. Chen, "CA-MAC: A Hybrid Context-Aware MAC Protocol for Wireless Body Area Networks," in *Proc. of 13th IEEE International Conference on e-Health Networking Applications and Services (Healthcom)*, pp. 213–216, 13-15 June 2011.

[22] W. Wang, H. Wang, D. Peng, and H. Sharif, "An Energy Efficient Pre-Schedule Scheme for Hybrid CSMA/TDMA MAC in Wireless Sensor Networks," in *Proc. of 10th IEEE Singapore International Conference on Communication systems*, pp. 1–5, October 2006.

[23] Y. K. Rana, B. H. Liu, A. Nyandoro, and S. Jha, "Bandwidth Aware Slot Allocation in Hybrid MAC," in *Proc. of 31st IEEE Conference on Local Computer Networks,* pp. 89–96, 14-16 November 2006.

[24] B. Shrestha, E. Hossain, and S. Camorlinga, "IEEE 802.15.4 MAC with GTS Transmission for Heterogeneous Devices with Application to Wheelchair Body-Area Sensor Networks," *IEEE Trans. on Information Technology in Biomedicine*, vol. 15, no. 5, pp. 767–777, September 2011.

[25] S. T. Sheu, Y. Y. Shih, and W. T. Lee, "CSMA/CF Protocol for IEEE 802.15.4 WPANs," *IEEE Transactions on Vehicular Technology*, vol. 58, no. 3, pp. 1501–1516, March 2009.

[26] R. Zhang, L. Cai, J. Pan, "Performance Study of Hybrid MAC Using Soft Reservation for Wireless Networks," in *Proc. of 2011 IEEE International Conference on Communications (ICC)*, pp. 1–5, 5-9 June 2011.

[27] R. Jurdak, A. G. Ruzzelli, and G. M. P. O'Hare, "Radio Sleep Mode Optimization in Wireless Sensor Networks," *IEEE Transactions on Mobile Computing*, vol. 9, no. 7, pp. 955–968, July 2010.

[28] M. Khanafer, M. Guennoun, and H. T. Mouftah, "Adaptive Sleeping Periods in IEEE 802.15.4 for Efficient Energy Savings: Markov-Based Theoretical Analysis," in *Proc. of IEEE ICC'11*, pp. 1–6, Japan, June 2011.

[29] Z. Xiao, C. He, and L. Jiang, "Slot-based Model for IEEE 802.15.4 MAC with Sleep Mechanism," *IEEE Communications Letters*, vol. 14, no. 2, pp. 154–156, February 2010.

[30] B. Shrestha, E. Hossain, S. Camorlinga, R. Krishnamoorthy, and D. Niyato, "An Optimization-based GTS Allocation Scheme for IEEE 802.15.4 MAC with Application to Wireless Body Area Sensor Networks," in *Proc. of IEEE ICC'10*, pp. 1–6, Cape Town, May 2010.

[31] M. H. S. Gilani, I. Sarrafi, M. Abbaspour, "An Adaptive CSMA/TDMA Hybrid MAC for Energy and Throughput Improvement of Wireless Sensor Networks," *Ad Hoc Networks(2011)*, pp. 1–8, 2011.

[32] S. Zhuo, Y. Song, Z. Wang, and Z. Wang, "Queue-MAC: A Queue-length Aware Hybrid CSMA/TDMA MAC Protocol for Providing Dynamic Adaptation to Traffic and Duty-cycle Variation in Wireless Sensor Networks," in *Proc. of 9th IEEE International Workshop on Factory Communication Systems (WFCS),* pp.105–114, 21-24 May 2012.

[33] M. Leconte,N. Jian, R. Srikant, "Improved Bounds on the Throughput Efficiency of Greedy Maximal Scheduling in Wireless Networks," *IEEE/ACM Transactions on Networking*, vol. 19, no. 3, pp. 709–720, June 2011.

[34] A. Seyedi and B. Sikdar, "Energy Efficient Transmission Strategies for Body Sensor Networks with Energy Harvesting," in *IEEE Transactions on Communications*, vol. 58, no. 7, pp. 2116–2126, July 2010.

[35] Z. Liu and I. Elhanany, "RL-MAC: A Reinforcement Learning Based MAC Pro-

tocol for Wireless Sensor Networks," *International Journal of Sensor Networks (IJSNET)*, vol. 1, no. 3/4, pp. 117–124, April 2006.

[36] G. D. Angel and T. L. Fine, "Optimal Power and Retransmission Control Policies for Random Access Systems," *IEEE/ACM Transactions on Networking*, vol. 12, no. 6, pp. 1156–1166, December 2004.

[37] C. V. Phan, Y. Park, H. H. Choi, J. Cho, and J. G. Kim, "An Energy-Efficient Transmission Strategy for Wireless Sensor Networks," *IEEE Transactions on Consumer Electronics*, vol. 56, no. 2, pp. 597–605, May 2010.

[38] N. Mastronarde and M. van der Schaar, "Fast Reinforcement Learning for Energy-Efficient Wireless Communications," *IEEE Transactions on Signal Processing* vol. 59, no. 12, pp. 6262–6266, December 2011.

[39] B. Shrestha, K. W. Choi, and E. Hossain, "A dynamic time slot allocation scheme for hybrid CSMA/TDMA MAC protocol," *IEEE Wireless Communications Letters*, vol. PP, no. 99, 2013.

[40] R. M. Adelson,"Compound Poisson distribution," *Operation Research,* vol. 17, no. 1, pp. 73–75, Mar. 1966.

[41] R. K. Patro, M. Raina, V. Ganapathy, M. Shamaiah, and C. Thejaswi, "Analysis and Improvement of Contention Access Protocol in IEEE 802.15.4 Star Network," in *Proc. of IEEE Conf. on Mobile Adhoc and Sensor Systems (MASS)*, pp. 1–8, Pisa, October 2007.

[42] P. Park, P. D. Marco, P. Soldati, C. Fischione, and K. H. Johansson, "A Generalized Markov Chain Model for Effective Analysis of Slotted IEEE 802.15.4," in *Proc. IEEE Int. Conf. on Mobile Ad-hoc and Sensor Systems*, pp. 130–139, Macau, 2009.

[43] P. Di Marco, P. Park, C. Fischione, and K. H. Johansson, "Analytical Modeling of Multi-hop IEEE 802.15.4 Networks," *IEEE Transactions on Vehicular Technology,* vol. 61, no. 7, pp. 3191–3208, September 2012.

[44] L. P. Kaelbling, M. L. Littman, and A. W. Moore, "Reinforcement Learning: A Survey," *Journal of Artificial Intelligence Research*, vol. 4, pp. 237–285, 1996.

[45] K. Y. Yazdandoost and K. Sayrafian-Pour, "Channel Model for Body Area Network (BAN)," *IEEE 802.15 Working Group Document, IEEE P802.15-08-0780-09-0006*, April 2009.

[46] Chipcon CC2420 2.4 GHz IEEE 802.15.4 / ZigBee-ready RF Transceiver, http://inst.eecs.berkeley.edu/ cs150/Documents/CC2420.pdf

[47] M. D. Francesco, G. Anastasi, M. Conti, S. K. Das, and V. Neri, "Reliability and Energy-Efficiency inIEEE 802.15.4/ZigBee Sensor Networks: An Adaptive and Cross-Layer Approach," *IEEE Journal on Selected Areas in Communications*, vol. 29, no. 8, pp. 1508–1524, September 2011.

[48] A. Soomro and D. Cavalcanti, "Opportunities and Challenges in Using WPAN and WLAN Technologies in Medical Environments," *IEEE Communications Magazine*, vol. 45, no. 2, pp. 114–122, February 2007.

[49] Y. Chu and A. Ganz, "A Mobile Teletrauma System Using 3G Networks," *IEEE Transactions on Information Technology in Biomedicine*, vol. 8, no. 4, pp. 456–462, November, 2004.

[50] A. Alesanco and J. Garcia, "Clinical Assessment of Wireless ECG Transmission in Real-time Cardiac Tele-monitoring," *IEEE Transactions on Information Technology in Biomedicine*, vol. 14, no. 5, pp. 1144–1152, April, 2010.

[51] S. Junnila, H. Kailanto, J. Merilahti, A.-M. Vainio, A. Zakrzewski, M. Vehkaoja, and J. Hyttinen, "Wireless, Multipurpose In-home Health Monitoring Platform: Two Case Trials," *IEEE Transactions on Information Technology in Biomedicine*, vol. 14, no. 2, pp. 447–455, March, 2010.

[52] P. Park, C. Fischione, and K. H. Johansson, "Performance Analysis of GTS Allocation in Beacon Enabled IEEE 802.15.4," in *Proc. 6th Annual IEEE Communications Society Conference on Sensor, Mesh and Ad Hoc Communications and Networks*, Italy, 2009, pp. 1–9.

[53] Private communications with Richard Rodd, Rehabilitation Engineer - Electronics, Health Sciences Centre, Winnipeg, email: rjrodd@hsc.mb.ca.

[54] D. Malone, K. Duffy, and D. Leith, "Modeling the 802.11 Distributed Coordination Function in Nonsaturated Heterogeneous Conditions," *IEEE/ACM Trans. on Networking*, vol. 15, no. 1, pp. 159–172, February 2007.

[55] P. E. Engelstad and O. N. Osterbo, "Non-Saturation and Saturation Analysis of IEEE 802.11e EDCA with Starvation Prediction," in *Proc. ACM SIGMETRICS Int. Conf. on Measurement and Modeling of Computer Systems*, June 06-10, 2005, Banff, Alberta, Canada, pp. 224–233.

[56] O. Tickoo and B. Sikdar, "Queueing Analysis and Delay Mitigation in IEEE 802.11 Random Access MAC Based Wireless Networks," in *Proc. IEEE Conf. on Computer Communications (INFOCOM 2004)*, vol. 2, China, 2004, pp. 1404–1413.

[57] G. Bianchi, "Performance Analysis of the IEEE 802.11 Distributed Coordination Function," *IEEE J. on Selected Areas in Communications*, vol. 18, no. 3, pp. 535–547, March 2000.

[58] S. Pollin, M. Ergen, S. C. Ergen, B. Bougard, L. V. D. Perre, F. Catthoor, I. Moerman, A. Bahai, and P. Varaiya, "Performance Analysis of Slotted Carrier Sense IEEE 802.15.4 MAC," in *Proc. IEEE Globecom'06*, CA, USA, Nov. 2006, pp. 1–6.

[59] Z. Tao, S. Panwar, D. Gu, and J. Zhang, "Performance Analysis and a Proposed

Improvement for the IEEE 802.15.4 Contention Access Period," in *Proc. IEEE Wireless Communications and Networking Conference*, Las Vegas, USA, 2006, pp. 1811–1818.

[60] T. J. Lee, H. R. Lee, and M. Y. Chung, "MAC Throughput Limit Analysis of Slotted CSMA/CA in IEEE 802.15.4 WPAN," *IEEE Communications Letters*, vol. 10, no. 7, pp. 561–563, July 2006.

[61] J. He, Z. Tang, H. H. Chen, and Q. Zhang, "An Accurate and Scalable Analytical Model for IEEE 802.15.4 Slotted CSMA/CA Networks," *IEEE Transactions on Wireless Communications*, vol. 8, no. 1, pp. 440–448, Jan. 2009.

[62] J. Gao, J. Hu, and G. Min, "A New Analytical Model for Slotted IEEE 802.15.4 Medium Access Control Protocol in Sensor Networks," in *Proc. WRI International Conference on Communications and Mobile Computing*, China, 2009, pp. 427–431.

[63] J. Mišić and V. B. Mišić, "Bridging between IEEE 802.15.4 and IEEE 802.11b Networks for Multiparameter Healthcare Sensing," *IEEE J. on Selected Areas in Communications*, vol. 27, no. 4, pp. 435–449, May 2009.

[64] E. Kim, M. Kim, S. Youm, S. Choi, and C. H. Kang, "Priority-based Service Differentiation Scheme for IEEE 802.15.4 Sensor Networks," *AEU-International Journal of Electronics and Communications*, vol. 61, no. 2, pp. 69–81, Feb. 2007.

[65] E. D. Ndih, N. Khaled, and G. D. Micheli, "An Analytical Model for the Contention Access Period of the Slotted IEEE 802.15.4 with Service Differentiation," in *Proc. IEEE Int. Conf. Communications*, Dresden, Germany, 2009, pp. 1–6.

[66] C. Y. Jung, H. Y. Hwang, D. K. Sung, and G. U. Hwang, "Enhanced Markov Chain Model and Throughput Analysis of the Slotted CSMA/CA for IEEE 802.15.4 Under Unsaturated Traffic Conditions," *IEEE Trans. on Vehicular Technology*, vol. 58, no. 1, pp. 473–478, Jan. 2009.

[67] J. Mišić, V. B. Mišić, and S. Shafi, "Performance of IEEE 802.15.4 Beacon Enabled PAN with Uplink Transmissions in Non-saturation Mode - Access delay for Finite Buffers," in *Proc. IEEE BroadNets 2004*, San Jose, CA, Oct. 2004, pp. 416–425.

[68] C. Buratti, "Performance Analysis of IEEE 802.15.4 Beacon-Enabled Mode," *Vehicular Technology, IEEE Transactions on* , vol. 59, no. 4, pp. 2031–2045, May 2010.

[69] P. Di Marco, P. Park, C. Fischione, and K. H. Johansson, "Analytical Modelling of IEEE 802.15.4 for Multi-hop Networks with Heterogeneous Traffic and Hidden Terminals," in *Proc. IEEE Globecom'10*, Florida, USA, 2010, pp. 1–6.

[70] J. Noga and V. Sarbua, "An Online Partially Fractional Knapsack Problem,"

in *Proceedings of International Symposium on Parallel Architectures, Algorithms and Networks (ISPAN'05)*, December 2005.

[71] Y. K. Huang, A. C. Pang, and H. N. Hung, "An Adaptive GTS Allocation Scheme for IEEE 802.15.4," *IEEE Transactions on Parallel and Distributed Systems*, vol. 19, no. 5, May 2008.

[72] A. Koubaa, M. Alves, and E. Tovar, "i-GAME: An implicit GTS Allocation Mechanism in IEEE 802.15.4 for Time-sensitive Wireless Sensor Networks," in *Proceedings of 18th Euromicro Conference on Real-Time Systems*, 2006.

[73] C. Na, Y. Yang, and A. Mishra, "An optimal GTS Scheduling Algorithm for Time-sensitive Transactions in IEEE 802.15.4 Networks," *Computer Networks*, vol. 52, no. 13, pp. 2543–2557, September 2008.

[74] L. Cheng, A. G. Bourgeois, and X. Zhang, "A New GTS Allocation Scheme for IEEE 802.15.4 Networks with Improved Bandwidth Utilization," in *Proceedings of International Symposium on Communications and Information Technologies (ISCIT'07)*, 2007.

[75] P. Kumar, M. Gunes, A. Al Mamou, and I. Hussain, "Enhancing IEEE 802.15.4 for Low-latency, Bandwidth, and Energy Critical WSN Applications," in *Proceedings of 4th International Conference on Emerging Technologies (ICET'08).*

[76] U. Varshney, "Pervasive Healthcare and Wireless Health Monitoring," *Mobile Networks and Applications*, vol. 12, no. 2-3, Springer Netherlands, June, 2007.

[77] T. H. Cormen, C. E. Leiserson, R. L. Rivest, and C. Stein, *Introduction to Algorithms* , The MIT press, 2001.

[78] T. Aoyagi, J. Takada, K. Takizawa, N. Katayama, T. Kobayashi, K. Y. Yazdandoost, H. Li, and R. Kohno, "Channel Models for Wearable and Implantable WBANs," *IEEE 802.15 Working Group Document, IEEE 802.15-08-0416-02-0006*, July 2008.

[79] J. Takada, T. Aoyagi, K. Takizawa, N. Katayama, T. Kobayashi, K. Y. Yazdandoost, H. Li, and R. Kohno, "Static Propagation and Channel Models in Body Area," *COST 2100 6th Management Committee Meeting, TD(08)639*, Lille, France, Oct. 2008

[80] A. Ahmad, A. Riedl, W. J. Naramore, N. Y. Chou, and M. S. Alley, "Scenario-based Traffic Modeling for Data Emanating from Medical Instruments in Clinical Environment," *2009 WRI World Congress on Computer Science and Information Engineering*, March 31-April 2, 2009.

[81] T. Baykas, C.-S. Sum, Z. Lan, J. Wang, M. A. Rahman, H. Harada, and S. Kato, "IEEE 802.15.3c: The First IEEE Wireless Standard for Data Rates over 1 Gb/s," *IEEE Commun. Mag.,* vol. 49, no. 7, pp. 114–121, Jul. 2011.

[82] C. Cordeiro, D. Akhmetov, and M. Park, "IEEE 802.11ad: Introduction and Performance Evaluation of the First Multi-Gbps WiFi Technology," in *Proc. mmCom 2010,* Chicago, IL, Sept. 2010.

[83] K. Ashrafuzzaman and K. S. Kwak, "On the Performance Analysis of the Contention Access Period of IEEE 802.15.4 MAC," *IEEE Commun. Lett.,* vol. 15, no. 9, pp. 986–988, Sept. 2011.

[84] C. W. Pyo and H. Harada, "Throughput Analysis and Improvement of Hybrid Multiple Access in IEEE 802.15.3c mm-wave WPAN," *IEEE J. Sel. Areas Commun.,* vol. 27, no. 8, pp. 1414–1424, Oct. 2009.

[85] J. W. Yang, J. K. Kwon, H. Y. Hwang, and D. K. Sung, "Goodput Analysis of a WLAN with Hidden Nodes under A Non-saturated Condition," *IEEE Transactions on Wireless Communications*, vol. 8, no. 5, pp. 2259–2264, 2009.

[86] Y. Liu, R. Sheahan, and H. P. Schwefel, "Towards Analytic Modeling for CSMA/CA based MAC Protocol in Wireless Multi-hop Networks - A Simulation Study," in *Proc. of 13th GI/ITG Conference on Measuring, Modelling and Evaluation of Computer and Communication Systems*, Nunberg, Germany, 2006, pp. 1–16.

[87] K. Kosek-Szott, "A survey of MAC Layer Solutions to the Hidden Node Problem in Ad-hoc Networks," *Ad Hoc Networks,* vol. 10, no. 3, pp 635–660, May 2012.

[88] A. Koubaa, R. Severino, M. Alves, and E. Tovar, "Improving Quality-of-Service in Wireless Sensor Networks by Mitigating Hidden-Node Collisions," *IEEE Transactions on Industrial Informatics*, vol. 5, no. 3, pp. 299–313, 2009.

[89] N. Kobatake and Y. Yamao, "High-Throughput Time Group Access SS-CSMA/CA for Wireless Ad-hoc Networks with Layered-tree Topology," *WMNC 2010 : Third Joint IFIP Wireless and Mobile Networking Conference*, Hungary, 13-15 Oct. 2010, pp. 1–5,

[90] L. J. Hwang, S. T. Sheu, Y. Y. Shih, and Y. C. Cheng, "Grouping Strategy for Solving Hidden Node Problem in IEEE 802.15.4 LR-WPAN," in *Proc. First International Conference on Wireless Internet*, Budapest, Hungary, 2005, pp. 26–32.

[91] K. Adere and G. R. Murthy, "Solving the Hidden and Exposed Terminal Problems using Directional-Antenna based MAC Protocol for Wireless Sensor Networks," in *Proc. of Seventh International Conference On Wireless And Optical Communications Networks (WOCN)*, Columbo, Sept. 2010, pp. 1–5.

[92] S. Parvin and T. Fujii, "A Novel Routing Scheme with High Sensitive Sensing for Multi Hop Wireless Mesh Network," in *Proc. of International Conference on Intelligent Networking and Collaborative Systems (INCOS)*, Greece, Nov. 2010, pp. 398–403.

[93] D. Halperin, J. Ammer, T. Anderson, and D. Wetherall, "Interference Cancellation: Better Receivers for a New Wireless MAC," in *Proc. of Hotnets*, 2007, pp. 339–350.

[94] H. Zhai and Y. Fang, "Physical Carrier Sensing and Spatial Reuse in Multirate and Multihop Wireless Ad-hoc Networks," in *Proc. of IEEE INFOCOM,* Apr. 2006, pp. 1–12.

[95] L. B. Jiang and S. C. Liew, "Hidden-Node Removal and Its Application in Cellular WiFi Networks," *IEEE Transactions on Vehicular Technology,* vol. 56, no. 5, pp. 2641–2651, 2007.

[96] Z. Yihong and S. M. Nettles, "Balancing the Hidden and Exposed Node Problems with Power Control in CSMA/CA-based Wireless Networks," in *Proc. of Wireless Communications and Networking Conference*, New Orleans, 2005, vol. 2, pp. 683–688.

[97] A. Jayasuriya, S. Perreau, A. Dadej, and S. Gordon, "A Hidden vs. Exposed Terminal Problem in Ad-hoc Networks," in *Proc. of the Australian Telecommunication Networks and Applications Conference*, Sydney, Australia, 8-10 Dec. 2004.

[98] P. Gupta and P. R. Kumar, "The Capacity of Wireless Networks," *IEEE Transactions on Information Theory,* , vol. 46, no. 2, pp. 488–404, 2000.

[99] C. Y. Jung, H. Y. Hwang, D. K. Sung, and G. U. Hwang, "Enhanced Markov Chain Model and Throughput Analysis of the Slotted CSMA/CA for IEEE 802.15.4 Under Unsaturated Traffic Conditions," *IEEE Transactions on Vehicular Technology,* vol. 58, no. 1, pp. 473–478, Jan. 2009.

Appendix A

Proof of uniqueness of solution of the equations (3.10) and (3.11)

For simplicity, assume $P_d = 0$ and $P_g = 0$. We can rewrite the equations (3.10) and (3.11) in terms of the constant parameters K_1, K_2 and C_n for particular value of $P_{cs} \in [0, 1]$ as follows:

$$\alpha_n = 1 - \alpha_n\beta_n C_n - K_1 \sum_{\substack{h=1 \\ h\neq n}}^{N} \alpha_h\beta_h - \sum_{\substack{h=1 \\ h\neq n}}^{N} \alpha_h\beta_h C_h \tag{A.1}$$

$$\beta_n = 1 - K_2 - \sum_{\substack{h=1 \\ h\neq n}}^{N} \alpha_h\beta_h C_h. \tag{A.2}$$

By comparing equations (3.10), (3.11), (A.1) and (A.2), one can easily find that K_1, K_2, and C_n are positive for $\forall n > 0$ since $P_{cs} \in [0, 1]$. Now let us define a $2N$ point function $\mathfrak{f} = [f_{\alpha,n}\ f_{\beta,n}]$ for $n = 1, 2, \cdots, N$, where

$$f_{\alpha,n} = 1 - \alpha_n - \alpha_n\beta_n C_n - K_1 \sum_{\substack{h=1 \\ h\neq n}}^{N} \alpha_h\beta_h - \sum_{\substack{h=1 \\ h\neq n}}^{N} \alpha_h\beta_h C_h \tag{A.3}$$

$$f_{\beta,n} = 1 - \beta_n - K_2 - \sum_{\substack{h=1 \\ h\neq n}}^{N} \alpha_h\beta_h C_h. \tag{A.4}$$

The problem is to prove that there exists unique values of α_n and β_n, where $f_{\alpha,n} = 0$ and $f_{\beta,n} = 0$. Our interested region for the solution is $\alpha_n > 0$ and $\beta_n > 0\ \forall n$. Let us consider the extreme point where $\alpha_n = 0$ and $\beta_n = 0\ \forall n$, and we have

$$\mathfrak{f} > 0_{1\times 2N}. \tag{A.5}$$

Therefore, at this extreme point, the function value is always positive. This is the lower extreme point.

Now let us consider $\alpha_n > 1$ and $\beta_n > 1$ $\forall n$. Then we get

$$\mathfrak{f} < 0_{1\times 2N}. \tag{A.6}$$

This indicates that $\alpha_n > 1$ and $\beta_n > 1$ lie in the region where the function value is always negative. Therefore, the upper extreme point is $\alpha_n = 1$, $\beta_n = 1$, $\forall n > 0$. We can say that the solution (i.e., $\mathfrak{f} = 0$) lies in the range $\alpha_n \in [0, 1]$ and $\beta_n \in [0, 1]$.

Now let us find the Jacobian matrix of the $2N$ point function $\mathfrak{f} = [f_{\alpha,1} \dots f_{\alpha,N}\ f_{\beta,1} \dots f_{\alpha,N}]$ with $2N$ unknowns $\mathfrak{X} = [\alpha_1 \dots \alpha_N\ \beta_1 \dots \beta_N]$, where for the purpose of finding the solution, each unknown is assumed independent of others.

$$\frac{\partial f_{\alpha,n}}{\partial \alpha_k} = -(1 + \beta_n C_n), \quad \text{if } n = k \tag{A.7}$$

$$\frac{\partial f_{\alpha,n}}{\partial \alpha_k} = -\beta_n (K_1 + C_n), \quad \text{if } n \neq k \tag{A.8}$$

$$\frac{\partial f_{\alpha,n}}{\partial \beta_k} = -\alpha_n C_n, \quad \text{if } n = k \tag{A.9}$$

$$\frac{\partial f_{\alpha,n}}{\partial \beta_k} = -\alpha_n (K_1 + C_n), \quad \text{if } n \neq k. \tag{A.10}$$

Similarly,

$$\frac{\partial f_{\beta,n}}{\partial \alpha_k} = 0, \quad \text{if } n = k \tag{A.11}$$

$$\frac{\partial f_{\beta,n}}{\partial \alpha_k} = -\beta_n C_n, \quad \text{if } n \neq k \tag{A.12}$$

$$\frac{\partial f_{\beta,n}}{\partial \beta_k} = -1, \quad \text{if } n = k \tag{A.13}$$

$$\frac{\partial f_{\beta,n}}{\partial \beta_k} = -\alpha_n C_n, \quad \text{if } n \neq k. \tag{A.14}$$

For any value of α_n and β_n in the interval (0,1), the gradient of the function $\mathfrak{f}$ is negative. This implies that the function is monotonically decreasing along the gradient path in the interval. This proves that there exists unique values of α and β where the function crosses the zero axis (i.e., has zero value). The same conclusion can be drawn with $P_d \in [0, 1]$ and $P_g \in [0, 1]$. Note that P_d cannot be greater than 0.5 in the IEEE 802.15.4 standard.

Appendix B

Derivation of total backoff

Note that $C_{1,n}$ is the probability of going to another backoff stage and $C_{3,n}$ is the probability of occurring collision transmission from any one of the $(m+1)$ backoff stages. If node n has collision from any of the $(m+1)$ backoff stages, it goes to another retransmission stage. z_n given in equation (3.12) is the average backoffs when node n is in the R^{th} retransmission plane. Let us assume $R = 2$. Then, considering every possible backoff a node n can take from any backoff stage of a retransmission plane, the total average backoff can be estimated as

$$\begin{aligned} TB_n &= (1-C_{1,n})\frac{W_0}{2}(1-C_{3,n}) + C_{3,n}[\dots] \\ &\quad +(1-C_{1,n})C_{1,n}\frac{W_1}{2}(1-C_{3,n}) + C_{3,n}[\dots] + \dots \\ &\quad +(1-C_{1,n})C_{1,n}^{m-1}\frac{W_{m-1}}{2}(1-C_{3,n}) + C_{3,n}[\dots] \\ &\quad +C_{1,n}^{m}\frac{W_m}{2}(1-C_{3,n}) + C_{3,n}[\dots] \end{aligned} \tag{B.1}$$

where

$$\begin{aligned} [\dots] &= (1-C_{1,n})\frac{W_0}{2}(1-C_{3,n}) + C_{3,n}z_n \\ &\quad +(1-C_{1,n})C_{1,n}\frac{W_1}{2}(1-C_{3,n}) + C_{3,n}z_n + \dots \\ &\quad +(1-C_{1,n})C_{1,n}^{m-1}\frac{W_{m-1}}{2}(1-C_{3,n}) + C_{3,n}z_n \\ &\quad +C_{1,n}^{m}\frac{W_m}{2}(1-C_{3,n}) + C_{3,n}z_n. \end{aligned}$$

After simple manipulations, we get

$$TB_n = z_n[(1-C_{3,n}) + (m+1)C_{3,n}(1-C_{3,n}) + (m+1)^2C_{3,n}^2].$$

Similarly, for R retransmission planes, the total average backoff is

$$\begin{aligned} TB_n &= z_n[((1-C_{3,n})\sum_{k=0}^{R-1}((m+1)C_{3,n})^k \\ &\quad +((m+1)C_{3,n})^R)]. \end{aligned} \tag{B.2}$$